R009-01
B 会場 ：11/24　PM1 （13:15-15:15）
13:15〜13:30

#村上 豪 [1)], Jones Geraint[2)], Benkhoff Johannes[2)]
([1]ISAS/JAXA, [2]ESA

Updated Status of BepiColombo and Overview of Mercury Flyby Observations

#Go Murakami[1)], Geraint Jones[2)], Johannes Benkhoff[2)]
([1]Institute of Space and Astronautical Science, Japan Aerospace Exploration Agency, [2]European Space Agency

The ESA-JAXA joint mission BepiColombo is now on the cruise to Mercury. The BepiColombo mission consists of two spacecraft, Mio (Mercury Magnetospheric Orbiter: MMO) and Mercury Planetary Orbiter (MPO). The 7-years interplanetary cruise of BepiColombo covers the heliocentric distance range of 0.3-1.2 AU and also includes 9 planetary flybys: once at the Earth, twice at Venus, and 6 times at Mercury. Even before arrival, we already obtained fruitful science data from Mercury during three Mercury flybys completed on 1 October 2021, 23 June 2022, and 19 June 2023. We performed science observations with almost all the instruments onboard Mio and successfully obtained comprehensive data of Mercury's magnetosphere such as magnetic fields, plasma particles, and waves. The fourth Mercury flyby is scheduled on 4 September 2024 and its trajectory is quite different from those of the first three flybys. Here we present the updated status of BepiColombo, initial results of the science observations during the Mercury flybys, and the upcoming operations plans.

R009-02
B 会場 ：11/24　PM1 （13:15-15:15）
13:30〜13:45

#尾崎 光紀 [1)], 近藤　岳琉 [1)], 山田 裕都 [1)], 八木谷 聡 [1)], 疋島 充 [2)], 大村 善治 [3)]
([1 金沢大, ([2 マグネデザイン株式会社, ([3 京大・生存圏

Whistler-driven electron precipitation by asymmetric loss cone in Mercury's miniature magnetosphere

#Mitsunori Ozaki[1)], Takeru Kondo[1)], Yuto Yamada[1)], Satoshi Yagitani[1)], Mitsuru Hikishima[2)], Yoshiharu Omura[3)]
([1Kanazawa University, ([2Magnedesign Corporation, ([3Research Institute for Sustainable Humanosphere, Kyoto University

Mercury has a large loss cone difference in both northern and southern hemispheres due to the northward shifted magnetic dipole. It is predicted that the asymmetric loss cones can affect the whistler instability by the effects of the asymmetric temperature anisotropy and the asymmetric Lorentz and mirror forces in the north and south polar regions. To understand the effects of the energetic electron precipitation through electron – whistler interactions in Mercury's miniature magnetosphere, we compute the pitch angle scattering in two different cases for symmetric (the same loss cone size at the north and south polar regions) and asymmetric (an assumption of 10-deg. wider at the south polar region) bounce loss cones. In the computation results of both cases, we see clear prompt electron precipitation events driven by whistler-mode waves. In particular, the computation result in the asymmetric loss cone case shows more active electron precipitation at the northern hemisphere in comparison with that for the symmetric loss cone, because the whistler instability in the southern hemisphere is enhanced by the effects of the larger loss cone. In this presentation, we will present the significant difference of the electron precipitation driven by the nonlinear whistler instability in the two hemispheres in Mercury's miniature magnetosphere.

R009-03
B 会場 ：11/24　PM1 （13:15-15:15）
13:45〜14:00

数値モデルとかぐや観測の比較に基づいた月面電位分布の解析

#加藤 正久 [1)], 原田 裕己 [1)], 西野 真木 [2)], 齋藤 義文 [2)], 横田 勝一郎 [3)], 高橋 太 [4)], 清水 久芳 [5)], Shaosui Xu[6)], Andrew Poppe[6)], Jasper Halekas[7)]
([1] 京大・理, [2] 宇宙研, [3] 大阪大, [4] 九大・理・地惑, [5] 東大・地震研, [6] カリフォルニア大学バークレー校, [7] アイオワ大学

Analysis of the lunar surface potential distribution based on a comparison between a numerical model and Kaguya observations

#Masahisa Kato[1)], Yuki Harada[1)], Masaki N Nishino[2)], Yoshifumi Saito[2)], Shoichiro Yokota[3)], Futoshi Takahashi[4)], Hisayoshi Shimizu[5)], Shaosui Xu[6)], Andrew R Poppe[6)], Jasper Halekas[7)]
([1]Department of Geophysics, Graduate School of Science, Kyoto University, [2]Institute of Space and Astronautical Science, Japan Aerospace Exploration Agency, [3]Osaka University, [4]Department of Earth and Planetary Sciences, Faculty of Sciences, Kyushu University, [5]Earthquake Research Institute, University of Tokyo, [6]Space Sciences Laboratory, University of California, Berkeley, US, [7]Department of Physics and Astronomy, University of Iowa, US

Since the Moon does not possess a dense atmosphere, the lunar surface directly interacts with its ambient plasma. Although the Moon has no global magnetic field, there are crustal magnetic field regions called magnetic anomalies. Thus, some characteristics of interaction between plasma and electromagnetic fields over magnetized regions are different from those over non-magnetized regions. In the context of lunar surface charging, the inhomogeneity of the lunar surface potential over a wide range of spatial scales is not fully characterized yet. In this study, we analyze electron observations by Kaguya in comparison with a numerical model of photo-emitted electron energy spectra to investigate the spatial distribution of the lunar surface potential. We identified more positive surface potential in the relatively strong crustal magnetic field regions. We discuss possible explanations for the inferred surface potential inhomogeneity.

月は濃い大気を持たないため、月面は周辺のプラズマと直接相互作用する。また、月は全球的な磁場を持たないが、磁気異常と呼ばれる地殻磁場領域が存在する。このため、磁化領域における電磁場とプラズマの間の相互作用の特徴が、非磁化領域での特徴と異なるものが存在する。月面帯電の文脈では、さまざまな空間スケールでの表面電位の不均一性はよく特徴づけがなされていない。本研究では、かぐやによる電子観測と太陽光によって放出された電子のエネルギースペクトルを求める数値モデルと比較することによって表面電位の水平分布について調べており、相対的に地殻磁場の強い領域において表面電位がより正に変化することを確かめた。推定される表面電位の不均一性がどのように説明されるかについて議論する。

R009-04
B 会場 ：11/24　PM1 （13:15-15:15）
14:00〜14:15

#荻野 晃平 [1)], 原田 裕己 [1)], 西野 真木 [2)], 齋藤 義文 [2)], 横田 勝一郎 [3)], 笠原 禎也 [4)], 熊本 篤志 [5)], 高橋 太 [6)], 清水 久芳 [7)]
([1] 京都大学大学院理学研究科, [2] 国立研究開発法人宇宙航空研究開発機構, [3] 大阪大学大学院理学研究科, [4] 金沢大学学術メディア創成センター, [5] 東北大学大学院理学研究科, [6] 九州大学理学研究院, [7] 東京大学地震研究所

Solar wind interaction with multiple lunar crustal magnetic anomalies: Kaguya low-altitude observations

#Kohei Ogino[1)], Yuki Harada[1)], Masaki N Nishino[2)], Yoshifumi Saito[2)], Shoichiro Yokota[3)], Yoshiya Kasahara[4)], Atsushi Kumamoto[5)], Futoshi Takahashi[6)], Hisayoshi Shimizu[7)]
([1]Department of Geophysics, Graduate School of Science, Kyoto University, [2]Japan Aerospace Exploration Agency, [3]Osaka University, [4]Emerging Media Initiative, Kanazawa University, [5]Department of Geophysics, Graduate School of Science, Tohoku University, [6]Department of Earth and Planetary Sciences, Faculty of Sciences, Kyushu University, [7]Earthquake Research Institute, University of Tokyo

The solar wind interaction with lunar crustal magnetic anomalies (LMAs) gives rise to various electromagnetic phenomena (e.g. formation of Hall electric fields due to ion-electron decoupling, nonadiabatic solar wind ion reflection, and plasma wave excitation). Understanding the nature of the solar wind-LMA interaction is important because it greatly affects the spatial structure and temporal variability of electromagnetic fields, which control the dynamics of charged particles near the lunar surface. However, the solar wind-LMA interaction has not been fully understood due to the small vertical spatial scales (<~50 km) of LMAs compared to the typical altitude of lunar orbiters (>~100 km) and the difficulty of direct observations of the interaction regions. In this study, we focus on Kaguya low-altitude observations, to comprehensively characterize the solar wind ion reflection and plasma wave excitation in the central region of the solar wind-LMA interaction over multiple LMAs with various horizontal extents. We observe relatively stronger solar wind ion reflection and whistler mode waves at 1-10 Hz over spatially extended LMAs than over spatially isolated LMAs. On the other hand, strong broadband electrostatic noise at 1-10 kHz tends to be observed over both spatially isolated and extended LMAs in the central interaction region. Also, our results suggest that direct measurements at low altitudes where Hall electric fields are formed are essential for understanding the detailed physics of the solar wind-LMA interaction. Based on the results derived from Kaguya low-altitude observations, we discuss implications for future low-altitude or lander missions to LMA.

R009-05
B 会場 ：11/24　PM1 （13:15-15:15）
14:15〜14:30

惑星探査用イオン質量分析器のグラフェンによる感度・質量分解能の向上

#関 宗一郎 [1)], 笠原 慧 [1)], 田尾 涼 [1)], 川島 桜也 [2)], 陶 由未加 [1)], 杉田 精司 [1)]
([1 東大, ([2 宇宙科学研究所

Improvement of sensitivity and mass resolution by graphene in ion mass spectroscopy for solar-system exploration

#Soichiro Seki[1)], Satoshi Kasahara[1)], Ryo Tao[1)], Oya Kawashima[2)], Yumika Sue[1)], Seiji Sugita[1)]
([1]The University of Tokyo, ([2]Institute of Space and Astronautical Science

The atmospheric compositions of planetary bodies are important for understanding their origins and evolutions. Ion mass spectrometers (MS) onboard spacecraft have been used to measure the atmospheric compositions of many planetary bodies. One of the main MS styles is time-of-flight (TOF), which is known for its light weight and high mass resolution. For many TOF MS for ion species in tenuous atmosphere often use ultra-thin carbon films installed at the MS entrance to knock out secondary electrons at the time of ion incidence. These electrons are used to trigger start signal to set the starting time of a flight time measurement. Because this start signal triggering is a necessary part for TOF MS, its efficiency and angular scattering of ion transmission as well as secondary electron emission efficiency influence the overall TOF-MS performances, such as sensitivity and mass resolutions. Thinner ion entrance films are better for TOF-MS resolution and sensitivity. However, mechanical strength high enough to withstand severe shock and vibration of a rocket launch and thermal extension/contraction in harsh space environments are required for space missions.

Since the 1990s, the thickness of ultrathin amorphous carbon films used in ion mass spectrometers has been about 50 Å. In contrast, graphene, discovered in the 2000s, has a thickness of ˜5 Å, about 10 times thinner than amorphous carbon. Consequently, energy loss and angular scattering of ions when they pass through the entrance film become much smaller. These contribute to improvement in mass resolution and detection sensitivity, respectively. In addition, because the interatomic bonds of molecular ion species often break down upon transmission through conventional amorphous carbon films, we cannot measure the original molecular ions accurately. In contrast, graphene does not change the original molecular states very much, enabling more accurate atmospheric composition measurements.

These excellent properties make graphene an extremely useful material for ion mass spectrometers. However, graphene is difficult to handle owing to its thinness, and there has been no flight heritage. In particular, frequent and serious damages occur during the process of placing graphene on TOF-MS entrances. More specifically, when transferring graphene from the base material to the holder of the analyzer, graphene surface is coated with acrylic resin for retention. After transferring the graphene to the holder, the acrylic coating is commonly dissolved by immersion in acetone. However, it is well known that graphene is damaged in this process.

The purpose of this study to establish a handling procedure for graphene and to demonstrate its compatibility with space/launch environment. More specifically, we newly used graphene consisting of multiple layers and performed the same procedure for transfer. Our experimental results show that we achieved a high graphene area coverage ($>$90%). On the other hand, residues of acrylic resin were found in places on the graphene even after soaking in acetone. In addition, vibration was applied to the transferred graphene to simulate a launch environment, and the changes in the graphene were examined. We found no significant damage was caused by the vibration, demonstrating high vibration resistance of graphene.

R009-06
B 会場 ：11/24　PM1 （13:15-15:15）
14:30〜14:45

#笠羽 康正 [1)], Baptiste Cecconi[2)], 土屋 史紀 [1)], 三澤 浩昭 [1)], 北 元 [3)], 安田 陸人 [1)], 加藤 雄人 [1)], 熊本 篤志 [1)], 木村 智樹 [4)], 三好 由純 [5)], 笠原 禎也 [6)], 松田 昇也 [6)], 八木谷 聡 [6)], 尾崎 光紀 [6)], 小嶋 浩嗣 [7)], 栗田 怜 [7)], J.-E. Wahlund[8)]
([1] 東北大, [2]Obs de Paris, [3] 東北工大, [4] 東京理大, [5] 名大, [6] 金沢大, [7] 京大, [8]IRF Uppsala

High-Frequency part of the Radio & Plasma Wave Investigation (RPWI) aboard JUICE: Lunar-Earth flyby in Aug 2024 and beyond

#Yasumasa Kasaba[1)], Cecconi Baptiste[2)], Fuminori Tsuchiya[1)], Hiroaki Misawa[1)], Hajime Kita[3)], Rikuto Yasuda[1)], Yuto Katoh[1)], Atsushi Kumamoto[1)], Tomoki Kimura[4)], Yoshizumi Miyoshi[5)], Yoshiya Kasahara[6)], Shoya Matsuda[6)], Satoshi Yagitani[6)], Mitsunori Ozaki[6)], Hirotsugu Kojima[7)], Satoshi Kurita[7)], Wahlund J.-E.[8)]
([1]Tohoku University, [2]Obs de Paris, [3]Tohoku Institute of Technology, [4]Tokyo University of Science, [5]Nagoya University, [6]Kanazawa University, [7]Kyoto University, [8]IRF Uppsala

This talk provides initial results of Radio & Plasma Wave Investigation (RPWI) aboard JUpiter ICy moons Explorer (JUICE) in the Lunar and Earth flybys (Aug 2024) and beyond, in the view for its high frequency radio observation capability in 80k − 45MHz.

JUICE was launched in April 2023. Lunar flyby was the first and last chance to observe an airless body before the arrival of Jupiter in 2030s. Earth flyby was also the first chance to observe a planet with magnetospheric activities. Next flybys are Venus (August 2025), Earth I (September 2026), and Earth II (January 2029). Arrival to Jupiter will be in July 2031.

RPWI provides unique opportunities to investigate electromagnetic fields and plasma environment around Jupiter and icy moons, with passive and active soundings by 4 Langmuir probes (LP-PWI; 3-axis E-field -1.6 MHz by four 10 cm diameter probes on the 3-m booms) and a search coil magnetometer (SCM; 3-axis B-field -20 kHz) + a tri-dipole antenna system (RWI; 3-axis E-field 0.08-45 MHz, 2.5-m tip-to-tip length) on the long MAG-Boom with JMAG. All antennas were successfully deployed in May 2023, and RPWI already has full observational capabilities. RPWI with other instruments covers the survey of harsh environment around Jupiter, environments and interaction with icy moons, and their surface and subsurface characteristics.

In lower frequency, RPWI enables to investigate electric field and electromagnetic interactions governing Jupiter - moon systems, cold plasmas in the ionospheres of icy moons for investigations of surfaces and salty conductive sub-surface oceans, and cold micrometeorite impacts.

The high frequency part of this system, i.e., Preamp of RWI and its High Frequency Receiver (HF) is procured by the RPWI Japan team, with the colleagues in Austria, France, Poland, and Sweden. This part enables the characterization of Jovian radio emissions (including gonio-polarimetry), passive radio sounding of the ionospheric densities of icy moons, and passive sub-surface radar measurements. It has an enough capability to detect Jovian radio emissions from magnetosphere (aurora etc.), atmosphere (lightning), and icy moons. Direction and polarization capabilities are first enabled in the Jovian system, to identify their source locations and characteristics.

During the Lunar flyby (passed in equatorial duskside with the closest altitude of 750 km, in the morning of Japan on 20 Aug.), we did a test observation for the ionospheres, surfaces, and subsurfaces of icy moons. We did unique test observations of the ionospheres below the spacecraft orbit by the occultation and reflection of terrestrial auroral kilometric radiation (AKR) in several 100s kHz, as an emulation using Jovian auroral radiations in several 100s to 10s MHz. The occultation of planetary auroral radiation investigates moons' ionospheric density profiles. The reflection of planetary auroral radiation is for the characterizing of moons' surfaces and subsurfaces, to try the passive subsurface radar (PSSR) concept which sounds the moons' crusts by the reflected radio waves. Although it was with strong RIME radar emission at 9MHz, this talk will report the test result of this first and last emulation for icy moons' flybys.

During the Earth flyby (passed in equatorial dawnside with the closest altitude of 6,800 km, in the morning of Japan on 21 Aug.), we did a continuous monitor of AKR and plasmaspheric waves above 80 kHz, including the test detection of HAARP radar emission at ˜9MHz. This test is for (1) first real test for the identifications of polarized emissions using real AKR, solar bursts, and magnetospheric waves, (2) critical calibration of the sensitivity and direction of three short RWI antennas, which only has 1.25-m and strongly affected by the couping with the spacecraft. Those are the first realistic test which cannot be executed on the ground without the deployment. This talk will report those test results, including the comparison of electromagnetic waves observed by Arase PWE.

Those observations require the low electric noise environment from the spacecraft. Unfortunately, large line noises as a harmonics of 200 kHz and wide-band noise in 4-10 MHz are emitted from the spacecraft. Those potentially suffers the observational capability, so we implemented the mask to the former in Jan 2024. We also report its effect to reduce the artificial noise, and will summarize plans with the proved performances for Jupiter and icy moons in 2030s.

R009-07
B 会場 ：11/24　PM1 （13:15-15:15）
14:45〜15:00

望遠鏡観測を用いた天王星大気の輸送速度の推定

#天田 耕太郎 [1)], 高木 聖子 [1)], 高橋 幸弘 [1)], 佐藤 光輝 [1)], 濱本 昴 [1)]
(1 北大理学院

Estimation of Component Transportation Velocity in Uranus' Atmosphere

#Kotaro Amada[1)], Seiko Takagi[1)], Yukihiro Takahashi[1)], Mitsuteru SATO[1)], KO HAMAMOTO[1)]
([1]Faculty of Science, Hokkaido University

Uranus is a planet that orbits with its axis tilted 98 degrees relative to its orbital plane. As of June 2023, the only close-up observation was the flyby by Voyager 2 in 1986, and since then, observations have continued through telescopes. After passing through the vernal equinox in 2007, a polar cap caused by methane deposition has been observed in the northern polar region since 2014 [Toledo et al., 2018]. Additionally, observations in the H-band (1.6 μ m) have confirmed the presence of local cloud regions that are brighter than other areas [Sromovsky et al., 2015].

Tracking of cloud top patterns by the Hubble Space Telescope (HST) has estimated that the maximum speed of zonal winds is about 250 m/s around 60° north and south [Soyuer et al., 2021]. While this zonal wind speed suggests interactions with the Uranian magnetic field and the interplanetary magnetic field (IMF) in the deep atmosphere, the understanding of atmospheric transport over several days has stalled due to the machine time constraints of the observational equipment [Soyuer et al., 2022]. To better understand the transport patterns in the Uranian atmosphere, continuous observations on Earth for about several days to one month are needed.

In this study, we conducted continuous observations of Uranus using the MSI imaging system [Watanabe et al., 2012] and the UVS spectrograph mounted at the Cassegrain focus of the 1.6 m Pirka telescope owned by Hokkaido University. We estimated the atmospheric transport speed at various altitudes by analyzing the temporal variation in the absorption due to methane and ammonia, which are components of Uranus's atmosphere.

From September 2022 to February 2023, spectroscopic imaging was performed in the wavelength range of 530-760 nm using the MSI. The transport speed was estimated from the temporal variation in absorption at the ammonia absorption wavelength of 552 nm and the methane absorption wavelength of 619 nm, compared to Uranus's rotation period. The results suggested transport speeds similar to those reported by [Soyuer et al., 2021] for the methane absorption wavelength, but faster speeds were calculated for the ammonia absorption wavelength.

After July 2023, observations aimed to estimate the vertical and longitudinal movement speed of atmospheric components based on the movement speed of local clouds observed on Uranus. To achieve this, observations were conducted using both the MSI and UVS, with improved spatial and wavelength resolution compared to previous observations. During the analysis process, we simulated the brightness changes at each wavelength associated with the movement of the polar cap and local clouds in the polar region of Uranus using Matlab for the high-speed imaging observations by the MSI.

In this presentation, we will compare the results of observations with the MSI and UVS to simulations conducted with Matlab and present the estimated positions of local clouds from the observations between July 2023 and November 2024. Additionally, we will discuss the future view for observations by comparing the results with the zonal wind speeds derived from observations between September 2022 and March 2023.

天王星は公転面に対し地軸が 98 ° 傾いた状態で公転する惑星である。2023 年 6 月現在、過去の接近観測は 1986 年のボイジャー 2 号によるフライバイ観測のみであり、この他は望遠鏡により観測が続けられている。2007 年に春分点を通過し、2014 年からは北極域にメタン沈降に起因する極冠が観察されている [Toledo et al., 2018]。また、H-band(1.6 μ m) における観測では他の部分よりも明るい局所雲領域が確認されている [Sromovsky et al., 2015]。

ハッブル望遠鏡 (HST) による雲頂模様のトラッキングから帯状風の最高速度は南北 60 ° 付近でそれぞれ約 250 m/s と推定されている [Soyuer et al., 2021]。この帯状風速度は、深部において天王星磁場および惑星間磁場 (IMF) との相互作用が示唆されているが、観測装置のマシンタイム制約により大気における数日スケールでの大気輸送について、理解が停滞している状況である [Soyuer et al., 2022]。天王星大気の輸送形態をより詳細に理解するため、地球における数日-1 ヶ月程度の継続観測が必要である。

本研究では、北海道大学が所有する 1.6 m ピリカ望遠鏡のカセグレン焦点に搭載された撮像装置 MSI[Watanabe et al., 2012] 及び分光装置 UVS を用いて天王星の継続観測を行い、天王星大気成分であるメタンとアンモニアによる吸収量の時間変動を用いて各高度における大気輸送速度の推定を行う。

2022 年 9 月から 2023 年 2 月の観測では、MSI で波長域 530 - 760 nm の波長域での分光撮像を行い、アンモニア吸収波長 552 nm とメタン吸収波長 619 nm における吸収量の時間変動と天王星の周期より輸送速度を推定した。この結果、メタン吸収波長では [Soyuer et al., 2021] と同程度の速度が推定されたが、アンモニア吸収波長においては速い速度が算出された。

2023 年 7 月以降の観測では、天王星に見られる局所雲の移動速度から大気成分の鉛直・経度方向における移動速度を推定することを目的とした。このため、MSI に加えて UVS を用い、従来よりも空間分解能・波長分解能を上げた観測を行った。解析過程では、MSI の高速撮像観測について、天王星極域の極冠・局所雲の移動に伴う各波長の輝度変化を Matlab を使用しシミュレートした。

本発表では、MSI および UVS の観測結果と Matlab によるシミュレーションを比較することにより、2023 年 7 月から 2024 年 11 月の観測結果における局所雲位置の推定の結果を提示する。また、2022 年 9 月から 2023 年 3 月の観測結果より導出された帯状風速度との比較を行った上で、今後の観測展望について議論を行う。

R009-08
B 会場 ：11/24　PM1 （13:15-15:15）
15:00〜15:15

LAPYUTA 計画の検討状況

#土屋 史紀 [1)], 村上 豪 [2)], 山崎 敦 [2)], 亀田 真吾 [3)], 鍵谷 将人 [1)], 吉岡 和夫 [4)], 古賀 亮一 [5)], 木村 淳 [6)], 木村 智樹 [7)], 垰 千尋 [8)], 益永 圭 [9)], 堺 正太朗 [1)], 中山 陽史 [3)], 生駒 大洋 [10)], 成田 憲保 [4)], 大内 正己 [4,10)], 田中 雅臣 [1)], 桑原 正輝 [3)], 鳥海 森 [2)], 野津 湧太 [11)], 行方 宏介 [12)]
([1] 東北大, [2] 宇宙科学研究所, [3] 立教大, [4] 東大, [5] 名市大, [6] 阪大, [7] 東京理科大, [8] 情報通信研究機構, [9] 山形大, [10] 国立天文台, [11] コロラド大学, [12] 京都大学, [13] 京都大学

Current status of LAPYUTA mission

#Fuminori Tsuchiya[1)], Go Murakami[2)], Atsushi Yamazaki[2)], Shingo Kameda[3)], Masato Kagitani[1)], Kazuo Yoshioka[4)], Koga Ryoichi[5)], Jun Kimura[6)], Tomoki Kimura[7)], Chihiro Tao[8)], Kei Masunaga[9)], Shotaro Sakai[1)], Akifumi Nakayama[3)], Masahiro Ikoma[10)], Norio Narita[4)], Masami Ouchi[4,10)], Masaomi Tanaka[1)], Masaki Kuwabara[3)], Shin Toriumi[2)], Yuta Notsu[11)], Kosuke Namekata[12)]
([1]Tohoku Univ., [2]ISAS/JAXA, [3]Rikkyo Univ., [4]The Univ. of Tokyo, [5]Nagoya City Univ., [6]Osaka Univ., [7]Tokyo Univ. Science, [8]NICT, [9]Yamagata Univ., [10]NAOJ, [11]Colorado Univ., [12]Kyoto Univ., [13]Kyoto Univ.

The LAPYUTA mission is an ultraviolet space telescope scheduled for launch in the early 2030s, as an ISAS M-class mission. We accomplish the following four objectives related to two scientific goals: understanding the ”habitable environment” and the ”origin of structure and matter” in the universe. The first objective focuses on the subsurface ocean environment of Jupiter’s icy moons and the atmospheric evolution of terrestrial planets. In the second objective, we characterize the atmospheres of exoplanets in the habitable zone by detecting their exospheric atmospheres and estimating the surface environments of the planets. In cosmology and astronomy, we will test whether the structures of present-day galaxies contain ubiquitous Ly α halos, reveal the physical origins of Ly α halos (Objective 3), and elucidate the heavy element synthesis process from observations of ultraviolet radiation from hot gas immediately after neutron star mergers (Objective 4).

The mission payload consists of a telescope with a 60 cm diameter primary mirror and focal plane instruments. The focal plane instruments consist of an ultraviolet spectrograph (medium-resolution spectrograph: MRS and high-resolution spectrograph: HRS), an ultraviolet slit imager (UVSI), and a fine-guide sensor (FGS). The MRS has a 100 arcsec field of view, wavelength range of 110-190 nm, and a spectral resolution of 0.02 nm, and a spatial resolution of 0.1 arcsec for slitless spectroscopy. The HRS has a field of view of ˜10 arcsec and a spatial resolution of 0.6 arcsec, but by using an echelle grating as a dispersive element, it has a wavelength resolution of 3 pm, enabling to resolve the absorption line profiles of the exoplanet atmosphere and to measure D/H in the atmospheres of Venus and Mars. The UVSI has a 180 arcsec field of view and 0.2 arcsec spatial resolution, enabling to resolve the spatial structure of Jupiter’s ultraviolet aurora. Multi-band observations with the filter turret will enable us to derive the characteristic energy of auroral electrons. LAPYUTA’s orbit is designed as an elliptical orbit with an apogee of 2,000 km and a perigee of 10,00 km to avoid the influence of the geocorona when observing oxygen and hydrogen atoms and the Earth’s radiation belt.

LAPYUTA 計画は、2030 年代初頭に ISAS 公募型小型計画での実現を目指す紫外線宇宙望遠鏡計画である。2024 年 8 月にプリプロジェクト候補移行審査を受け、2026 年に予定されているダウンセレクションに向け、科学検討と技術検討を進めている。

宇宙での「生命生存可能環境」と「構造と物質の起源」の理解を目指し、4 つの科学課題の達成を目的としている。課題 1 では、宇宙で最も詳細な観測が可能な太陽系内天体のうち、氷衛星とイオを含む木星系の物質輸送と地球型惑星の大気進化に焦点を当て、太陽や磁気圏からのエネルギー流入により変化する惑星・衛星大気の観測を通して、惑星大気・衛星表層の進化の知見を獲得する。課題 2 ではハビタブルゾーン内にある系外惑星を対象に外圏大気の広がり検出することによって大気の特徴づけを行い、惑星表層環境の推定を目指す。宇宙論・天文学では、銀河周辺物質の構造の観測を通して宇宙構造形成の枠組みで予言されたガスの流入による星形成を検証し (課題 3)、中性子星合体直後の高温ガスの紫外線放射の観測から重元素合成過程の解明 (課題 4) を目標とする。

ミッション部は口径 60cm の主鏡をもつ望遠鏡部と焦点面装置からなり、焦点面装置は、紫外分光器（中分散分光器 (MRS) と高分散分光器 (HRS))、紫外スリットイメージャ (UVSI)、ファインガイドセンサ (FGS) で構成される。MRS は視野 100 秒角、波長範囲 110-190nm、波長分解能 0.02nm で、スリットレス分光の場合は 0.1 秒角の高空間分解能を設計目標値としており、木星系の衛星大気の空間構造や惑星超高層大気の高度分布を分解できる。HRS は視野˜10 秒角、空間分解能 0.6 秒角ながら、分散素子にエシェル回折格子を用いることによって 3pm の波長分解能を持つ。系外惑星大気の吸収線プロファイルを分解し、金星・火星大気の D/H 観測が可能となる。UVSI は 180 秒角の視野と 0.2 秒角の空間分解能を持ち、木星紫外オーロラの空間構造を分解すると同時に、フィルターターレットによる多波長観測によって、オーロラの空間構造と電子の特性エネルギーの導出が可能になる。軌道は、酸素原子や水素原子の観測におけるジオコロナの影響を回避するため、遠地点 2,000km、近地点 1,000km を予定している。

R009-09
B 会場 ：11/24　PM2 （15:30-18:15）
15:30〜15:45

#関 華奈子 [1)], 原 拓也 [2)], 坂田 遼弥 [3)], 松本 洋介 [4)], Brain David[5)], 寺田 直樹 [3)], McFadden James P.[2)], Halekas Jasper S.[6)], DiBraccio Gina A.[7)], Curry Shannon[5)]
[(1] 東大理・地球惑星科学専攻, [(2]SSL, University of California, Berkeley, [(3] 東北大学理学研究科, [(4] 千葉大学, [(5]LASP, University of Colorado, Boulder, [(6]Department of Physics and Astronomy, University of Iowa, [(7]NASA Goddard Space Flight Center

Kelvin-Helmholtz instability at Mars: Properties of plasma boundaries with a large density gradient

#Kanako Seki[1)], Takuya Hara[2)], Ryoya Sakata[3)], Yosuke Matsumoto[4)], David A. Brain[5)], Naoki Terada[3)], James P. McFadden[2)], Jasper S. Halekas[6)], Gina A. DiBraccio[7)], Shannon Curry[5)]
[(1]Department of Earth and Planetary Science, Graduate School of Science, University of Tokyo, [(2]SSL, University of California, Berkeley, [(3]Graduate School of Science, Tohoku University., [(4]Institute for Advanced Academic Research, Chiba University, [(5]LASP, University of Colorado, Boulder, [(6]Department of Physics and Astronomy, University of Iowa, [(7]NASA Goddard Space Flight Center

Momentum and mass transport mechanisms at a velocity-sheared boundary between the shocked solar wind and the ionosphere are important processes that affect the ion escape from Mars. Kelvin − Helmholtz instability (KHI) is a promising mechanism to facilitate transport. Although previous studies have suggested KHI occurrence both around the ionopause (e.g., Gurnett et al., 2010) and magnetic pileup boundary (e.g., Poh et al., 2021), theory predicts that compressibility prevents KHI excitation at boundaries with large density gradients because of previously considered boundary structures where density varies with velocity. Based on the observations of a large density gradient boundary by MAVEN at Mars, where we can observe an extreme case, we show that it is the entropy that varies with the velocity in the real velocity-sheared boundary. The entropy-based boundary structure places the velocity shear in a lower-density region than the traditional density-based structure and weakens the compressibility effect (Seki et al., 2024). This new boundary structure thus enables KHI excitation even at large density gradient boundaries around the ionopause of unmagnetized planets. The result suggests the ubiquitous occurrence of KHI in the plasma universe and emphasizes its important role in planetary cold plasma escape from unmagnetized planets. In the presentation, role of KHI in the ion escape and its dependence of the density ratio across the boundary will be also discussed.

References:
Gurnett et al., Icarus, 206, 83-94, https://doi.org/10.1016/j.icarus.2009.02.019, 2010.
Poh et al., J. Geophys. Res., 126, https://doi.org/10.1029/2021JA029224, 2019.
Seki et al., Front. Astron. Space Sci., 11, https://doi.org/10.3389/fspas.2024.1394817, 2024.

R009-10
B 会場 ：11/24　PM2 （15:30-18:15）
15:45〜16:00

#堺 正太朗 [1,2)], 中川 広務 [1)], Deighan Justin[3)], Jain Sonal[3)], 益永 圭 [4)], 土屋 史紀 [2)], 寺田 直樹 [1)], Mayyasi Majd[5)], Schneider Nicholas[3)], Mitchell David[6)], Mazelle Christian[7)], Benna Mehdi[8,9)], Lillis Robert[6)], 村上 豪 [10)], Curry Shannon[3)], 関 華奈子 [11)]
([1 東北大・理・地球物理, [2 東北大・理・惑星プラズマ大気, [3LASP, Univ. Colorado Boulder, [4 山形大・学士課程基盤教育機構, [5CSP, Boston Univ., [6SSL, Univ. California, Berkeley, [7IRAP, CNRS, Univ. Toulouse, UPS-OMP, CNES, [8CSST, Univ. Maryland, Baltimore County, [9SSED, NASA GSFC, [10JAXA 宇宙科学研究所, [11 東大・理・地球惑星

C^+ emission mechanisms on Mars revealed by MAVEN: Implications for response to thermospheric and ionospheric variations

#Shotaro Sakai[1,2)], Hiromu Nakagawa[1)], Justin Deighan[3)], Sonal K. Jain[3)], Kei Masunaga[4)], Fuminori Tsuchiya[2)], Naoki Terada[1)], Majd Mayyasi[5)], Nicholas M. Schneider[3)], David L. Mitchell[6)], Christian Mazelle[7)], Mehdi Benna[8,9)], Robert J. Lillis[6)], Go Murakami[10)], Shannon M. Curry[3)], Kanako Seki[11)]
([1Dept. Geophysics, Grad. Sch. Sci., Tohoku Univ., [2PPARC, Grad. Sch. Sci., Tohoku Univ., [3LASP, Univ. Colorado Boulder, [4IAS, Yamagata Univ., [5CSP, Boston Univ., [6SSL, Univ. California, Berkeley, [7IRAP, CNRS, Univ. Toulouse, UPS-OMP, CNES, [8CSST, Univ. Maryland, Baltimore County, [9SSED, NASA GSFC, [10JAXA / ISAS, [11Dept. Earth and Planetary Science, Grad. Sch. Sci., Univ. Tokyo

C^+ emission is generated by electron impact, dissociative ionization, photoionization, and resonant scattering with carbon-related atoms, molecules, and ions in the Martian ionosphere and thermosphere. The contribution of each mechanism to emission, however, has not been revealed due to the difficulty of observation and the fact that a part of the emission cross section is uncertain. This paper isolates the C^+ emission mechanism using remote-sensing and in-situ observations onboard MAVEN (Mars Atmosphere and Volatile EvolutioN). Observational data from the Imaging Ultraviolet Spectrograph instrument are analyzed to obtain C^+ emission from the remote-sensing method and compared to C^+ emission obtained from in-situ observations of Solar Wind Electron Analyzed and Neutral Gas and Ion Mass Spectrometer. Both electron impact and dissociative ionization/photoionization contribute to C^+ emission below 150 km altitude when the CO density is high, but only dissociative ionization/photoionization contributes to the emission for the low CO density case, while only dissociative ionization/photoionization dominates the emission at altitudes between 150 km and 165 km for both CO density cases. It is difficult to estimate the total flux of suprathermal electrons in the ionosphere from remote-sensing observations of C^+ emission because the contribution of electron impact to C^+ emission is small. In contrast, C-atom remote-sensing observations might provide a better understanding of the total flux of suprathermal electrons in the ionosphere than C^+ emission, and global ultraviolet observations could be utilized as a tool for monitoring the ionosphere. The total flux of suprathermal electrons estimated from C-atom emission may be utilized to isolate the contribution of each C^+ emission process to the brightness more accurately. This suggests that the C^+ and C-atom emissions might be tracers of spatiotemporal variations in the Martian ionosphere and thermosphere.

R009-11
B 会場 ：11/24　PM2 （15:30-18:15）
16:00〜16:15

#沖山 太心 [1)], 関 華奈子 [1)], 中村 勇貴 [1)], Lillis Robert J.[2)], Rahmati Ali[2)], Larson Davin E.[2)], DiBraccio Gina A.[3)], Schneider Nicholas M.[4)], Jain Sonal K.[4)], Curry Shannon[4)]
[(1] 東京大学, [(2] カリフォルニア大学バークレー校, [(3]NASA ゴダード宇宙飛行センター, [(4] コロラド大学ボルダー校

Effects of magnetic field structure on the Martian diffuse aurora

#Taishin Okiyama[1)], Kanako Seki[1)], Yuki Nakamura[1)], Robert J. Lillis[2)], Ali Rahmati[2)], Davin E. Larson[2)], Gina A. DiBraccio[3)], Nicholas M. Schneider[4)], Sonal K. Jain[4)], Shannon Curry[4)]
[(1]The University of Tokyo, Tokyo, Japan, [(2]The University of California, Berkeley, USA, [(3]NASA Goddard Space Flight Center, Greenbelt, USA, [(4]The University of Colorado at Boulder, Boulder, USA

Mars does not have intrinsic magnetic field except parts of southern hemisphere, where crustal magnetic fields exist. In such an environment, solar wind magnetic fields drape around Mars and form induced magnetosphere, which is variable due to the variation of solar wind conditions. The nightside structures of the draped magnetic fields during extreme solar events are especially not well understood, despite the importance of these periods for understanding the ion loss from Mars. In some of extreme solar events, global auroras, called diffuse aurora, are observed. The Martian diffuse aurora are global ultraviolet emissions including CO_2^+ ultraviolet doublet (UVD) on the nightside, caused by solar energetic particles (SEPs) consisting of electrons and protons (Schneider et al., 2015; Schneider et al., 2018; Nakamura et al., 2022). The auroral emissions caused by the electrons can vary with nightside magnetic fields around Mars, while those by protons are less affected by the magnetic fields due to the larger Larmor radii than electrons. However, the effect of nightside magnetic fields on the electron-induced Martian diffuse auroras are far from understood. Our previous study indicates that the auroral emission at altitudes of 80-100 km caused by SEP electrons can systematically change with the dip angle of the magnetic fields. Since the diffuse auroral observations can be useful to infer the nightside induced magnetic field structures during extreme solar events, it is important to understand effects of the magnetic fields on diffuse auroral emission profiles.

In order to understand the effects, we investigated the relationship between Martian diffuse auroral emissions, SEP flux, and magnetic fields based on MAVEN observations. Basically, increase of precipitating SEP flux leads to increase of the auroral intensity. Therefore, we investigated the non-correspondence of time variations of auroral intensity to those of SEP proton and electron fluxes in the solar wind or magnetosheath regions, which may include the effects of magnetic fields. As diffuse auroral events, we use December 2014 and September 2017 events in this study. Results show that the time variations of the auroral intensity at low altitudes (50-70 km) corresponded to the time variations of the upstream SEP proton flux as expected. On one hand, the high-altitude (90-110 km) auroral emissions, which are mainly caused by SEP electrons, were sometimes enhanced even during the decreasing periods of upstream SEP electron flux. In order to understand the cause of this non-correspondence, we investigated those time intervals in detail with a focus on the effects of the draped magnetic field structure, crustal magnetic fields, and observational geometry on auroral emissions. Based on the results, possible effects of the magnetic fields on diffuse aurora will be discussed.

R009-12
B 会場 ：11/24　PM2 （15:30-18:15）
16:15〜16:30

火星夜側電離圏の上流太陽風・IMF 条件及び地殻磁場に対する全球的な依存性の統計的研究

#竹内 直之 [1)], 原田 裕己 [1)], Sánchez-Cano Beatriz[2)]
([1] 京大・理, [2] レスター大学

Statistical study of how the Martian nightside ionosphere globally depends on the solar wind, IMF direction, and crustal magnetism

#Naoyuki Takeuchi[1)], Yuki Harada[1)], Beatriz Sánchez-Cano[2)]
([1]Graduate School of Science, Kyoto University, [2]University of Leicester

On the night side of Mars, a more tenuous and variable ionosphere exists compared to the day side (e.g., Zang et al., 1990; Němec et al., 2010; Girazian et al., 2017), which is primarily generated by day-to-night plasma transport and electron impact ionization (Fox et al., 1993). Previous studies have shown that these processes are either suppressed or enhanced by the upstream solar wind and interplanetary magnetic field (IMF) conditions, and crustal magnetic fields mainly distributed in the southern hemisphere of Mars (Acuna et al., 1999). Dieval et al. (2014) conducted a statistical study of the dependences of the Martian nightside ionosphere on these upstream and local conditions. However, their data set is limited to approximately seven months during the simultaneous observation period of the Mars Express (MEX) and Mars Global Surveyor (MGS) spacecraft under specific conditions. Additionally, the upstream solar wind and IMF conditions were determined based on proxies inferred from the MGS observations at 400 km altitude, presenting challenges in terms of temporal and spatial coverage, as well as the accuracy of the solar wind and IMF conditions.

To address these challenges, this study re-investigated the upstream solar wind and IMF dependences of the Martian nightside ionosphere statistically, using a much larger data set from MEX and Mars Atmosphere and Volatile EvolutioN (MAVEN) spacecraft from October 2014 to October 2022. We process the data from the radar sounder observations of the nightside ionosphere at solar zenith angles $>110^\circ$ conducted by MARSIS onboard MEX and organize the nightside ionospheric peak density according to MAVEN in-situ observations of the upstream solar wind. This enables a global statistical analysis of the nightside ionosphere over a much extended period compared to previous studies, revealing new aspects of the nightside ionosphere of Mars. For example, Dieval et al. (2014) reported very high-density ionospheres primarily under westward IMF conditions, but we identify that this trend is specific to certain regions, including some strong crustal magnetic field regions. With the wider and denser geographic coverage, we find that high-density ionospheres are detected under eastward IMF conditions in the northern hemisphere and different strong crustal magnetic field regions that were poorly sampled in the previous study. Therefore, it is suggested that both westward and eastward IMF conditions globally influence the generation of high-density nightside ionospheres. We will present the global dependence of the Martian nightside ionosphere on external factors such as upstream solar wind and IMF conditions, crustal magnetic fields, and solar activity levels along with the relationship with Martian discrete aurorae.

火星の夜側には昼側と比較してより希薄で変動に富む電離圏が存在しており（e.g. Zang et al., 1990; Němec et al., 2010; Girazian et al., 2017）、主にプラズマの昼夜間輸送や電子衝突電離がその発生機構として考えられている（Fox et al., 1993）。夜側電離圏の生成・輸送機構は上流太陽風・IMF 及び主に火星の南半球に局在する地殻磁場（Acuna et al., 1999）の影響により抑制・促進されることが先行研究で示されており、夜側電離圏密度の統計的な調査が Dieval et al. (2014) において行われた。しかしながら、その対象期間は探査機 Mars Express (MEX) と Mars Global Surveyor (MGS) の同時観測期間において特定の条件を満たす約 7 ヶ月間と短期間であり、また、上流太陽風・IMF 条件は MGS の 400 km 高度での観測に基づく代替データで決定されているため、時間的・空間的な網羅性と太陽風・IMF 条件の精度に課題がある。

本研究ではこれらの課題を踏まえ、探査機 MEX と Mars Atmosphere and Volatile EvolutioN (MAVEN) の同時観測期間のうち 2014 年 10 月から 2022 年 10 月を対象に、MEX に搭載のレーダーサウンダー MARSIS が 110° 以上の太陽天頂角で夜側電離圏を遠隔計測し、MAVEN が上流太陽風をその場観測しているようなデータを用い、火星夜側電離圏最大電子密度の上流太陽風・IMF 条件を統計的に再調査した。先行研究と比較して長期間かつ全球的な夜側電離圏の観測データを蓄積し、大規模な統計解析を行うことが可能となった。例えば、Dieval et al. (2014) では高密度の電離圏が西向き IMF 条件下で多く観測されていたが、これは一部の強地殻磁場領域をはじめとする地域に見られる傾向であり、東向き IMF 条件下においても北半球やその他の強地殻磁場領域で高密度の電離圏が検出されることが明らかとなった。したがって、IMF の向きが高密度の夜側電離圏の発生に全球的に影響を及ぼすことが示唆されている。本発表では上流太陽風・IMF 条件、及び地殻磁場や太陽活動度などの外的要因に対する火星夜側電離圏の全球的な依存性を検証するとともに、近年研究が進んでいる火星ディスクリートオーロラとの関連も調査し議論する予定である。

R009-13
B 会場 ：11/24　PM2 （15:30-18:15）
16:30〜16:45

MAVEN 及び Mars Express の観測に基づく太陽活動イベント時における火星のイオン散逸に関する統計的研究

#亀井 りま [1)], 関 華奈子 [1)], 桂華 邦裕 [1)], Ramstad R.[2)], Brian D. A.[2)], Hara T.[3)], McFadden J. P.[3)], Hanley K. G.[3)], Fowler C.[4)], Halekas J. S.[5)], DiBraccio G. A.[6)], Curry S. M.[2)]
([1] 東大理・地球惑星科学専攻, [2] コロラド大学ボルダー校 大気宇宙物理学研究所, [3] カリフォルニア大学バークレー校 宇宙科学研究所, [4] ウェストバージニア大学物理学・天文学部, [5] アイオワ大学物理学・天文学部, [6]NASA ゴダード宇宙飛行センター

Statistical study of ion escape from Mars during ICME and CIR events based on MAVEN and Mars Express observations

#R. Kamei[1)], K. Seki[1)], K. Keika[1)], R. Ramstad[2)], D. A. Brian[2)], T. Hara[3)], J. P. McFadden[3)], K. G. Hanley[3)], C. Fowler[4)], J. S. Halekas[5)], G. A. DiBraccio[6)], S. M. Curry[2)]
([1]Department of Earth and Planetary Science, Graduate School of Science, The University of Tokyo, [2]Laboratory for Atmospheric and Space Physics, University of Colorado, Boulder, CO, USA, [3]Space Sciences Laboratory, University of California, Berkeley, CA, USA, [4]Department of Physics and Astronomy, West Virginia University, Morgantown, WV, USA, [5]Department of Physics and Astronomy, University of Iowa, Iowa City, Iowa, USA, [6]NASA Goddard Space Flight Center, Greenbelt, MD, USA

It is important to clarify responses of each atmospheric escape mechanism to solar activities for understanding of the planetary atmospheric evolution. This is especially significant for Mars, which lacks an intrinsic magnetic field, allowing direct interaction between the solar wind and its atmosphere. While various mechanisms can contribute to the atmospheric escape, we here focus on the ion escape driven by solar activity events, such as Interplanetary Coronal Mass Ejections (ICMEs) and Corotating Interaction Regions (CIRs). ICMEs occur when large amounts of plasma are ejected into interplanetary space following solar flares, while CIRs are formed when fast solar wind overtakes slower one, creating interaction regions, Both ICMEs and CIRs often facilitate high solar wind dynamic pressure condition and disturb the Martian induces magnetosphere and influence atmospheric escape. MAVEN observations and their comparison with global MHD simulation results show that atmospheric escape rates increased significantly during an ICME event in March 2015 [1]. On the other hand, Ramstad and Barabash (2021) pointed out that the ion escape rate from Mars does not have clear dependence on the solar wind dynamic pressure based on statistical analysis [2]. These contradictory observations indicate the need for careful investigation of effects of ICMEs and CIRs on the ion loss from Mars. Observationally there are two major escape channels for ions from Mars: polar plumes accelerated by the convective electric field of the solar wind and the tailward escape, a bulk ion outflow through Martian magnetotail [2]. Statistical studies of the polar plumes [3] and tailward escape [4] both indicate that the spatial distributions of the ion escape flux are highly localized in terms of the MSE coordinates determined by the direction of the solar wind electric field. In this study, we aim to evaluate the impact of solar wind on the ion escape from Mars during ICMEs and CIRs by carefully investigating the localization effects of the both ion escape channels.

Utilizing simultaneous observations by Mars Express and MAVEN from 2015 to 2019, we identified ICMES and CIRS. First, the data satisfying the following criteria were selected: (1) the maximum daily solar wind density exceeded 15 cm^{-3}, and (2) the difference in velocity over two days was greater than 100 km/s. Among the selected data, events where density and velocity increased simultaneously were classified as CMEs, while those where velocity increased following a density rise were classified as CIRs. We also used the ENLIL simulation model to identify events where both CIR and CME occurred simultaneously. As a result, we found 7 CMEs, 120 CIRs, and 8 events where both CIR and CME arrived simultaneously over the five-year period. We used the Supra-Thermal And Thermal Ion Composition (STAIC) onboard MAVEN to investigate spatial distributions of escaping ions. Distributions of O^+ and $O_2{}^+$ fluxes are separately examined both in the Mars-Solar-Orbital (MSO) coordinates and the Mars-Solar-Electric field (MSE) coordinates to differentiate the effects of the crustal magnetic field and acceleration by solar wind electric field. Based on the statistical results focusing only during the solar event intervals (ICME and CIRs), effects of ICMEs and CIRs on the ion loss from Mars are discussed.

References
[1] Jakosky et al. (2015), Science, 350, aad0210, doi:10.1126/science.aad0210.
[2] Ramstad and Barabash (2021), Space Sci. Rev., 217, 36, doi:10.1007/s11214-021-00791-1.
[3] Dong et al. (2015), Geophys. Res. Lett., 42, 8942 – 8950, doi:10.1002/2015GL065346.
[4] Inui et al. (2019), J. Geophys. Res., 124, 5482 – 5497, doi:10.1029/ 2018JA026452.
[5] Sakakura et al. (2022), J. Geophys. Res., 127, e2021JA029750, doi:10.1029/2021JA029750.

R009-14
B 会場 ：11/24　PM2 （15:30-18:15）
17:00〜17:15

火星 GCM でシミュレーションされた水循環におけるレゴリス－大気間の相互作用の役割

#古林 未来 [1,2], 黒田 剛史 [1,3], Forget François[2], 鎌田 有紘 [1], 黒川 宏之 [4,5], 青木 翔平 [6], 中川 広務 [1], 寺田 直樹 [1]
([1] 東北大学大学院理学研究科地球物理学専攻, [2] ソルボンヌ大学 LMD/IPSL, [3] 東北大学高等研究機構, [4] 東京大学大学院総合文化研究科, [5] 東京大学大学院理学系研究科地球惑星科学専攻, [6] 東京大学大学院新領域創成科学研究科

Role of the regolith-atmosphere interaction on the water cycle simulated with a Mars GCM

#Mirai Kobayashi[1,2], Takeshi Kuroda[1,3], François Forget[2], Arihiro Kamada[1], Hiroyuki Kurokawa[4,5], Shohei Aoki[6], Hiromu Nakagawa[1], Naoki Terada[1]
([1]Department of Geophysics, Graduate School of Science, Tohoku University, [2]LMD/IPSL, Sorbonne Université, [3]Organization for Advanced Studies, Tohoku University, [4]Graduate School of Arts and Sciences, The University of Tokyo, [5]Department of Earth and Planetary Science, Graduate School of Science, The University of Tokyo, [6]Graduate School of Frontier Sciences, The University of Tokyo

The Martian regolith exchanges water vapor with the atmosphere via adsorption (Fanale & Cannon, 1971; Zent et al., 1993). Diurnal variations in adsorption and desorption correspond to changes in ground temperature, and water vapor is thought to be trapped on regolith grains at night and released into the atmosphere during the day (Savijärvi et al., 2020, 2021). According to one-dimensional models that account for water vapor exchange between the regolith and the atmosphere (the regolith-atmosphere interaction), the diurnal variations in relative humidity near the surface observed by the Curiosity rover and Phoenix lander are well reproduced when this interaction is considered (Savijärvi et al., 2016, 2019, 2020). However, the impact of this interaction on the seasonal water cycle has not been well explored. Previous global climate modeling studies have shown that the regolith-atmosphere interaction is significantly influenced by the initial subsurface water amount, which in turn affects the atmospheric water vapor amount (Houben et al., 1997; Richardson & Wilson, 2002; Tokano, 2003; Böttger et al., 2005). In other words, relatively dry regolith at the start of the calculation ultimately dries out the atmosphere, while wet regolith makes the atmosphere too wet, making it impossible to quantitatively discuss the role of the regolith-atmosphere interaction on the seasonal water cycle on Mars. In this context, we investigate the effects of the regolith-atmosphere interaction on the Martian water cycle with a quasi-steady state of adsorbed water mass as an initial condition, which is obtained by long-term calculations. This makes the calculated water cycle comparable to the observations and the effects of the regolith-atmosphere interaction can be quantitatively evaluated. In this study, we use a Mars Global Climate Model (MGCM) coupled with a regolith model. Our MGCM traces the Martian seasonal water cycle, including seasonal caps, frost formation, turbulent fluxes in the atmospheric boundary layer, and simple cloud microphysics that have been considered in previous MGCMs (Kuroda et al., 2005, 2013; Montmessin et al., 2004). We have developed a regolith model that includes the water vapor exchange between the regolith and the atmosphere, water diffusion, adsorption, and condensation in the regolith. Our regolith model has been developed based on several previous models (Böttger et al., 2005; Steele et al., 2017; Kamada et al., 2024) and uses an adsorption coefficient as a free parameter. In this study, in order to obtain the quasi-steady state of the adsorbed water mass in the regolith, we perform “spin-up” calculations for several decades with the regolith-atmosphere interaction turned off in advance. In this case, the total atmospheric water vapor amount is conserved, while the total subsurface water amount can be changed. The regolith-atmosphere interaction is then turned on (active regolith simulation) to compute the Martian water cycle. Conventional water cycle, except for the regolith model, is also calculated (inactive regolith simulation). Our results show that the active regolith simulation results in 5 pr-μm wetter mid- and low-latitude atmosphere during the northern fall and winter (Ls=210° − 320°) compared to the inactive regolith simulation when the atmospheric water vapor masses over the polar cap in the northern summer are similar (100 pr-μm) in both cases. The seasonal variations in water vapor flux exchanged between the regolith and the atmosphere show a water supply from the regolith at mid-latitudes in the northern hemisphere in Ls=180° − 240° . This suggests that the mid- and low-latitude regolith releases water vapor into the atmosphere during the fall and winter in the northern hemisphere. Thus, while the regolith-atmosphere interaction does not have drastic effects as previously suggested (Tokano, 2003; Böttger et al., 2005), it moistens mid- and low-latitudes, indicating that the regolith is a seasonal water source.

火星表層を構成するレゴリスは、吸着を介し、大気との間で水蒸気を交換している (Fanale & Cannon, 1971; Zent et al., 1993)。吸着・脱着の日変動は地温の変化に対応しており、水蒸気は夜間にレゴリス粒子表面に捕捉され、日中に大気中へ放出されると考えられている (Savijärvi et al., 2020, 2021)。火星のレゴリス－大気間の水蒸気交換を考慮した一次元モデルによれば、キュリオシティ・ローバーやフェニックス・ランダーによって観測された地表面付近 (~1.5 m) の相対湿度の日内変動は、レゴリス－大気間の水蒸気交換を考慮する場合にとても良く再現される (Savijärvi et al., 2016, 2019, 2020)。しかし、この相互作用が火星の季節的な水循環に与える影響は十分に検討されているとは言えない。これまでの全球気候モデルによる研究では、レゴリス－大気間の水蒸気交換は計算開始時の地下水量が大気中の水蒸気総量に

大きく影響を与えることが示されている。つまり、初期条件の時点で比較的乾燥したレゴリスは最終的に大気を乾燥させ、湿ったレゴリスは大気を湿潤にしすぎてしまうという問題があり、観測された大気中の水蒸気量を再現しながらレゴリスー大気間の水蒸気交換の役割を定量的に議論することができなかった (Houben et al., 1997; Richardson & Wilson, 2002; Böttger et al., 2005)。これを踏まえ、本研究ではレゴリス中の吸着水量の準定常状態を予め計算することにより、大気中の水蒸気量を再現しながらレゴリスー大気間の水蒸気交換が火星の水循環に与える影響を調べる。本研究では、レゴリスモデルと結合された火星全球気候モデル (MGCM) を用いる。我々の MGCM は、これまでの MGCM で考慮されてきた、季節的なキャップや地表面における霜の形成、大気境界層における乱流フラックスおよび単純な雲微物理を含み、火星の季節的な水循環をトレースする (Kuroda et al., 2005, 2013; Montmessin et al., 2004)。そこに新たにレゴリスー大気間の水蒸気交換、水蒸気拡散、吸着および凝結を含むレゴリスモデルを開発した。我々のレゴリスモデルは、いくつかの過去のモデルに基づいて開発され (Böttger et al., 2005; Steele et al., 2017; Kamada et al., 2024)、吸着係数をフリーパラメータとしている。また、レゴリスー大気間の水蒸気交換のオン・オフを切り替えることができる。本研究では、レゴリス中の吸着水量の準定常状態を求めるために、事前にレゴリスー大気間の水蒸気交換をオフにして数十年間の「スピンアップ」計算を行う。このとき、大気中の水蒸気総量は保存し、地下水の総量は変化する。その後、レゴリスー大気間の水蒸気交換をオンにして（アクティブ・レゴリス・シミュレーション）、火星の水循環を計算する。また、レゴリスモデルを除いた従来の水循環過程も同様に計算を行った（インアクティブ・レゴリス・シミュレーション）。その結果、アクティブ・レゴリス・シミュレーションでは、北半球の秋から冬にかけて (Ls=210° – 320°)、中・低緯度の大気を湿潤にすることがわかった。従来の水循環過程では、北半球の夏における極冠上空の水蒸気量が少ないとき、中・低緯度の供給される水蒸気も同時に減少していた。しかし、アクティブ・レゴリス・シミュレーションでは、北半球の夏における極冠上空の水蒸気量がインアクティブ・レゴリス・シミュレーションと同程度 (100 pr-μ m) であっても湿潤な中・低緯度 (25 – 30 μ m) を実現でき、中・低緯度はインアクティブ・レゴリス・シミュレーションと比較して約 5 pr-μ m 湿潤になる。また、レゴリスー大気間で交換された水蒸気フラックスの季節変動を見ると、Ls=180° – 240° に北半球の中緯度でレゴリスからの水の供給が見られる。これは、中・低緯度のレゴリスが北半球の秋から冬にかけて大気中に水蒸気を放出していることを示唆している。従って、レゴリスー大気間の水蒸気交換は従来のモデルで示唆されたほど季節的な水循環に対して劇的な影響を持つわけではないが、中・低緯度を湿潤にしており、レゴリスが季節的な水の供給源となっていることを示している。

R009-15
B 会場 ：11/24　PM2 （15:30-18:15）
17:15〜17:30

#西岡 知輝 [1)], 関 華奈子 [1)], 坂田 遼弥 [2)], 堺 正太朗 [2)], 寺田 直樹 [2)], 品川 裕之 [3)], 中山 陽史 [4)]
([1] 東京大・理, [2] 東北大・理, [3] 九州大学国際宇宙惑星環境研究センター, [4] 立教大・理

Effects of hot oxygen corona on the ion escape from Venus-like planets

#Tomoaki Nishioka[1)], Kanako Seki[1)], Ryoya Sakata[2)], Shotaro Sakai[2)], Naoki Terada[2)], Hiroyuki Shinagawa[3)], Akifumi Nakayama[4)]
([1]Graduate School of Science, University of Tokyo, [2]Graduate School of Science, Tohoku University, [3]International Research Center for Space and Planetary Environmental Science, Kyushu University, [4]College of Science, Rikkyo University

Since Venus has no substantial planetary magnetic field, the fast-flowing solar wind plasma interacts directly with its upper atmosphere. Venusian extended oxygen corona in the exosphere, as well as thermal atomic oxygen in the thermosphere, is a source of the ion loss. Ionized oxygen loss is thought to be the main mechanism of atmospheric escape at current Venus. Therefore, to understand the atmospheric evolution of a Venus-like planet, it is important to understand how much hot oxygen corona contributes to the ion escape. Venusian exosphere has been studied based on spacecraft observations and numerical simulations for many years (e.g., Nagy et al., 1981; Gröller et al., 2010). These studies focus on current Venus, but it is important to note that the structure of Venusian upper atmosphere is strongly influenced by X-ray and extreme ultraviolet (XUV) radiation from the host star (Sun). In the past, the Sun is thought to be emitted XUV radiation that was tens of times stronger than it is today. Similarly, close-in exoplanets in the habitable zones (HZ) around M dwarfs are expected to be exposed to extreme levels of XUV radiation. This could mean that the contribution of the oxygen corona to ion escape in such extreme XUV environments was different from current Venus.

In this study, we investigated the effect of the hot oxygen corona on the ion escape from Venus-like planets under various XUV environments and stellar wind conditions. We combined a Monte Carlo code for calculating hot oxygen transport in the thermosphere with the multi-species MHD simulation model REPPU-Planets (Terada et al., 2009; Sakata et al., 2022). The hot oxygen density above the exobase is calculated by using Liouville's equation (Schunk and Nagy, 2009). We assumed a Venus-like atmospheric composition that depends on the stellar XUV flux as the input neutral atmosphere based on Kulikov et al. (2007). The stellar XUV flux is set between 1 and 100 times the current Venus value. As stellar wind conditions, number density and velocity were varied from 4.5 to 450 cm^{-3} and from 470 to 4700 km s^{-1}, respectively, and the temperature was fixed at 1.3×10^6 K, by referring to previous studies (Nishioka et al., 2023; Dong et al., 2020). Interplanetary magnetic field (IMF) was assumed to be a Parker spiral with an angle of 45 degrees and a magnitude of 12 nT.

We first confirmed a good agreement of the model results for the current Venus with the observations of the hot oxygen corona by the Pioneer Venus Orbiter. The results of the parameter surveys show that the contribution of the oxygen corona decreases under high-XUV environment or low-density stellar wind. This is because increased XUV radiation causes the thermospheric component to dominate over the nonthermal component, and reduced stellar wind density decreases ionization of the corona through charge exchange and electron impact ionization. This study reveals that the hot oxygen corona plays a crucial role in the ion escape from close-in exoplanets in the HZ around inactive M dwarfs. In the presentation, effects of the stellar wind number density, velocity, and XUV radiation on the ion escape mechanism will be also reported in detail.

R009-16
B 会場 ：11/24　PM2 （15:30-18:15）
17:30〜17:45

#能勢 千鶴 [1)], 益永 圭 [2)], 土屋 史紀 [1)], 笠羽 康正 [1)], 堺 正太朗 [1,3)], 吉川 一朗 [4)], 山崎 敦 [5)], 村上 豪 [5)], 木村 智樹 [6)], 北 元 [7)], Chaufray Jean-Yves[8,9)], Leblanc François[8,9)]
([1] 東北大・理・惑星プラズマ大気, [2] 山形大学, [3] 東北大・理・地球物理, [4] 東大, [5]ISAS/JAXA, [6]Tokyo University of Science, [7] 東北工業大学, [8]LATMOS/ CNRS, [9]Sorbonne University

Influence of the solar wind on the hydrogen airglow in the Venusian upper atmosphere observed by Hisaki

#Chizuru Nose[1)], Kei Masunaga[2)], Fuminori Tsuchiya[1)], Yasumasa Kasaba[1)], Shotaro Sakai[1,3)], Ichiro Yoshikawa[4)], Atsushi Yamazaki[5)], Go Murakami[5)], Tomoki Kimura[6)], Hajime Kita[7)], Jean-Yves Chaufray[8,9)], François Leblanc[8,9)]
([1]Planetary Plasma and Atmospheric Research Center, Graduate School of Science, Tohoku University, [2]Yamagata University, [3]Department of Geophysics Graduate School of Science, Tohoku University, [4]University of Tokyo, [5]Institute of Space and Astronautical Science, Japan Aerospace Exploration Agency, [6]Tokyo University of Science, [7]Tohoku Institute of Technology, [8]LATMOS/ CNRS, [9]Sorbonne University

Variations in the Venusian hydrogen atmosphere are important for understanding the dynamics of the upper atmosphere, such as atmospheric escape. Observations from Venus Express have shown the presence of hot and cold components in the Venusian hydrogen corona at different scale heights. It was suggested that charge exchange between the cold component and ionospheric or solar wind protons plays a significant role in producing the hot component (Chaufray et al. 2012). However, the temporal variation in the two hydrogen components and the influence of the solar wind on them have not been fully understood. We analyzed the variations in global hydrogen column densities, calculated from the brightness of resonantly scattering Ly-α (121.6 nm) and Ly-β (102.6 nm) observed by Hisaki, the solar wind velocity by ASPERA-4 on Venus Express and the solar UV irradiance at Ly-α and Ly-β obtained from Flare Irradiance Spectral Model (FISM) for Planets. The analysis periods were from March 7th to April 3rd, 2014 (P1) and from April 25th to May 23rd, 2014 (P2). High-speed solar wind arrivals were confirmed in P1 but not in P2. In P1, when the high-speed solar wind arrived, the hydrogen column density derived from Ly-α increased by approximately 10% over a few days, and then remained almost constant for weeks. The column density derived from Ly-β decreased slightly during this period. In contrast, in P2, the column density remained almost constant for both Ly-α and Ly-β. One possible explanation for the ˜10% variations in Ly-α and the slightly decrease in Ly-β seen in P1 is an increased high-altitude hot hydrogen abundance due to charge exchange and momentum transfer between neutral hydrogen and ionospheric ions. We considered the charge exchange between thermospheric hydrogen and ionospheric ions as a production process and the charge exchange between hot hydrogen and the solar wind as a loss process and estimated their reaction time scales. We found that these scales are consistent with the observed variation. Another candidates is an increase in the low-altitude cold hydrogen abundance or an increase in hydrogen temperature. We will discuss how we could consider the hydrogen density and temperature variations in the Venusian upper atmosphere.

R009-17
B 会場 ：11/24　PM2 （15:30-18:15）
17:45〜18:00

#大野 辰遼 [1)], 高橋 幸弘 [2)], 佐藤 光輝 [3)], 高木 聖子 [4)], 今井 正尭 [5)]
([1] 北海道大学, [2] 北大・理・宇宙, [3] 北大・理, [4] 北海道大学, [5] 東大 天文センター

Development of Planetary Lightning Detector (PLD) and Venusian lightning Model comparing with JEM-GLIMS data

#Tatsuharu Ono[1)], Yukihiro Takahashi[2)], Mitsuteru SATO[3)], Seiko Takagi[4)], Masataka Imai[5)]
([1]Department of Cosmosciences, Graduate School of Science, Hokkaido University, [2]Faculty of Science, Hokkaido University, [3]Faculty of Science, Hokkaido University, [4]Hokkaido University, [5]Institute of Astronomy, The University of Tokyo

Lightning is the electric discharge through the atmosphere that occurs not only on Earth. The previous observations detected the possible signal originating from Venusian lightning. LAC onboard AKATSUKI recorded a potential signal on March 1, 2020 (Takahashi et al., 2020). If the lightning discharge generated its signal, the occurrence rate is similar to the estimated rate by the ground-based telescope observation (Hansell et al., 1995). Lightning could help understand the Venusian atmospheric dynamics. Moist convection is one of the possible mechanisms for generating lightning discharge in dense clouds. Lightning activity has correlated with the convection activity. However, there are many unknowns about Venusian lightning's existence, mechanism, and distribution due to a lack of global observations and continuous monitoring over several years.

To enable us to achieve high-frequency monitoring observations, we have developed the Planetary Lightning Detector (PLD) for the 1.6-m Pirka telescope of Hokkaido University. PLD can distinguish between the lightning and the variation of the other light sources using two-band simultaneous photon counting. The first photomultiplier tube observes the wavelength of Venusian lightning(777 nm, FWHM = 1nm). The second photomultiplier tube simultaneously observes the background variation with the broadband filter, 700 nm (FWHM = 10 nm). If the PMT's signal of 777 nm has a considerable count increasing above the trigger level estimated by the noise amplitude, unlike the second PMT, the candidate waveform has been detected. From the data of observing Venus since 2021, we triggered several possible signals. We cannot rule out the possibility that all recorded light curves originate from noise or Cosmic rays. It might be disputable to conclude that we have detected lightning. To understand the Venusian lightning optical waveform, we developed the Venusian lightning scattering model compared with the Earth lightning model and Earth lightning light curve observed by JEM-GLIMS to test if the observed lightning is possible. JEM-GLIMS observed the VLF and optical light curve at the same time. We can understand the difference between the optical and lightning current duration time. Assume that the emission waveform of lightning can be represented by the convolution of a single photon scattering waveform and the waveform of an electric current. We analyze the waveform of the Earth's lightning to confirm the relationship using the scattering model and data of the Earth's lightning. The atmospheric conditions of the same model are adjusted to Venus, and Venusian lightning is discussed. Only a few milliseconds of lightning emission duration waveforms were obtained from a single flash when considering Venusian atmospheric conditions. LAC observed waveforms on the scale of 100 milliseconds. This difference in time scale needs to be discussed.

R009-18
B 会場 ：11/24　PM2 （15:30-18:15）
18:00〜18:15

#佐藤 毅彦 [1)], 佐藤 隆雄 [2)], 今村 剛 [3)], 黒田 剛史 [4)]
([1] 宇宙研, [2] 情報大, [3] 東京大学, [4] 東北大・理

Growth and decline of enormous cloud cover observed by Akatsuki/IR2 in Venus' night-side hemisphere

#Takehiko Satoh[1)], Takao M Sato[2)], Takeshi Imamura[3)], Takeshi Kuroda[4)]
([1]Institute of Space and Astronautical Science, Japan Aerospace Exploration Agency, [2]Hokkaido Information University, [3]Graduate School of Frontier Sciences, The University of Tokyo, [4]Department of Geophysics, Tohoku University

Akatsuki/IR2 observed the enormous cloud cover (or the cloud discontinuity) in the night-side of Venus several times (Peralta et al., 2020) with the best continuous coverage from 09 August to 06 September 2016 (every 9 days). The data recorded evolution of this remarkable phenomenon but what changes of the aerosol properties caused this remained unclear because IR2 night-side data were severely affected by the light spread from the intense day crescent. Satoh et al. (2021) introduced the Restoration by Simple Subtraction (RSS) method to overcome this issue and enabled photometric studies using IR2 night-side data for the first time. In addition to the original RSS, we have developed an alternative RSS using the 2.02-um data which has a potential of producing better quality "cleaned" night-side data. Utilizing these tools, we have performed two-color (2.26 um and 1.735 um) analysis of the enormous cloud cover for four occasions (0809, 0818, 0827, and 0906).

After RSS processing, the data were corrected for limb darkening and then projected on the longitude-latitude grid map. Rectangular measurement areas were placed both west (normal region) and east (enormous cloud covered region) of the discontinuity. Measured radiance in two filters (2.26 um and 1.735 um) is plotted in a shear-transformed two-color coordinates (M3L introduced by Satoh et al., 2021). In the first and the last data (0809 and 0906), the changes from the normal region to the cloud covered region can be explained mostly by the increase of Mode 2' particles with slight addition of Mode 3 particles. On the other hand, the third data (0827) can be explained mostly by the increase of Mode 3 particles with varying amount of Mode 2' particles. The 0818 data appear completely different, requiring significant increase of Mode 3 particles and simultaneous decrease of Mode 2' particles. We interpret these four occasions as the growth phase (from 0809 to 0818) and the decline phase (from 0827 to 0906) of the phenomenon. Quantitative estimates of the amount of sulfuric acid vapor required to explain these changes will be discussed.

R009-19
B 会場 ：11/25　AM1 （9:00-10:15）
9:00〜9:15

金星大気の全球非静力学計算：鉛直対流の影響

#樫村 博基 [1)], 八代 尚 [2)], 西澤 誠也 [3)], 富田 浩文 [3)], 高木 征弘 [4)], 杉本 憲彦 [5)], 小郷原 一智 [4)], 黒田 剛史 [6)], 中島 健介 [7)], 石渡 正樹 [8)], 高橋 芳幸 [1)], 林 祥介 [1)]
([1] 神戸大学, [2] 国立環境研究所, [3] 理化学研究所, [4] 京都産業大学, [5] 慶應義塾大学, [6] 東北大学, [7] 九州大学, [8] 北海道大学

Non-hydrostatic global simulations of the Venus atmosphere: effects of vertical convection

#Hiroki Kashimura[1)], Hisashi Yashiro[2)], Seiya Nishizawa[3)], Hirofumi Tomita[3)], Masahiro Takagi[4)], Norihiko Sugimoto[5)], Kazunori Ogohara[4)], Takeshi Kuroda[6)], Kensuke Nakajima[7)], Masaki Ishiwatari[8)], Yoshiyuki O. Takahashi[1)], Yoshi-Yuki Hayashi[1)]
([1]Kobe University, [2]NIES, [3]RIKEN, [4]Kyoto Sangyo University, [5]Keio University, [6]Tohoku University, [7]Kyushu University, [8]Hokkaido University

Venus is fully covered by thick clouds of sulfuric acid, and its atmospheric circulation and inherent phenomena are poorly understood.

Recent observations by the Venus Climate Orbiter/Akatsuki have revealed a variety of atmospheric phenomena, from the planetary-scale bow-shaped structure (Fukuhara et al., 2017) and streak-structure (Kashimura et al., 2019) to a front-like structure to small-scale vortices and waves of several hundred kilometers (Limaye et al., 2018). There have also been active attempts to reproduce these phenomena using Venusian atmospheric global models and to understand the mechanisms involved. In particular, AFES-Venus (Sugimoto et al., 2014) has realized high-resolution simulations of the Venus atmosphere, and many structures have been analyzed (e.g., Kashimura et al., 2019; Takagi et al., 2018; Sugimoto et al., 2022; Takagi et al., 2022). However, AFES-Venus is a hydrostatic model, which cannot explicitly express vertical convection. The vertical convection in the cloud layer is not only interesting in itself but is also very important in the Venusian atmosphere because the neutral or low-stability layer resulting from convection is closely related to the formation of the planetary-scale bow-shaped structure and the streak-structure. Though non-hydrostatic regional models have been used to study convective activities and the resulting gravity waves (e.g., Baker et al., 1998; Imamura et al., 2014; Yamamoto 2014; Lefèvre et al., 2017), due to the limitation of the domain size, effects of the convective activities on large-scale phenomena have not been investigated.

We are developing a non-hydrostatic Venusian atmospheric global model to realize a global simulation that explicitly represents convective activities in the cloud layer. We utilized SCALE-GM (http://r-ccs-climate.riken.jp/scale/) for the dynamical core. We imported the solar heating and Newtonian cooling functions used in AFES-Venus (Tomasko et al., 1980; Crisp et al., 1986; Sugimoto et al., 2014) to SCALE-GM. Then, we performed numerical experiments with zonally uniform heating and cooling and obtained features such as the superrotation and streak-structure similar to those obtained by AFES-Venus. Here, note that the used thermal forcing leads the atmosphere to a hydrostatically stable state (though it is close to neutral) and does not directly drive convective motions in the cloud layer.

In this study, we attempted to perform global simulations with vertical convection by providing a thermal forcing that brings a hydrostatically unstable state. Specifically, the forcing stability (i.e., the stability of the reference temperature field for Newtonian cooling) at 55-60 km altitude was changed from 0.1 K/km to negative values (e.g., -1.0 K/km), and a diurnal component of solar heating was added. Simulations were performed at several resolutions from dx ˜52 km to 3.3 km.

Numerical results show that vertical convection occurs in the region of the night side at every resolution. However, the horizontal scales of the expressed vertical convection depend on the resolution. We will show the basic features of the circulation and temperature structures and discuss the location, morphology, and role of convection in the Venus atmosphere.

Acknowledgments: This research was supported by MEXT as ”Exploratory Challenge on Post-K computer” (Elucidation of the Birth of Exoplanets [Second Earth] and the Environmental Variations of Planets in the Solar System) and “Program for Promoting Researches on the Supercomputer Fugaku” (Structure and Evolution of the Universe Unraveled by Fusion of Simulation and AI). The supercomputer Fugaku provided by RIKEN was used for the numerical calculations. This research was also supported by JSPS Grants-in-Aid for Scientific Research JP19H05605, JP20K04062, and JP24H00021 and JST FOREST Program, Grant Number JPMJFR212R.

金星は全球が濃硫酸の分厚い雲で覆われており、その大気の循環構造や内在する諸現象の全貌は明らかになっていない。しかし近年、金星探査機「あかつき」の観測によって、惑星規模の弓状構造 (Fukuhara et al., 2017) や筋状構造 (Kashimura et al., 2019)、前線状の構造、数百 km 程度の小規模な渦や波 (Limaye et al., 2018) など様々な大気現象が発見

されている。また、これらの現象を大気大循環モデルで再現し、メカニズムに迫る試みも活発に行われている。なかでも、地球シミュレータに最適化された全球大気モデル「AFES」(Ohfuchi et al., 2004; Enomoto et al., 2008) をもとに開発された AFES-Venus (Sugimoto et al., 2014) によって、高解像度計算が実現され、様々な構造が解析されてきた (e.g., Kashimura et al., 2019; Takagi et al., 2018; Sugimoto et al., 2022; Takagi et al., 2022)。しかし、AFES は静力学平衡を仮定した大気モデルであり、水平数十 km 規模以下の現象には適しておらず、雲層の対流活動を陽に扱うこともできない。雲層の対流活動は、それ自身が興味深いだけでなく、対流の結果として生じる中立あるいは低安定度の層が、惑星規模の弓状構造や筋状構造の成因に深く関わっており、金星大気大循環の特徴を理解する上で非常に重要だと考えられる。これまでに、非静力学の領域モデルによって雲層の対流活動やそこから生じる重力波などが研究されている (e.g., Baker et al., 1998; Imamura et al., 2014; Yamamoto 2014, Lefèvre et al., 2017) が、計算領域が限定されるがゆえに、大規模現象に対する影響を調べることは出来ていない。

そこで我々は、雲層の対流活動を陽に表現した金星大気の全球計算を実現すべく、非静力学の全球金星大気モデルの開発を進めている。大気運動や座標系を担う力学コアには「SCALE-GM」(http://r-ccs-climate.riken.jp/scale/) を利用している。SCALE-GM は、完全圧縮方程式系を正二十面体準一様格子 (Tomita et al., 2001, 2002) 上で有限体積法で解く力学コアである。これまでに、AFES-Venus で用いられている太陽加熱・ニュートン冷却 (Tomasko et al., 1980; Crisp et al., 1986; Sugimoto et al., 2014) を導入し、東西一様な加熱冷却強制の下で計算を試行し、AFES-Venus と同様な平均東西風分布や惑星規模筋状構造が表現されることを確認してきた (樫村他, 2021)。ただし、この加熱冷却強制は、(中立には近いものの、対流運動による静的不安定解消後の) 静的安定な場へと近づけるものであり、雲層付近の鉛直対流を直接駆動しない設定であった。

そこで本研究では、静的不安定な場へと近づける加熱冷却強制を与えることで、鉛直対流が直接駆動される全球計算を試みた。具体的には、高度 55 – 60 km における安定度強制 (ニュートン冷却の基準温度場の安定度) を、従来の 0.1 K/km から、負の値 (– 1.0 K/km など) に変更し、太陽加熱の日変化成分も加えた。計算は、水平格子間隔 dx ˜52 km から 3.3 km まで段階的に複数の解像度で行った。

計算の結果、全ての解像度で夜面の高度 50-60 km 付近で鉛直対流が生じることが確認された。ただし、表現された鉛直対流の水平規模は dx ˜52 km で 500 km 程度、dx ˜3.3 km で 50 km 程度と解像度に依存する。講演では、平均東西風をはじめとした基本的な循環構造や温度構造を紹介した後、鉛直対流の出現場所、形態、および熱・運動量の鉛直輸送への寄与を議論する予定である。

謝辞：本研究は、文部科学省「富岳」成果創出加速プログラム「宇宙の構造形成と進化から惑星表層環境変動までの統一的描像の構築」及び「シミュレーションと AI の融合で解明する宇宙の構造と進化」の一環として実施しました。 数値計算には、理化学研究所の大型計算機「富岳」を使用しました。 本研究は JSPS 科研費 JP19H05605、JP20K04062、JP24H00021 及び JST 創発的研究支援事業 JPMJFR212R の支援を受けました。

R009-20
B 会場 ：11/25　AM1 （9:00-10:15）
9:15〜9:30

金星周回機あかつきの紫外画像から得られた金星雲頂高度における二酸化硫黄と未同定紫外吸収物質の分布

#岩中 達郎 [1)], 今村 剛 [2)], 青木 翔平 [2)], Marcq Emmanuel[3)], 佐川 英夫 [4)]
([1] 東京大学大学院理学系研究科, [2] 東京大学大学院新領域創成科学研究科, [3]Laboratoire Atmosphères, Observations Spatiales / IPSL, Université de Versailles Saint-Quentin, [4] 京都産業大学理学部

Distributions of sulfur dioxide and the unidentified UV absorber retrieved using UV images taken by Akatsuki UVI

#Tatsuro Iwanaka[1)], Takeshi Imamura[2)], Shohei Aoki[2)], Emmanuel Marcq[3)], Hideo Sagawa[4)]
([1]Graduate School of Science, The University of Tokyo, [2]Graduate School of Frontier Sciences, The University of Tokyo, [3]Laboratoire Atmosphères, Observations Spatiales / IPSL, Université de Versailles Saint-Quentin, [4]Faculty of Science, Kyoto Sangyo University

The clouds on Venus, composed of sulfuric acid droplets, are a crucial factor affecting the solar energy absorbed by Venus through its albedo. The series of processes by which sulfur dioxide, a precursor of the clouds, is transported from the cloud formation region to the cloud top altitude and then converted into sulfuric acid through photochemical reactions needs to be better understood. Additionally, the unidentified UV absorber, which absorbs the near-UV to visible rays where solar energy is most intense, affects the solar energy incident on Venus. Therefore, their distribution and variation are essential for understanding the climate system. To observe the distribution and variation of sulfur dioxide and the unidentified absorber, the Venus orbiter Akatsuki has continuously taken UV images of Venus (Nakamura et al., 2016; Yamazaki et al., 2018). However, since Akatsuki's UV images are taken using band-pass filters and the absorption wavelengths of sulfur dioxide and the unidentified absorber overlap within observational wavelengths of UVI (UltraViolet Imager), quantitative analysis was difficult using only one image. Therefore, in this study, we developed a code for radiative transfer calculations suitable for retrievals from the disk images taken from the orbit and a method to separate these two absorbers using images taken at two wavelengths (283 nm and 365 nm) nearly simultaneously. As a result, we obtained the distributions of sulfur dioxide and the unidentified absorber on the Venus disk from approximately 15,000 UV images from 2016 to 2022. In this study, we first derived the local time and latitudinal mean distributions using this long-term, high-temporal resolution dataset. The average mixing ratio of sulfur dioxide on the dayside was 80-200 ppbv, consistent with the results from the solar occultation observations by Venus Express/SOIR (Belyaev et al., 2012). The latitudinal distribution has a minimum of around mid-latitudes, while the local time distribution has a single maximum in the afternoon. Although the latitudinal distribution was consistent with the nadir spectroscopic observations by Venus Express/SPICAV-UV (Marcq et al., 2020), the local time distribution did not match. The distribution of the unidentified absorber was higher in the low-latitude region and lower in the mid-latitudes, with a subtle maximum in the morning and increasing towards both the morning and evening terminators. The distribution of sulfur dioxide, with a single maximum in the afternoon as found in this study, was consistent with the results of the general circulation model incorporating photochemical reactions (Stolzenbach et al., 2023) and the vertical movement of air induced by thermal tides as calculated by Takagi et al. (2018).

硫酸液滴で構成される金星の雲は，アルベドを通して金星が吸収する太陽エネルギーに影響を与える重要な要素である．雲の前駆物質である二酸化硫黄が，雲下層領域から雲頂高度まで輸送され，光化学反応により硫酸へ変化する一連の過程は詳しく解明されていない．また，太陽エネルギーが最大となる波長域である近紫外から可視領域にかけて吸収をもつ未同定の紫外線吸収物質は，金星に入射する太陽エネルギーに影響を与え，その分布と変動は気候システムを理解するうえで重要である．二酸化硫黄や未同定の紫外吸収物質の分布やその変動を観測するため，金星周回機あかつきは軌道上から金星の紫外画像を継続的に撮影してきた (Nakamura et al., 2016; Yamazaki et al., 2018)．あかつきの紫外画像はバンドパスフィルタによる撮像であること，二酸化硫黄と未同定の紫外吸収物質の吸収波長はあかつきの観測波長で重複するため，単一波長の画像だけでは，これらの物質の定量的な解析は難しかった．そこで本研究では，軌道上からのディスク画像からのリトリーバルに適した放射輸送計算コードと，ほぼ同時刻に撮影された 283 nm と 365 nm の 2 波長での画像を用いてこれらの 2 物質を分離する手法を開発した．それにより，2016 年から 2022 年までに撮影された約 15,000 枚の紫外画像から二酸化硫黄，未同定の紫外吸収物質の金星ディスク上での分布が得られた．このような 7 年間の 2 時間毎という長期間かつ高時間分解能のデータセットを用いた解析として，本研究ではまず地方時・緯度平均分布を導出した．その結果，昼面の二酸化硫黄の混合比の平均値は 80-200 ppbv であり，Venus Express/SOIR の太陽掩蔽観測による結果 (Belyaev et al., 2012) と矛盾のない結果であった．緯度方向には中緯度付近で極小をもち，地方時方向には午後側で単一の極大をもつ分布で， Venus Express/SPICAV-UV による直下視分光観測 (Marcq et al., 2020) とは，緯度方向には整合的であったが，地方時方向には一致しなかった．未同定の紫外吸収物質の分布は，緯度方向には低緯度域で多く，中緯度で少ない分布で，地方時方向には午前側に明瞭でない極大をもち，朝方，夕方の終端に向かって増加するような分布であった．本研究によって得られた，二酸化硫黄が午後側で単一の極大をもつ分布は，光化学反応を組み込んだ大気大循環モデルによる計算結果 (Stolzenbach et al., 2023) や，Takagi et al. (2018) の大気大循環モデルによって計算された，熱潮汐波が励起する空気の鉛直変位と整合的な結果であった．

R009-21
B 会場 ：11/25　AM1 （9:00-10:15）
9:30〜9:45

金星模擬環境下における NO2 による酸化を通じた SO2 の硫酸液滴への取り込みに関する室内実験

#生方 颯真 [1)], 狩生 宏喜 [1)], 玄 大雄 [2)], 中川 広務 [1)], 小山 俊吾 [1)], 南川 陸登 [2)], 黒田 剛史 [1)], 寺田 直樹 [1)]
([1] 東北大・理・地球物理, [2] 中央大・理工・応用化学

Laboratory Experiments on SO2 Uptake into Sulfuric Acid Droplets through Oxidation by NO2 under Venus-analogous Conditions

#Soma Ubukata[1)], Hiroki Karyu[1)], Masao Gen[2)], Hiromu Nakagawa[1)], Shungo Koyama[1)], Rikuto Minamikawa[2)], Takeshi Kuroda[1)], Naoki Terada[1)]
([1]Department of Geophysics, Graduate School of Science, Tohoku University, [2]Department of Applied Chemistry, Faculty of Science and Engineering, Chuo University

Sulfur dioxide (SO2) has both direct and indirect effects on the thermal structure of the Venusian atmosphere: while SO2 causes a warming of the planetary atmosphere through its greenhouse effect, it also causes a cooling by increasing albedo as a precursor to clouds. We can constrain the photochemical processes involving SO2 and their subsequent impact on the thermal structure of the Venusian atmosphere by identifying the factors that determine the mixing ratio of SO2.

According to observations from instruments such as SPICAV on Venus Express and ISAV on VEGA, the volume mixing ratio of SO2 decreases by approximately three orders of magnitude from the lower cloud to the cloud top. However, the SO2 depletion cannot be explained by gas-phase chemistry alone, suggesting the presence of missing sinks of SO2 in the cloud layers. A potential mechanism for SO2 depletion is the reactive uptake of SO2 by cloud droplets of sulfuric acid (H2SO4), which is very significant in the Earth's atmosphere, particularly when oxidants co-exist. It is highly uncertain whether the reactive uptake mechanism can substantially deplete SO2 in the cloud layers of Venus because the solubility of SO2 in H2SO4 is extremely low. This unaccounted-for pathway necessitates experimental validation under Venus-analogous conditions.

Here, we perform laboratory experiments to examine the uptake of SO2 by H2SO4 droplets in the presence of oxidants. NO2 was used as a potentially important oxidant to oxidize dissolved SO2 in an H2SO4 droplet. An H2SO4 droplet of ˜10 μ m in radius was levitated using an electrodynamic balance (EDB) at the ambient temperature (˜298 K) and pressure (1 atm), corresponding to an altitude of 50-55 km on Venus. The relative humidity in the EDB was kept at ˜1%, and hence the droplet concentration was ˜77 wt% H2SO4. Uptake experiments were performed in an open system under continuous mixed flow of carbon dioxide (CO2: ˜100%) and SO2 (100 ppm) gases, representative of the Venusian cloud layers. NO2 was also introduced at 0-100 ppm to initiate the reaction. The size increase during the reactive uptake of SO2 was measured by the Mie scattering method and converted to the H2SO4 formation rate to estimate the SO2 uptake coefficient.

We find that the growth rate of an H2SO4 droplet increases with NO2 concentration. The reactive uptake coefficient is expressed as a function of the partial pressure of NO2. To the best of our knowledge, the present study reports the first experiments demonstrating the reactive uptake of SO2 by H2SO4 droplets promoted by NO2 oxidants. Reactive uptake of SO2 by H2SO4 droplets may be a potentially important contributor to the SO2 depletion, warranting future observations of oxidants in the Venusian atmosphere.

二酸化硫黄 (SO2) は、金星大気の温度構造に対して直接的・間接的に影響を及ぼす。SO2 はその温室効果によって惑星を温める一方、雲の前駆物質でもあり、アルベドを上げて惑星を冷やす効果がある。SO2 の混合比を決める要因を同定することで、SO2 に伴う光化学反応と、それに伴う惑星大気の熱構造への影響を制約することができる。

Venus Express の SPICAV や VEGA の ISAV などの観測によると、SO2 の体積混合比は、雲層下部から雲層上部にかけて 3 桁近く減少している。しかし、この SO2 の減少は気相の化学種だけを考慮したモデルでは説明できず、雲層における未知の SO2 消失メカニズムが存在することが示唆されている。SO2 減少の潜在的なメカニズムとして、硫酸雲粒による SO2 の取り込みが考えられる。このプロセスは地球大気において、特に酸化剤が共存する場合に非常に重要となることがわかっている。しかし、濃硫酸に対する SO2 の溶解度は極めて低いため、このプロセスが金星の雲層で SO2 の減少に大きな役割を果たしているかどうかは不明である。よって、硫酸液滴による SO2 の取り込み過程について、金星類似の条件下での実験的検証が必要である。

そこで私たちは、酸化剤の存在下での硫酸液滴による SO2 の取り込みを調べるための実験を行った。 SO2 を酸化する可能性のある重要な酸化剤として、二酸化窒素 (NO2) を使用した。電気力学天秤 (EDB) を用いて、半径約 10 μ m の硫酸液滴を室温 (約 298 K) および室内圧力 (1 atm) で浮遊させ、金星の高度 50-55 km に相当する条件を再現した。EDB 内の相対湿度は約 1% に保たれ、その条件下での硫酸液滴の濃度は約 77 wt% と見積もられた。実験は、CO2 (約 100%) 、SO2 (100 ppm) および NO2(0-100 ppm) の混合ガスを連続的に流す開放系で行った。SO2 の取り込みによる硫酸液滴のサイズ増加は Mie 散乱法により測定した。そして、測定されたサイズ増加を硫酸生成速度に変換して SO2 の取り込み係数を推定した。

実験の結果、NO2 濃度の増加に伴い硫酸液滴の成長率が増加することがわかった。取り込み係数は NO2 の分圧の関数として表された。私たちの知る限り、本研究は硫酸液滴による SO2 の取り込みが NO2 によって促進されることを実証する初めての実験である。硫酸液滴による SO2 の取り込みは、金星での SO2 の減少に重要な寄与をする可能性があり、金星大気中の酸化剤の将来観測が必要となる。

R009-22
B 会場 ：11/25　AM1 （9:00-10:15）
9:45〜10:00

金星大気の対流圏界面高度と大気重力波の変動

#杉浦 美優 [1)], 今村 剛 [2)], 安藤 紘基 [3)]
[(1] 東京大学, [(2] 東京大学, [(3] 京産大

Variations of tropopause height and gravity waves in the Venusian atmosphere

#Miyu Sugiura[1)], Takeshi Imamura[2)], Hiroki Ando[3)]
[(1]Graduate School of Frontier Science, The University of Tokyo, [(2]Graduate School of Frontier Sciences, The University of Tokyo, [(3]Kyoto Sangyo University

At 50-70km altitudes in the Venusian atmosphere, there is a thick cloud layer composed of H_2SO_4 and H_2O liquid. Around the cloud base, the clouds absorb infrared radiation from the lower atmosphere and then the atmosphere is heated. On the other hand, the atmosphere near the cloud top is cooled by emitting infrared radiation to space. This drives convection in the lower cloud layer. Atmospheric gravity waves, with this convection being one of the excitation sources, propagate vertically and transport momentum between distant altitude regions. Thus, they play important roles in atmospheric dynamics.

In the previous studies, the latitudinal and local-time dependences of the convective layer thickness and the gravity wave activity were suggested. Unlike Earth, observations of Venus Express and Akatsuki radio occultation showed that the convective layer is thicker at higher latitudes (Tellmann et al. 2009; Ando et al. 2020). As the solar heating in the upper cloud layer decreases with latitude, convection will be enhanced at higher latitudes (Imamura et al. 2014). The enhancement of gravity wave activity in high latitudes (Tellmann et al. 2012; Ando et al. 2015) might be attributed to such latitude-dependent convection. On the other hand, the Venus Express radio occultation observed a periodical variation of the polar atmospheric temperature with a period of 3.1 Earth days, which was attributed to a planetary-scale wave (Ando et al. 2017). However, the variations of the convective layer and gravity wave activity associated with such waves have not been studied. Clarifying these aspects is crucial for understanding the dynamics of Venus's atmosphere from micro to planetary scales and is also expected to play an important role in comparative studies with other planetary atmospheres.

Through my analysis of data obtained during two periods of radio occultation observations by Venus Express, it was discovered for the first time that the tropopause height in the polar atmosphere changes with the same period as the temperature variations associated with the propagation of planetary-scale waves. Although it was predicted that stronger convection would result in a higher tropopause height and larger amplitudes of atmospheric gravity waves, only a weak correlation was found between the tropopause height and the amplitude of atmospheric gravity waves in both periods. Furthermore, when comparing the vertical wave number spectra between cases with high and low tropopause altitudes, an unexpected trend was observed in short-wave gravity waves: the lower the tropopause height, the larger the amplitude of atmospheric gravity waves.

In this study, we conduct a detailed analysis of this reverse trend using the Full Spectrum Inversion (FSI), a type of radio holography that has a higher vertical resolution than GO(Geometrical Optics).

金星には、濃硫酸から成る厚い雲層が高度 50-70 km において全球的に存在する。雲底付近では雲が下層大気からの赤外放射を吸収することで雲層下部が加熱される一方、雲頂付近では宇宙空間への赤外放射によって大気が冷却されるため、雲層下部（高度 50-55 km）で鉛直対流が生じている。この鉛直対流を励起源の一つとする大気重力波は鉛直方向に伝播し離れた高度間での運動量輸送に寄与するため、金星の大気大循環を考える上で重要である。

先行研究では、金星大気における対流層の厚さや大気重力波活動の緯度依存性や地方時依存性が示唆されている。例えば、金星では地球とは逆に、高緯度ほど対流層が厚くなっていることが欧州の金星探査機 Venus Express や「あかつき」の電波掩蔽観測によって示されている (Tellmann et al. 2009; Ando et al. 2020)。これは、高緯度では雲頂付近での太陽光加熱が小さくなるので、高緯度ほど対流が強化されることに起因する可能性があると指摘されている (Imamura et al. 2014)。高緯度での大気重力波活動の強化 (Tellmann et al.2012; Ando et al. 2015) はそのような対流層の強さの緯度依存性に起因する可能性がある。一方、Venus Express の電波掩蔽観測によって、金星極域大気の温度が約 3.1 日周期で変動する様子が捉えられており、約 3.1 日周期の惑星規模波動が伝播していることが先行研究からわかっている (Ando et al. 2017)。しかし、このような波に伴う対流層構造や大気重力波活動の変動の研究は行われておらず、これらを解明することは微細スケールから惑星規模に至るまでの金星大気の動力学を理解する上で重要であり、地球大気といった他の惑星大気との比較研究においても重要な役割を果たすと考えられる。

これまでに Venus Express の電波掩蔽観測で得られた 2 つの期間でのデータを自身で解析した結果、極域大気において惑星スケール波の伝播に伴う温度変動と同じ周期で対流圏界面高度も変動していることが初めて分かった。また、対流が強いほど対流圏界面高度が高く大気重力波の振幅が大きくなると予想したが、どちらの期間でも対流圏界面高度と大気重力波の振幅との間にほぼ相関はなかった。さらに、鉛直波数スペクトルを対流圏界面高度が高い場合と低い場合で比較したところ、短波重力波において、対流圏界面高度が低いほど大気重力波の振幅が大きいという、予想とは逆傾向の結果となった。

本研究では、幾何光学より高い鉛直分解能を実現できる電波ホログラフィーの一種である Full Spectrum Inversion (FSI) 法を用いて解析して、この逆の傾向について詳しい解析を行う。

R009-23
B 会場 ：11/25　AM1 （9:00-10:15）
10:00〜10:15

金星雲頂に見られるメソスケールの構造の時間発展

#松井 龍郎 [1)], 今村 剛 [2)]
([1 東大院・理, ([2 東京大学

Temporal Evolution of Mesoscale Structures seen in UV images of the Venusian Cloud Top

#Tatsuro Matsui[1)], Takeshi Imamura[2)]
([1school of science, the university of Tokyo, ([2Graduate School of Frontier Sciences, The University of Tokyo

Venusian cloud images show mesoscale cellular structures at the cloud tops with a horizontal scale of approximately 1,000 km or less. AKATSUKI's Ultraviolet Imager (UVI) takes a series of images every two hours, allowing us to see the temporal evolution of the cellular structure. The 365-nm channel of UVI provides the spatial distribution of the unidentified UV absorbers. The purpose of this study is to investigate the origin and mechanism of mesoscale atmospheric dynamics at the cloud tops by analyzing the temporal evolution of cellular structures using 365nm. Data were taken from June-July 2016. From each image data, a region moving along the super-rotation was cut out and an animation was created to observe the temporal evolution of the identical cloud. In the animation, we observed that the clouds originated near the equator and that the cellular structure tended to be stretched toward the polar regions. In order to quantify the characteristics of the shapes observed in the animation, we divided the mesoscale structures of the UV absorber using the maximum value of brightness, and ellipse fitting was applied to each of them. The ellipse flatness tended to increase as the clouds were stretched toward the poles and to decrease significantly when the clouds were torn apart and split. Future analysis will include analysis of the inclination of the major axis of the ellipse and its latitudinal dependence, as well as proceeding with a similar analysis at 2.02 μ m.

金星探査機あかつきで撮影された金星雲画像には、雲頂に水平スケールおよそ 1000km 以下のメソスケールの筋状構造が確認されている。 あかつきに搭載された紫外線カメラは 2 時間おきに連続した画像を撮影しているため、筋状構造の発展の様子を見ることができる 。本研究では、筋状構造の分析を通して金星雲頂で生じる大気運動のメカニズムの解明を目的にしている。UVI カメラによって波長 365nm で撮影された紫外画像を使用し未同定の紫外線吸収物質の空間分布の時間発展を調べた。データは 2016 年 6〜7 月のものを使用した。各画像データから金星のスーパーローテーションに沿って移動する領域を切り出し、同一の雲の時間変化を観測するアニメーションを作成した。アニメーション内では、雲が赤道付近から生じる様子や、セル状構造が極域に向かって引き伸ばされる傾向が確認された。

次にアニメーション内で観測された形状の特徴を定量化 するために、紫外線吸収物質のメソスケールの塊状の構造を輝度の極大値を用いて分割し、それぞれの輪郭に対して楕円フィッティングを適用した。楕円の扁平率は、雲が極域に向かって引き伸ばされるにつれて増加し、雲がちぎれて分割する時に大きく減少する傾向が確認された。 今後の解析として、楕円の長軸の傾きや緯度依存性の分析や、2.02 ミクロンで同様の解析を進めることを考えている。

R009-P01
ポスター 4 ：11/26　AM1/AM2 （9:00-12:00）

#鍵谷 将人 [1)], 笠羽 康正 [1)]
[(1] 東北大・理・惑星プラズマ大気研究センター

Daytime monitoring of Mercury's sodium exosphere with Haleakala T60 adaptive optics

#Masato Kagitani[1)], Yasumasa Kasaba[1)]
[(1]Planetary Plasma and Atmospheric Research Center, Graduate School of Science, Tohoku University

We report on the development of a visible adaptive optics (AO) system for Tohoku 60cm telescope (T60) at Haleakala Observatory in Hawaii. The current goal is to join the ground-based support observation for the ESA-JAXA joint Mercury mission BepiColombo on the orbit in 2025 through 2028.

Mercury has tenuous surface-bounded exosphere containing H, He, O, Na, Ca, and K. The resonant scattering emission of the Na D-lines (589.0 nm and 589.6 nm) is bright enough to be observable from Earth. The typical time scales for variability expected from the interaction with the solar wind are on the order of a few minutes. Previous ground-based observations have shown that the north-south ratio of brightness in the Na exosphere changes on a time scale of several tens of minutes, which is consistent with the brightness response due to magnetospheric particle sputtering. There are also some global brightness patterns in Na exosphere. However, previous observations using the slit scanning technique took about an hour to get Mercury's global Na brightness distribution. Using a high-resolution spectrograph (R=50,000) equipped with an integral field unit (IFU) installed on the T60, our objective is to obtain 2-dimensional spectroscopic observation with a cadence of 5 minutes.

Mercury's maximum elongation from the Sun is only about 20 degrees. Therefore, using a regular telescope, the observation time after sunset or before sunrise is less than an hour typically. To monitor the Mercury's exospheric Na brightness through the coordinated observation with the BepiColombo mission, it is necessary to carry out continuous observations not only during short periods after sunset or before sunrise, but also during the daytime when the atmospheric seeing condition is poor (2 to 5" typically). Our visible AO system installed on T60 (T60-AO) aims to stably observe Mercury with a spatial resolution of 1 arc-seconds even during daytime with poor seeing conditions.

T60-AO consists of a 12x12 140-element MEMS deformable mirror (Boston Micromachine) and a Shack-Hartmann wavefront sensor. Field-of-view and number of pupil division for the wavefront sensor are 22" and 14.2, respectively. We updated the focal plane array of wavefront sensor in August 2024, then higher closed-loop AO control frequency 540 Hz was achieved for higher wavefront resolution 0.69"/pixel.

Then we conducted test observation of T60-AO on 9 August 2024. The result shows FWHMs of point spread function (PSF) with T60-AO were $<$1.0" under seeing conditions of 2-3" at around local time 13:00. Figure 1 shows the observed Mercury's disk image with 10 nm bandwidth centered at 590nm without(left) and with (right) T60-AO. White lines indicate circles of Mercury's disk diameter 10.5". The nighttime observation of a star with magnitude 2.2 shows the FWHM of PSF was improved from 2.0" to 0.50" with the T60-AO.

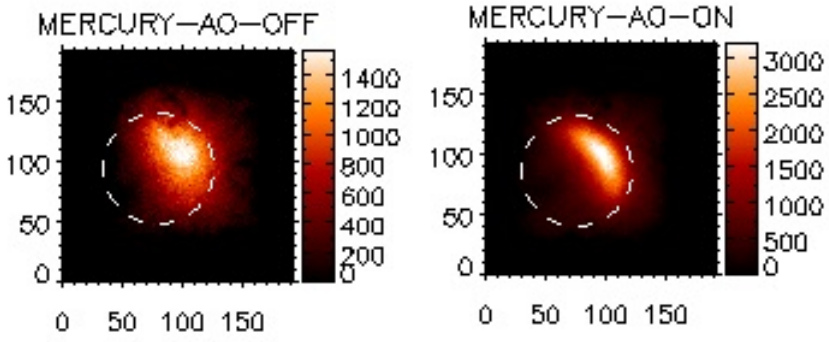

R009-P02
ポスター 4 ：11/26　AM1/AM2 （9:00-12:00）

LUPEX 搭載３回反射型リフレクトロン TRITON エンジニアリングモデルの性能評価

#齋藤 義文 [1)], 米田 匡宏 [2)], 川島 桜也 [1)], 横田 勝一郎 [4)], 齋藤 直昭 [5)], 笠原 慧 [3)], 浅村 和史 [6)], 西野 真木 [7)]
([1] 宇宙研, [2] 京大理, [3] 東京大学, [4] 大阪大, [5] 産総研, [6] 宇宙研, [7] 宇宙機構

Performance of the Engineering Model of Triple-Reflection Reflectron (TRITON) for Lunar Polar Exploration (LUPEX)

#Yoshifumi Saito[1)], Masahiro Yoneda[2)], Oya Kawashima[1)], Shoichiro Yokota[4)], Naoaki Saito[5)], Satoshi Kasahara[3)], Kazushi Asamura[6)], Masaki N Nishino[7)]
([1]Institute of Space and Astronautical Science, Japan Aerospace Exploration Agency, [2]Graduate School of Science, Kyoto University, [3]The University of Tokyo, [4]Osaka University, [5]National Institute of Advanced Industrial Science and Technology, [6]Japan Aerospace Exploration Agency, [7]Japan Aerospace Exploration Agency

For the purpose of investigating the presence and amount of the water (ice) molecules in the regolith 1 to 1.5 m below the lunar surface, a compact neutral particle mass spectrometer TRITON (Triple-reflection Reflectron) is under development. TRITON is a sub-system of REIWA (Resource Investigation Water Analyzer) onboard the LUPEX (Lunar Polar Exploration) Moon rover. REIWA also includes two other sub-systems, ADORE (Aquatic Detector using Optical Resonance) and LTGA (Lunar Thermogravimetric Analyzer) in addition to TRITON. TRITON will perform mass analysis of the neutral gas generated by LTGA.

A standard Reflectron Time-of-Mass Spectrometer consists of an ion source, ion acceleration part, free flight part, ion reflection part and an ion detector. Ionized neutral particles are accelerated in the ion acceleration part by a pulsed high voltage whose pulse timing is used as a start signal. The accelerated ions enter into the free flight part and reflected in the single-stage ion reflection part. Reflected ions again fly through the free flight part and detected by a detector. Ion mass is determined by the time difference between the start signal and the particle detection.

In order to increase the mass resolution as much as possible within the allocated volume, we have decided to modify the standard reflectron by adding a second reflector that enables triple reflections and doubles the flight length (triple reflection mode). The triple-reflection TOF mass spectrometer can be operated also as a standard reflectron by changing the voltage applied to the analyzer (single reflection mode). Triple-reflection mode is suitable for high mass resolution measurement and standard single reflection mode is suitable for high sensitivity measurement.

Engineering Model (EM) analyzer of TRITON was designed and built based on the test results of the Test Model (TM) analyzer with improved performance, taking into account the structure adapted to the flight environment. Initial performance tests of TRITON EM confirmed that TRITON can measure the atoms, molecules and their isotopes up to mass number 200 with mass resolution as high as 150 using triple reflection mode. The electronics part of TRITON EM is currently under fabrication, and the testing of the whole part of TRITON EM will be performed in the near future.

月面から約 1.5m の深さまでのレゴリス中に水（氷）分子が存在するかどうか、そして存在する場合にはその量を調べるため、小型の中性粒子質量分析器 TRITON の開発を進めている。TRITON は、月極域探査 LUPEX のローバーに搭載される水資源分析計 REIWA のサブシステムである。REIWA には TRITON と熱重量分析計 LTGA、微量水分・同位体分析装置 ADORE が含まれており、TRITON は LTGA で加熱されたレゴリスから放出される中性ガスの質量分析を行う。

通常のリフレクトロン型飛行時間式質量分析器は、イオン源、イオン加速部、自由飛行部、リフレクトロン、イオン検出器で構成される。イオン源でイオン化された中性粒子は、イオン加速部でパルス高電圧により加速され、そのパルスタイミングがスタート信号として使用される。加速されたイオンは自由飛行部に入り、リフレクトロンで反射される。反射されたイオンは再び自由飛行部を飛行した後、イオン検出器で検出される。イオンの質量は、スタート信号から粒子検出までの時間差を用いて測定することができる。

限られた装置サイズで質量分解能を可能な限り高めるため、通常のリフレクトロンに加えて第２リフレクトロンを加えることでイオンを 3 回反射させ、自由飛行部のイオンの飛行長を 2 倍にすることのできる３回反射型リフレクトロン TRITON を考案した。TRITON は、イオン源と、アナライザーの電極に印加する電圧を変えることにより、通常の１回反射型リフレクトロンとしても動作させることができる。３回反射モードは高質量分解能計測に、１回反射モードは高感度計測に適している。

TRITON アナライザのエンジアリングモデルは、テストモデルアナライザの試験結果を反映させて性能を向上させた他、フライト可能な構造を考慮して設計・製作した。初期的な性能試験を実施した結果、３回反射モードでは、質量数 200 までの原子・分子とその同位体を質量分解能 150 以上で測定できることを確認することができた。現在、TRITON 電子回路部エンジアリングモデルの製作中であり、近い将来、TRITON エンジアリングモデル全体の試験を行う予定である。

R009-P03
ポスター 4 ：11/26　AM1/AM2 （9:00-12:00）

#荻野 晃平 [1)], 原田 裕己 [1)], 西野 真木 [2)], 齋藤 義文 [2)], 横田 勝一郎 [3)], 高橋 太 [4)], 清水 久芳 [5)]
([1] 京都大学大学院理学研究科, [2] 国立研究開発法人宇宙航空研究開発機構, [3] 大阪大学大学院理学研究科, [4] 九州大学理学研究院, [5] 東京大学地震研究所

A search for magnetic reconnection signatures on lunar crustal magnetic fields: Kaguya low-altitude observations

#Kohei Ogino[1)], Yuki Harada[1)], Masaki N Nishino[2)], Yoshifumi Saito[2)], Shoichiro Yokota[3)], Futoshi Takahashi[4)], Hisayoshi Shimizu[5)]
([1]Department of Geophysics, Graduate School of Science, Kyoto University, [2]Japan Aerospace Exploration Agency, [3]Osaka University, [4]Department of Earth and Planetary Sciences, Faculty of Sciences, Kyushu University, [5]Earthquake Research Institute, University of Tokyo

The Moon is an airless obstacle with no intrinsic global magnetic field, while the solar wind interaction with lunar crustal magnetic anomalies (LMAs) forms mini-magnetospheres. The spatial scales of LMAs are smaller than local ion gyroradii and inertial length, thus solar wind ions are demagnetized near LMAs while electrons are still magnetized. An important question related to the solar wind-LMA interaction concerns the possible occurrence of magnetic reconnection between interplanetary magnetic fields and LMAs. A recent study based on ARTEMIS observations at 15 km altitude has reported a closed magnetic field line structure containing solar wind electrons, suggestive of magnetic reconnection occurred at some point between the solar wind interplanetary magnetic field and lunar crustal magnetic field (Sawyer et al., 2023). Also, 2D fully kinetic simulations show an intermittent electron-only magnetic reconnection in the solar wind-LMA interaction region (Stainer et al., 2024). In this study, we analyze magnetic field data obtained by Kaguya at low altitudes (<~30 km), in order to find potential magnetic reconnection signatures on LMAs. We identified several tens of candidate events of flux rope-like magnetic field structures near the solar wind-LMAs interaction regions. We discuss the possibility that the flux ropes can be an indicator of the occurrence of magnetic reconnection between interplanetary magnetic fields and LMAs.

R009-P04
ポスター 4 ：11/26　AM1/AM2 （9:00-12:00）

#益永 圭 [1)], 原田 裕己 [2)], 横田 勝一郎 [3)], 寺田 直樹 [4)], 堺 正太朗 [5)], 桂華 邦裕 [6)], 松岡 彩子 [7)], 齋藤 義文 [8)], 加藤 大羽 [9)]
([1] 山形大, [2] 京大・理, [3] 大阪大, [4] 東北大・理, [5] 東北大・理・地球物理, [6] 東大・理, [7] 京都大学, [8] 宇宙研, [9] 日立製作所

Mass analysis of low-energy ions originating from the lunar surface and exosphere: Feasibility study for MMX/MSA observations

#Kei Masunaga[1)], Yuki Harada[2)], Shoichiro Yokota[3)], Naoki Terada[4)], Shotaro Sakai[5)], Kunihiro Keika[6)], Ayako Matsuoka[7)], Yoshifumi Saito[8)], Daiba Kato[9)]
([1]Institute of Arts and Sciences, Yamagata University, [2]Graduate School of Science, Kyoto University, [3]Osaka University, [4]Graduate School of Science, Tohoku University, [5]Department of Geophysics, Graduate School of Science, Tohoku University, [6]Department of Earth and Planetary Science, Graduate School of Science, The University of Tokyo, [7]Graduate School of Science, Kyoto University, [8]Institute of Space and Astronautical Science, Japan Aerospace Exploration Agency, [9]Hitachi, Ltd.

We analyzed ˜1 year of the time-of-flight (TOF) data obtained from the Ion Mass Analyzer (IMA) on the Kaguya spacecraft to study the ion species originating from the lunar surface and exosphere. In this study, we especially investigated ion species coming from lunar highlands and lunar mare defined by iron abundance data obtained from the Gamma ray spectrometer on Lunar Prospector. At every time step of IMA observations, we calculated the motional electric field of the solar wind using the ion energy analyzer and the magnetometer and searched its footprint on the lunar surface. We divided the TOF data into two cases according to whether the footprint was in lunar highlands or in lunar mare. Integrating low-energy ions ($<$300 eV) of the TOF data, we identified C+, O+, and several metal ions such as Na+, Ti+, and Fe+. We found that these ions were more abundant in mare compared to highlands, which is consistent with other remote observations of the lunar surface. This indicates that with low-energy ion measurements we can study the elemental composition of the lunar surface. This technique will be used for future observations of Mass Spectrum Analyzer (MSA) on the Martian Moons eXploration (MMX) mission to study the Phobos surface.

R009-P05
ポスター 4 ：11/26　AM1/AM2 （9:00-12:00）

Comet Interceptor Mission 搭載の彗星水素コロナ撮像器の光学性能評価

#御任 勇成 [1)], 吉岡 和夫 [2)], 山崎 朝 [3)], 鈴木 雄大 [4)]
([1] 東大, [2] 東大・新領域, [3] 東大, [4]JAXA/ISAS

Optical Performance Evaluation of the Comet Hydrogen Corona Imager onboard the Comet Interceptor Mission

#Yusei Mitoh[1)], Kazuo Yoshioka[2)], Ashita Yamazaki[3)], Yudai Suzuki[4)]
([1]The University of Tokyo, [2]Graduate School of Frontier Sciences, The University of Tokyo,, [3]University of Tokyo, [4]Institute of Space and Astronautical Science, Japan Aerospace Exploration Agency

In-situ observations of comets by spacecraft began with the Giacobini-Zinner mission in 1985, and spacecrafts have explored comets since then. However, most of the comets visited were short-period comets, and no spacecraft has made detailed in-situ observations of long-period comets, which still have more state of the past state of the solar system. The ESA-led Comet Interceptor mission aims to explore long-period comets and extrasolar comets that have maintained their primordial nature.

The scientific objectives of this mission are to investigate the composition of primitive cometary comets' coma, the connection between the coma and the nucleus (activity), and the nature of coma's interaction with the solar wind. Comets are highly active bodies with high gas and dust emission rates, and as they approach the Sun, volatile material is ejected from the cometary nucleus, resulting in coma and tail structures. These are often asymmetric and localized, including the nucleus. By comparing their characteristics and relationships with measurements and simulations, we can clarify the environment surrounding the comet, such as the connection between the nucleus and coma and their interaction with the solar wind. However, with ground-based observations, the gas and dust around cometary nucleus make it difficult to observe the nucleus surface morphology and spatial distribution of the gas in detail ,and high spatial resolution data from close-up observations are required.

The Hydrogen Imager (HI) on one of the three spacecrafts will image the cometary corona at Ly-α (121.6 nm) to determine the spatial structure of hydrogen and derive the water emission rate based on the assumption that hydrogen atoms are produced by the photodislocation of water molecules. The water emission rate is an indicator of comet activeness and is an important value for comparison with short-period comets. The spatial structure of hydrogen also provides insight into the interaction with the environment outside the comet, such as the solar wind, and chemical reactions within the coma. The instrument will provide observation data for these questions by revealing the hydrogen distribution in the coma extending from 10^5 to 10^7 km from the comet nucleus to the vicinity of the nucleus below 10^3 km by using 2D images taken.

For these requirements, it is necessary to confirm that HI has the optical performance to resolve the structure on a scale of 10^3 km or less and still capture light from the dark region of the coma more than 10^7 km away from the nucleus. The instrument consists of a Cassegrain-type telescope and optical filters; Ly-α is an ultraviolet light with a wavelength of 121.6 nm, and it is difficult to make the reflectance on the mirror surface as high as that of visible light, so the effect must be considered together with the attenuation by the optical filters. In this study, the point spread function was first evaluated from point source imaging to assess the telescope's imaging performance. Next, the effect of the optics on the Ly-α intensity was investigated. By measuring the Ly-α reflectance to the spherical mirror and the transmittance of the optical filter, and by considering the results of ray tracing by optical simulation, the efficiency of the entire HI optics system was determined. In this presentation, these results will be introduced, and the optical performance of the HI will be evaluated and discussed in terms of imaging and Ly-α transmission performance.

探査機を用いた彗星のその場観測は 1985 年のジャコビニ・ツィナー彗星探査に始まり、それ以降も数々の探査機が彗星を探査してきた。しかし、訪れた彗星のほとんどは短周期彗星であり、太陽系の過去の状態をより多く記憶している長周期彗星を詳細にその場で観測した探査機はいない。そこで始原性を維持した長周期彗星や太陽系外彗星の近接探査を目的としたミッションが ESA 主導の Comet Interceptor である。

このミッションの科学的目標は、始原的彗星のコマの構成・コマと核（の活動）の関係・太陽風とコマの相互作用を調べることである。彗星は高いガス放出率やダスト放出率を持った活動性の高い天体で、太陽に近づいて揮発性の物質が彗星核から放出されることでコマやテイルなどの構造をもつ。これらは往々にして、核も含めて非対称性・局所性を持っている。その特徴や関係性を実測およびシミュレーションと比較することで核とコマの繋がりや太陽風との相互作用といった彗星周囲の環境を明らかにできる。しかし、ガスとダストの影響から地上観測では核表面の形態やガスの空間分布などの詳細な観察が難しく、近接観測による高空間分解能データの取得が求められている。

探査機の 2 つの子機の一方に搭載される「水素コロナ撮像器（Hydrogen Imager: HI）」は彗星コロナを Ly-α（121.6nm）で撮像し、水素の空間構造の把握および水素原子が水分子の光解離によって生成するという仮定により水の放出率を導出する。水の放出率は彗星の活動性を示す指標となり、短周期彗星と比較する上でも重要な値となる。また、水素の空間構造は太陽風など彗星外側の環境との相互作用やコマ内の化学反応について知見を与える。本装置では撮影

した 2 次元画像により彗星核から 10^5〜10^7km まで広がるコマに対し、10^3km 以下の核近傍まで水素分布を明らかにし、これらの問いに対する観測データを与える。

このような要求から、HI が 10^3km 以下のスケールの構造を分解し、なおかつ核から 10^7km 以上離れたコマの暗い領域も捉えられる光学性能を有していることを確認する必要がある。装置はカセグレン式の反射望遠鏡と光学フィルターで構成されている。Ly-α は波長 121.6nm の紫外光であり鏡面での反射率を可視光ほど高くすることが難しく、光学フィルターによる減衰と合わせて影響を考慮しなければならない。本研究では、まず望遠鏡の結像性能評価のために点光源の撮影から点広がり関数を評価した。次に、光学系が Ly-α 強度に与える影響を調べた。Ly-α の球面鏡に対する反射率と光学フィルターの透過率を測定し、光学シミュレーションによる光線追跡の結果を考慮することで、HI 光学系全体の効率を決定した。本発表ではこれらの結果を示し、HI の光学性能について結像性能・Ly-α 透過性能を評価・議論する。

R009-P06
ポスター 4 ：11/26　AM1/AM2 （9:00-12:00）

#笠原 慧 [1)], 田尾 涼 [1)], 川島 桜也 [2)], 関 宗一郎 [1)], 佐藤 祐貴 [2)], 横田 勝一郎 [3)], 浅村 和史 [2)], 齋藤 義文 [2)]
([1] 東京大学, [2] 宇宙航空研究開発機構, [3] 大阪大, [4] 宇宙研

Development of the engineering model of the ion mass spectrometer for the Comet Interceptor mission

#Satoshi Kasahara[1)], Ryo Tao[1)], Oya Kawashima[2)], Soichiro Seki[1)], Yuki Sato[2)], Shoichiro Yokota[3)], Kazushi Asamura[2)], Yoshifumi Saito[2)]
([1]The University of Tokyo, [2]Japan Aerospace Exploration Agency, [3]Osaka University, [4]Department of Solar System Sciences, Institute of Space and Astronautical Science, Japan Aerospace Exploration Agency

Comets are pristine small bodies and thus provide key information about the solar system's evolution. Remote observations by ground observatories have characterized various comets, while in-situ observations by spacecraft have brought much more detailed information on several comets. However, the direct observations by spacecraft fly-by or rendezvous have been limited to the short-period comets, which neared the sun many times in the past and thus lost some of (or even most of) their primitive characteristics. The Comet Interceptor mission, led by ESA, aims at a long-period comet or an interstellar object. JAXA will provide an ultra-small (~35 kg) daughter spacecraft (probe B1), whose closest approach will be less than 1,000 km, allowing the first-ever multi-spacecraft fly-by observations of a comet. Here we report our recent progress on the development of engineering of the ion mass spectrometer onboard probe B1.

R009-P07
ポスター 4 ：11/26　AM1/AM2 （9:00-12:00）

彗星探査機 Comet Interceptor における磁力計センサアライメント検定手法の開発

#久連松 良温 [1)], 松岡 彩子 [1)], 村田 直史 [3)], 原田 裕己 [1)], 笠原 慧 [2)], 佐藤 泰貴 [3)], 宮崎 康行 [3)], 白鳥 弘英 [3)], 中島 晋太郎 [3)], 五十里 哲 [2)], 船瀬 龍 [3)]
([1] 京大・理, [2] 東京大学, [3]JAXA, [4] 京大・理, [5] 東京大学

Examination of the Method to Estimate the Magnetometer Sensor Alignment on Comet Interceptor

#Yoshiharu Kurematsu[1)], Ayako Matsuoka[1)], Naofumi Murata[3)], Yuki Harada[1)], Satoshi Kasahara[2)], Yasutaka Satoh[3)], Yasuyuki Miyazaki[3)], Hirohide Shiratori[3)], Shintaro Nakajima[3)], Satoshi Ikari[2)], Funase Ryu[3)]
([1]Graduate school of Science, Kyoto University, [2]The University of Tokyo, [3]Japan Aerospace Exploration Agency, [4]Graduate School of Science, Kyoto University, [5]The University of Tokyo

Comets are samples of small celestial bodies retaining the characteristics at the early era of the solar system and providing essential information to understand the origin and evolution of the solar system. Previous missions to explore the comets have targeted short-period ones with orbital period of less than 200 years. However, these comets have approached the Sun many times, making it difficult to distinguish whether their surface features are original or affected by the solar illumination. The European Space Agency (ESA) and Japan's JAXA are planning the Comet Interceptor mission, the first-ever mission to explore a long-period comet whose characteristics have not been affected by the solar illumination. In this mission three spacecraft will be launched to observe a comet simultaneously, aiming to gain new insights into the formation and evolution of the solar system and the interaction between the solar wind and the comet. The spacecraft are scheduled to launch in 2029; ESA provides the main spacecraft (A) and one of the daughter spacecraft (B2), while JAXA provides the other daughter spacecraft (B1).

All these three spacecraft are equipped with magnetometers. On Spacecraft B1, to prevent artificial magnetic noise from the spacecraft itself from degrading the precise measurement of natural magnetic fields, the magnetometer sensor is mounted at the tip of a 1.5-meter-long boom. The boom, which is compactly stored at the launch, will be deployed after the launch. However, there are concerns that the magnetometer sensor might not be correctly aligned as designed, because the boom could be distorted after the deployment. Since this alignment error directly impacts the accuracy of magnetic field data, the boom distortion is a significant issue. In previous missions such as the Selenological and Engineering Explorer (SELENE) and the Jupiter Icy Moons Explorer (JUICE), two coils are implemented inside the spacecraft to generate a known magnetic field for the calibration of the magnetometer sensor alignment. However, for the Comet Interceptor mission, it is not realistic to install coils since the weight restraint is the high priority. Therefore, we are aiming to develop an alternative method to estimate the magnetometer sensor alignment using magnetic noise generated by the instruments originally installed.

For the calibration, we are considering using the three reaction wheels that control the spacecraft's attitude as potential noise sources. In October, we plan to conduct an experiment to measure the magnetic field strength and direction generated by these wheels. In our presentation, we will show the results of the experiment and discuss whether we can estimate the magnetometer sensor alignment by these results. We will also talk about how accurate we may finally calibrate the alignment. After the experiment, we plan to build a simulation device that can reproduce the magnetic noise from the wheel to establish the method to determine the alignment of the magnetometer sensor. As the preliminary research, using magnetic experiment data of a previous project, EQUULEUS, we are developing the programs to analyze magnetic noise and evaluate the results. This preliminary research would enable us to start smoothly the examination for the Comet Interceptor case. The EQUULEUS CubeSat was developed by the University of Tokyo's Nakasu & Funase Laboratory (ISSL) and JAXA. EQUULEUS, same as Comet Interceptor, uses three reaction wheels for the attitude control. We would also like to present the analysis result of the magnetic field noise from the wheels of the EQUULEUS flight-model simulator. The magnetic experiment for the EQUULEUS flight-model simulator was carried in the same Magnetic Shield Room at JAXA's Institute of Space and Astronautical Science, where our experiment of the wheels for Comet Interceptor will take place. During these tests, time variations of the three-axis magnetic field components were measured by two magnetometer sensors placed at different locations, for different axes and various speeds of the rotation of the reaction wheels. From the measured magnetic field data, we calculated the directions of the maximum, intermediate and minimum magnetic field variation, and defined a coordinate system based on these directions. Using this coordinate system, we plotted hodograms to examine the characteristics of the magnetic field generated by the reaction wheels and feasibility to decide the axis directions determined by the field variation. We then evaluated how well this noise can be used for estimation of the magnetometer sensor alignment.

彗星は太陽系の形成初期における微小天体のサンプルであり、太陽系の起源や進化を理解するための重要な手がかりで

ある。これまでの探査ミッションでは、周期が 200 年未満の短周期彗星がターゲットであったが、それらは太陽に何度も接近しているため、表面の特徴が元々のものか、太陽に接近する過程で変化したものかを見分けるのが難しいという問題がある。このため、ESA（欧州宇宙機関）と日本の JAXA（宇宙航空研究開発機構）により、史上初めて長周期彗星の探査を目指す Comet Interceptor ミッションが計画されている。このミッションでは、3 機の衛星を用いて彗星を同時に観測することにより、太陽系の形成や進化、太陽から吹き出す荷電粒子である太陽風と彗星との相互作用について、新しい知見が得られることが期待されている。衛星は 2029 年に打ち上げ予定であり、ESA が親機（A 衛星）と子機の一つ（B2 衛星）を、JAXA が残りの子機一つ（B1 衛星）を提供する予定である。

それら 3 機の探査機には磁力計が搭載予定であり、JAXA が担当する B1 衛星では、探査機本体が発する人工的な磁場ノイズが自然界の磁場の観測に影響を与えることを防ぐため、長さ 1.5m の「ブーム」と呼ばれる棒状の伸展物の先に磁力計のセンサが設置される。打ち上げ時にはブームは小さく収納されているが、打ち上げ後にセンサが衛星本体から離れる方向に伸ばされる。しかし、ブーム伸展後に生じる歪みにより磁力計センサの方向（アライメント）が不確定性を有することが懸念されており、そのアライメント誤差が磁場データの誤差に直結するため、重要な課題となっている。従来の磁力計を搭載した探査ミッションのうち、月周回衛星「かぐや」や木星氷衛星探査衛星「JUICE」などでは、アライメントを正確に推定するために、衛星本体内部に既知の磁場を発生させるコイルを装備し、その磁場をセンサで計測することでアライメントのずれを検証していた。しかし、今回のミッションでは探査機の小型化の優先度が高いため、アライメント較正磁場を生成するコイルを搭載することができず、新たな較正手法の開発が求められている。そこで本研究では、探査機内部の機器が発生する磁場ノイズを逆に利用し、ブーム伸展後の磁力計センサのアライメントを推定する手法の開発を目指す。

今回の較正に用いるノイズ源として、衛星の姿勢制御のために使用される 3 つのホイール（リアクションホイール）を候補としており、今年の 10 月には、衛星に搭載されるホイールと同様のホイールが発する磁場の強さと向きを詳しく測る実験を予定している。今回の発表では、その実験で得たデータの解析結果を紹介し、その結果をもとに磁力計センサのアライメント推定の実現可能性や、最終的に目標とするアライメントの決定精度に言及したい。さらに実験後は、測定された磁場ノイズを再現できる模擬装置を作成し、方向推定方法の確立を目指す。現在は、過去に行われた別のプロジェクトの磁気試験データを用いて、磁場ノイズを解析するためのプログラムの作成とその結果の評価を行っており、10 月の磁場測定実験後に解析をスムーズに開始できるよう準備している。過去の磁気試験データには、Comet Interceptor と同様に姿勢制御のための 3 個のリアクションホイールを搭載した、東京大学中須賀・船瀬研究室 (ISSL) と JAXA が開発した深宇宙探査 CubeSat EQUULEUS のシミュレータを用いており、そのデータの解析内容に関しても今回合わせて紹介したい。EQUULEUS の磁気試験は、私たちが 10 月に実験を行う施設と同じ JAXA 宇宙科学研究所の磁気シールドルームで行われたものであり、回転させるホイールの軸を変更したり、回転数を変化させたりするのに応じた 3 軸成分の磁場の時間変化が、異なる場所に置かれた 2 台の磁力計によって記録されている。その磁場データから磁場変動の最大方向と、最小方向を計算し、これらの方向を基準にして座標系を作って、その座標系で Hodogram（ホドグラム）というグラフを描く。こうして得られるグラフから、リアクションホイールの発する磁場の特徴と、それによって決定される軸方向を捉え、リアクションホイールの磁場ノイズを用いたアライメント推定の有効性を議論する。

R009-P08
ポスター 4 ：11/26　AM1/AM2 （9:00-12:00）

電位差観測波形の歪と衛星電位の関係から求める光電子の到達距離

#中川 朋子 [1)], 今野 翼 [1)], 伊藤 穂尚 [1)], 眞野 航平 [1)], 堀 智昭 [2)], 笠羽 康正 [3)], 三好 由純 [2)], 松田 昇也 [4)], 笠原 禎也 [4)], 篠原 育 [5)]
([1] 東北工大・工・情報通信, [2] 名大 ISEE, [3] 東北大・理, [4] 金沢大学, [5] 宇宙機構／宇宙研

Spatial extent of photoelectrons estimated from the spacecraft potential at electric-field waveform distortion

#Tomoko Nakagawa[1)], Tsubasa Konno[1)], Hodaka Ito[1)], Kouhei Mano[1)], Tomoaki Hori[2)], Yasumasa Kasaba[3)], Yoshizumi Miyoshi[2)], Shoya Matsuda[4)], Yoshiya Kasahara[4)], Iku Shinohara[5)]
([1]Information and Communication Engineering, Tohoku Institute of Technology, [2]Institute for Space-Earth Environmental Research, Nagoya University, [3]Planetary Plasma and Atmospheric Research Center, Tohoku University, [4]Kanazawa University, [5]Japan Aerospace Exploration Agency/Institute of Space and Astronautical Science

The Electric Field Detector (EFD) of the Plasma Wave Experiment (PWE) instrument on board the Arase satellite measures an electric potential difference between each probe and the satellite body while it spins, and the sinusoidal waveform of the electric potential gives an electric field vector in a rest frame perpendicular to the spin axis. However, the measured waveform often deviates from a sinusoidal curve but has a higher harmonic component, accompanied by a spurious sunward electric field. It is due to the photoelectrons emitted from the spacecraft body. The typical double-peaked waveform was observed when the spacecraft potential was around 2 V. Too low spacecraft potential allows the photoelectrons flow away, while too high spacecraft potential traps the photoelectrons in a deep potential well and limits them within a small distance from the spacecraft. Photoelectrons in an energy range from |q|(Φ sc-Φ (r)) and |q| Φ sc are trapped within a distance r from the spacecraft, where Φ sc is the spacecraft potential and Φ (r) is an electric potential. Using the spacecraft potential 2V at the time of waveform distortion, we can estimate the spatial extent of the photoelectrons.

磁気圏電場を測る方法としてよく使われるダブルプローブ法では、人工衛星の自転により DC 電場が正弦波として観測されることを利用し、オフセット成分を分離して自然電場を得る。しかし、実際に観測された電位差波形は正弦波となっていないことがよくある。ジオスペース探査衛星「あらせ」のプラズマ波動・電場観測器 (Plasma Wave Experiment / Electric Field Detector, PWE/EFD) においても歪んだ電位差波形が観測されている。中でも、日照中において、スピン 1 周期に 2 つの極小を持つ特徴的な波形がしばしば観測され、それと同時に太陽方向を向いた偽の電場が観測されている。これは衛星から放出された光電子がプローブの軌道中心よりも太陽側にずれた位置に集まることによると考えられる。この歪んだ波形から光電子の位置や電荷量を逆算すれば、光電子の影響を観測データから除去できるのではないかと期待される。しかし、このような波形歪がない場合は、光電子の影響を推定できない。そのため、どのような時に 1 スピン 2 山の波形が現れるかを調査した。

その結果、スピン 1 周期に 2 つの極小を持つ特徴的な波形が見られるのは、衛星電位がおよそ 2V となる範囲に集中していることが分かった。衛星電位が 2V 未満の時は 1 スピンに 1 つの山がある波形となる場合がほとんどであった。他方、衛星電位が 3V 以上のところでは 1 スピンに 1 山の波形と 2 山の波形の場合が同程度の割合で混在していた。

光電子の影響が顕著になるのは、十分な数の光電子が電場計測用プローブに影響を及ぼす距離まで来る場合と考えられる。光電子のエネルギー分布を考えると、電位Φ sc の衛星から放出された光電子のうち、電位差に打ち勝って電位Φ (r) の距離 r まで到達できるのはエネルギーが |q|(Φ sc-Φ (r)) 以上のものである。このうち、エネルギーが |q| Φ sc 以上の電子は流出したまま戻ってくることはない。エネルギー範囲 |q|(Φ sc-Φ (r)) 以上 |q| Φ sc 以下の電子が、衛星からの距離 r までの範囲にとどまることができる。衛星電位が低すぎると放出された光電子はほとんど流出してしまい衛星周辺にとどまることがなく、逆に衛星電位が非常に高いときは、放出された光電子は衛星付近の深いポテンシャルにとらえられて遠くまで出てくることができない。

光電子の影響が顕著となる衛星電位Φ sc=2V の情報を使い、光電子の典型的なエネルギーが上述のエネルギー範囲に入るようにすることにより、衛星近傍にとどまる光電子の分布範囲を推定することができる。光電子の典型的なエネルギーが衛星電位に近いほど、とらえられた光電子は遠くまで分布することができる。例えば衛星周辺電位Φ (r) を簡単のために球対称な形 (a/r) exp(-(r-a)/λ) （a は衛星の大きさ）と仮定し光電子の典型的なエネルギーを 1.9V、ブラックカプトンの光電子放出量を 14-18 μ A/m^2 [1] とすると衛星表面の光電子密度 400 cm^{-3} 程度、λは約 0.5m となり、光電子の到達距離は約 1m となる。実際の電位構造は球対称ではなく、衛星構造に沿ってより遠くまで光電子が達する可能性や誘導電場により光電子分布が偏る可能性を考える必要がある。

[1] Ewang et al., (2017), I.RE.AS.E.,10-3.

R009-P09
ポスター 4 ：11/26　AM1/AM2 （9:00-12:00）

#松下 奈津子 [1)], 土屋 史紀 [1)], 笠羽 康正 [1)], 吉岡 和夫 [2)], 佐藤 晋之祐 [1)], 堺 正太朗 [1,3)], 眞田 聖光 [4,5)], 山崎 敦 [6)], 村上 豪 [6)], 木村 智樹 [7)], 北 元 [8)], 吉川 一朗 [2)]
([1] 東北大・理・惑星プラズマ大気, [2] 東大・新領域, [3] 東北大・理・地球物理, [4]University of Texas at San Antonio, [5]Southwest Research Institute, [6]JAXA/宇宙研, [7] 東京理科大, [8] 東北工業大学

Plasma parameters at Europa's orbit estimated from the Hisaki observation

#Natsuko Matsushita[1)], Fuminori Tsuchiya[1)], Yasumasa Kasaba[1)], Kazuo Yoshioka[2)], Shinnosuke Satoh[1)], Shotaro Sakai[1,3)], Saniya Sanada[4,5)], Atsushi Yamazaki[6)], Go Murakami[6)], Tomoki Kimura[7)], Hajime Kita[8)], Ichiro Yoshikawa[2)]
([1]Planetary Plasma and Atmospheric Research Center, Graduate School of Science, Tohoku University, [2]Graduate School of Frontier Sciences, The University of Tokyo, [3]Department of Geophysics, Graduate School of Science, Tohoku University, [4]University of Texas at San Antonio, [5]Southwest Research Institute, [6]Institute of Space and Astronautical Science, Japan Aerospace Exploration Agency, [7]Tokyo University of Science, [8]Tohoku Institute of Technology

Europa (9.4 R_J from Jupiter) has a tenuous molecular oxygen atmosphere, produced by magnetospheric plasma sputtering on its surface. To improve our understanding of the production and loss of the atmosphere, the density and temperature of the magnetospheric plasma around the satellite must be known. However, plasma observations at Europa's orbit are still limited.

In this study, we used JAXA's Hisaki data observed in May 2015 to estimate the plasma parameters at Europa's orbit.

An ultraviolet spectrograph (EXCEED) aboard Hisaki measured the sulfur and oxygen ion emission lines in the extreme ultraviolet (EUV) wavelength range (55-145 nm). The Jovian magnetosphere is filled with plasmas originating from satellite Io (5.9 R_J). The torus emission intensity peaks around Io's orbit and decays with increasing radial distance from the planet. At Europa's orbit, the brightness was so weak that contaminations from the terrestrial radiation belt and foreground emissions (geocorona) were carefully removed, and the spectrograph data were integrated for one week (over 1,080 min).

The emission intensity is a product of the ion density and natural transition probability along the line of sight. The torus ions are excited by electron impact, so that the ion density of a certain energy level depends on the density and temperature of the electrons. We used the CHIANTI atomic database to find the best-fit plasma parameters of the observed spectrum by minimizing the chi-square, a method known as plasma diagnosis.

The sulfur and oxygen ion emission lines were identified at Europa's orbit. Their brightness was 1.5 Rayleigh at 68.0 nm and 0.3 Rayleigh at 76.5 nm, which were approximately 2 to 6 % of those at Io's orbit. The signal-to-noise ratio (S/N) >2 was satisfied for the S^+, S^{2+}, and S^{3+} emission lines in 65-80 nm, O^+ and O^{2+} line at 83.4 nm, and S^{3+} lines at 106-108 nm. In the wavelength range longer than Ly-α (121.6 nm), S/N decreased because the intensity of the torus emission was comparable to that of the scattered geocoronal emission. The emission lines with S/N <2, including sulfur ion emission lines longer than 121.6 nm were excluded from plasma diagnosis.

We assumed that the plasma in the torus (S^+, S^{2+}, S^{3+}, O^+, O^{2+}, H^+, and e^-) was quasi-charge-neutral and O^{2+}/ O^+ was fixed at 0.1. The temperature of hot electrons was fixed to 300 eV. From plasma diagnosis, we found that the density of electron was 310 $\pm$ 200 cm^{-3}, the temperature of core electron was 4.6 $\pm$ 3.7 eV, and the fraction of hot electrons was 25 $\pm$ 27 % at Europa's orbit. The electron density in our result was larger than that in Galileo's PLS data, 63-190 cm^{-3}, while the core electron temperature in our result was cooler than that in Bagenal et al. (2015), 10-30 eV.

In plasma diagnosis, the emission lines of both short and long wavelengths are necessary to separate the density and temperature of the cold electrons, and the fraction of hot electrons. However, using only the emission lines in the short wavelength range ($<$121.6 nm), it is difficult to separate the density and temperature of cold electrons because the response of the volume emissivity in the shorter wavelength lines to these two parameters is similar. The hot fraction can be evaluated with only the emission lines shorter than 121.6 nm, but the longer emission lines are required for better accuracy. To resolve this, we plan to extend the integration time to more than 10,000 min to improve the S/N of the torus emission lines at longer wavelengths.

R009-P10
ポスター 4 ：11/26　AM1/AM2 （9:00-12:00）

木星衛星圏での物質輸送過程の解明に向けたガリレオ衛星におけるナトリウム輝線の分光観測

#長谷川 龍 [1)], 佐川 英夫 [1)], 木村 淳 [2)], 高木 聖子 [3)], 窪田 暉 [1)]
[(1] 京産大, [(2] 阪大, [(3] 北海道大学

Toward an understanding of material transport in the Jovian moons: Observation of sodium emissions in the Galilean moons

#Ryu Hasegawa[1)], Hideo Sagawa[1)], Jun Kimura[2)], Seiko Takagi[3)], Hikaru Kubota[1)]
[(1]Kyoto Sangyo University, [(2]Osaka University, [(3]Hokkaido University

When discussing habitability in space, it is important to consider not only an environment that holds liquid water, but also what kind of materials, especially those containing essential elements for life, are present in that environment. In the solar system, the existence of subsurface oceans in the interior of the icy moons of the Jovian system (i.e., Europa, Ganymede, and Callisto) has been suggested, and the importance of investigating the materials that exist in these environments has increased in recent years. Another unique feature of the Jovian system is the presence of Io. It is known that active volcanic eruptions of Io release large amounts material into space. Whether or not Io-derived materials are continuously transported to other Jovian satellites is one of the important research subjects of the Jovian system as it directly leads to the discussion of the possibility that the material transport from Io affects the formation of habitability in Jovian icy moons. In this study, we focus on sodium, one of the elements essential for life on Earth, among the materials released from Io, and aim to observationally constrain the presence of material transport processes in the Jovian moons.

In the Jovian moons, sodium is known to be spread in cloud-like distributions (sodium clouds) around Io and Europa, but no such distribution has been found on Ganymede and Callisto (e.g., Brown, 1997). Leblanc et al. (2005) showed that the variability of sodium clouds around Europa can be explained to most extent by variations in solar radiation and the Jovian magnetospheric particle fluxes to Europa. However, it is also suggested the possibility that the sodium clouds around Europa may be influenced by Io when Io and Europa are in a particular position. To quantitatively verify such a possibility, it is necessary to understand the spatial and temporal variation of sodium distributions in the Jovian moons with respect to its positional relationship with other satellites.

We have carried out continuous ground-based observations of sodium in the Jovian moons since 2023. Observations are made using the high-resolution spectropolarimeter VESPolA (Arasaki et al., 2015), which is attached to the Araki Telescope (diameter of 1.3 m) at the Koyama Astronomical Observatory of Kyoto Sangyo University. The instrument is capable of acquiring spectra at 577-780 nm wavelengths at once, and can simultaneously acquire emission lines of potassium at 766.48 and 769.89 nm, in addition to the D-lines of sodium at wavelengths of 588.99 and 589.59 nm. In the 2023 season, data were obtained for 6 nights (11/28, 12/13, 12/20, 12/28, 01/09, 01/11). As an initial result of the analysis, we are able to detect significant sodium emission lines at Io, and have confirmed that the intensity of the emission lines varies from day to day. In this presentation, we will discuss the temporal variation of the observed sodium emission and its correspondence to the volcanic distribution on Io's surface, the results of the potassium analysis, and comparison with the observations of other icy moons.

宇宙におけるハビタビリティを議論する際に重要となるのは、液体の水を保持する環境の有無に加え、その環境にどのような物質、特に、生命必須元素を含んだ物質が存在するかという点である。太陽系内では木星系の氷衛星（エウロパ、ガニメデ、カリスト）において、その内部に長期安定的な地下海の存在が示唆されており、そこに存在する物質の調査の重要性が近年より一層増している。また、木星系の特徴として、衛星イオの存在が挙げられる。イオには太陽系内で最大規模の火山が多数存在しており、その噴火によってイオ由来の物質が宇宙空間に大量に放出されている。イオ由来の物質が他の木星衛星にも継続的に輸送されるか否かは、木星氷衛星におけるハビタビリティの形成にイオからの物質輸送が影響している可能性を議論することに直結し、木星衛星圏研究において欠かせないテーマの一つである。本研究では、イオから放出されている物質のうち、地球上の生命における必須元素の一つでもあるナトリウムに着目し、木星衛星圏での輸送過程の有無を観測的に制約することを目標としている。

木星衛星圏において、ナトリウムはイオおよびエウロパの周囲に雲状（ナトリウム雲）に広がっていることが知られているが、ガニメデおよびカリストではそのような雲状の分布は見つかっていない (e.g., Brown, 1997)。近年、エウロパ表面に塩化ナトリウムの存在も検出されている (Trumbo et al., 2019)。その分布が地下海からの物質が表出しやすいと考えられる地形に対応していたことから、この塩化ナトリウムはエウロパの地下海の成分が表面に出てきたものと考察されている。その一方で、エウロパにおけるナトリウムが外的な起源を持つとする考えもいくつか示されており (e.g., Brown & Hill, 1996)、この考えは未だ完全には棄却されていない。Leblanc et al. (2005) では、エウロパ周辺におけるナトリウム雲の変動が、日射量や木星磁力線のエウロパへの接し具合の変動を理由としてある程度は説明できることが示されてい

る。しかし、その中でも、イオおよびエウロパが特定の位置になった際に、エウロパ周辺のナトリウム雲がイオからの影響を受けている可能性が言及されている。この可能性を定量的に検証するためには、木星衛星圏におけるナトリウムの存否だけでなく、その空間分布や他衛星との位置関係に着目した時間変動を理解する事が必要である。

こうした観点から、本研究では地上望遠鏡を用いた木星衛星ナトリウム輝線の継続観測を 2023 年度より実施している。観測は、京都産業大学神山天文台の荒木望遠鏡 (口径 1.3 m) に取り付けられている可視光分光器 VESPolA(Arasaki et al., 2015) を用いている。この装置は、波長 577-780 nm の分光スペクトルを一度に取得できる装置であり、波長 588.99 および 589.59 nm に存在するナトリウムの D 線以外にも、766.48 および 769.89 nm に存在するカリウムの輝線を同時取得することができる。波長分解能は $\lambda/\Delta\lambda$=8000 と 20000 の二つのモードがあり、本研究では主に $\lambda/\Delta\lambda$=8000 のモードを利用した。また、VESPolA は 1/2 波長板を回転させることで偏光度を測定できるが、本研究ではその機能は利用していない。2023 年度シーズンの観測では、木星が前半夜に見える 2023 年 11 月から 2024 年 1 月の期間で、イオやエウロパが木星やお互いに近接し過ぎないタイミングのうち天候が良かった 6 晩 (11/28, 12/13, 12/20, 12/28, 01/09, 01/11) のデータが取得できている。現在、観測データの解析を進めているが、初期解析結果としてイオにおけるナトリウム輝線を有意に検出できており、輝線強度が日によって変化している事が確認できている。講演では、観測されたナトリウム輝線強度の時間変動とイオ表面の火山分布との対応や、カリウムの解析結果、そしてエウロパ、ガニメデの観測結果との比較などを議論する。

R009-P11
ポスター 4 ：11/26　AM1/AM2 （9:00-12:00）

#佐藤 晋之祐 [1)], 坂田 遼弥 [2)], 土屋 史紀 [1)], 堺 正太朗 [1,2)], 寺田 直樹 [2)], 笠羽 康正 [1)], 松下 奈津子 [1)], 関 華奈子 [3)], 品川 裕之 [4)]
([1] 東北大学 惑星プラズマ・大気研究センター, [2] 東北大学 理学研究科地球物理学専攻, [3] 東京大学 理学系研究科地球惑星科学専攻, [4] 九州大学 国際宇宙惑星環境研究センター

A Multi-Fluid MHD Simulation for Europa's Ionosphere Affected by Variations in the Jovian Magnetospheric Plasma and Magnetic Field

#Shinnosuke Satoh[1)], Ryoya Sakata[2)], Fuminori Tsuchiya[1)], Shotaro Sakai[1,2)], Naoki Terada[2)], Yasumasa Kasaba[1)], Natsuko Matsushita[1)], Kanako Seki[3)], Hiroyuki Shinagawa[4)]
([1]Planetary Plasma and Atmospheric Research Center, Graduate School of Science, Tohoku University, [2]Department of Geophysics, Graduate School of Science, Tohoku University, [3]Department of Earth and Planetary Science, Graduate School of Science, The University of Tokyo, [4]International Research Center for Space and Planetary Environmental Science, Kyushu University

Europa acts as an obstacle to the plasma corotating with Jupiter's magnetosphere. Through the interaction between Europa's O_2 atmosphere and the magnetospheric plasma, chemical processes generate plasma originating from the atmosphere to form an ionosphere. Europa's ionosphere was observed in several observing events of Galileo's radio occultations, and in some cases, the peak electron density was derived on the order of 10^4 cm^{-3} at an altitude of ~50 km (McGrath et al., 2009). However, Galileo's observations also indicate that the electron distribution varies both in time and space significantly.

The ionization rate in the ionosphere is expected to vary in response to changes in Europa's atmosphere and those in Jupiter's magnetospheric plasma and magnetic field near Europa. A three-dimensional multi-fluid magnetohydrodynamic (MHD) simulation is suitable for characterizing the spatio-temporal variations in Europa's plasma interaction because it calculates the production and loss rates of each ion fluid separately. Several studies presented two- or three-ion-fluid MHD models for Europa's plasma interaction and considered the effects of variations in Europa's atmosphere (Rubin et al., 2015; Harris et al., 2021; Harris et al., 2022). However, the observed variations in the ionosphere have not been fully explained yet.

Inhomogeneity of the magnetospheric plasma due to the interchange instability and the plasma injection was observed by Galileo near the orbit of Europa (e.g., Russell et al., 2005). Occurrence probability of the plasma injection was found to be even higher between the orbits of Europa and Ganymede (Mauk et al., 1999). To describe how the inhomogeneity of the magnetospheric plasma affects Europa's ionosphere, we have performed MHD simulations for Europa's plasma interaction based on the MAESTRO code (Sakata et al., 2024). Firstly, we performed multi-species MHD simulations to optimize the simulation codes for the plasma environment around Europa. Chemical reactions for the simulations are the same as Rubin et al. (2015) and Harris et al. (2021), and the ion species include magnetospheric $O_2{}^+$ and the ionospheric $O_2{}^+$ and O^+ based on the previous studies. We confirmed that the optimized codes can reproduce density distributions of the ionospheric ions consistent to the results in Harris et al. (2021). After the optimization, we have performed multi-fluid simulations with three ion fluids, the same as the multi-species simulations described above. Electron pressure is separately calculated. Both photoionization and electron-impact ionization are the sources of the ionosphere. We consider the variability of the magnetospheric plasma and the magnetic field based on the Galileo observations and do not consider the changes in the neutral atmosphere.

The multi-fluid MHD simulations can also evaluate the ion escape rate from Europa. The results will be directly compared with Juno's in-situ measurements (Szalay et al., 2024) and Hisaki's spectroscopic observation (Matsushita et al., presentation at the Magnetospheres of Outer Planets 2024) to constrain the ion composition in Jupiter's inner magnetosphere.

R009-P12
ポスター 4 ：11/26　AM1/AM2 （9:00-12:00）

プラズマ照射実験に基づくエウロパ内部海起源 NaCl の表層での結晶構造の解明

#小林 愛結 [1)], 木村 智樹 [1)], 星野 亮 [1)], 大槻 美沙子 [1)], 奥本 海友 [1)], Sadgrove Mark[1)], 仲内 悠祐 [2)], 土屋 史紀 [3)], 丹 秀也 [4)], 木村 淳 [5)]
([1] 理科大, [2] 立命館大学, [3] 東北大・理・惑星プラズマ大気, [4] 国立研究開発法人海洋研究開発機構, [5] 阪大

Crystal Structure of NaCl on Europa's Surface Originated from Subsurface Ocean Based on Plasma Irradiation Experiments

#Kobayashi Ayumi[1)], Kimura Tomoki[1)], Hoshino Ryo[1)], Otuki Misako[1)], Okumoto Miyu[1)], Sadgrove Mark[1)], Nakauchi Yusuke[2)], Tsuchiya Fuminori[3)], Tan Shuya[4)], Kimura Jun[5)]
([1]Tokyo University of Science, [2]Ritsumeikan University, [3]Planetary Plasma and Atmospheric Research Center, Graduate School of Science, Tohoku University, [4]Japan Agency for Marine-Earth Science and Technology, [5]Osaka University

Europa, an icy satellite of Jupiter, has an interior ocean that is expected to be habitable for life. Since material transport between the ocean and surface layer has been suggested, understanding the chemical composition of the surface layer could provide insights into the ocean's chemistry. However, the surface material composition is still unknown because it must be altered immediately after transport from the ocean due to exposure to Jupiter's magnetospheric plasma and other elements. The telescopic data showed absorption signatures in the solar reflectance spectrum at wavelengths of 450 nm and 230 nm in the Tara Regio, which is over 1,000 kilometer-wide area of the Chaos Terrain and is likely active in the eruption of the ocean materials [Trumbo et al.,2022]. These are consistent with the spectral absorption generated by laboratory electron irradiation of NaCl, which would be 'color centers' corresponding to lattice defects in the NaCl crystal [Trumbo et al.,2022]. However, the relationship between the spectral absorption depth of the color centers and irradiation conditions is still unresolved, which leads to difficulty in estimating the NaCl crystal structure from the spectral observation. Therefore, the alteration state of NaCl in the Europa surface layer has not been unveiled.

In this study, we attempted for the first time to relate the absorption structure of the color centers, irradiation conditions, and crystal structure by applying multiple optical analyses to NaCl samples, which are irradiated with electrons and ions that model Jupiter's magnetospheric plasma interacting with Europa's surface layer. Powdered NaCl was irradiated with electron beams at 10 keV energy at room temperature (300 K) while maintaining a constant fluence (2.3×10^{14}-3.2×10^{18}/cm^2) or flux (1.9×10^{12}-1.5×10^{15}/s/cm^2). As a result, the F center around 460 nm decreased and the M center around 720 nm increased with increasing fluence. This indicates that the F center may have changed to the M center after being saturated via alteration by the irradiation, similar to the results of the electron irradiation experiment by Denman et al. [2022]. Under constant values of fluence, both F and M centers increased with increasing flux, but more M centers were produced. In addition, the irradiation of NaCl with both electrons and $H_2{}^+$ resulted in the F and M centers generated by the electron irradiation being attenuated due to the $H_2{}^+$ irradiation. This suggests that ion sputtering on the sample surface suppressed the formation of color centers. A comparison of Europa's F center observed by the Hubble Space Telescope with the electron irradiation experiment suggested that photobleaching may also decay F centers and not reach M center production [Denman et al., 2022]. These results indicate that sputtering and photobleaching may attenuate the F and M centers produced by electron irradiation on Europa's surface.

We are directly evaluating the crystal structure of the irradiated NaCl samples after irradiation using the cathodoluminescence method developed by Sadgrove et al. [2022], which is a crystal structure analysis that does not easily alter samples. We will correlate lattice defects with color centers and analyze surface conditions more rigorously to estimate Europa's surface age.

References

1. S. K. Trumbo et al, Planet. Sci. J. 3 27(2022).
2. William T. P. Denman et al, Planet. Sci. J. 3 26 (2022).
3. M. Sadgrove et al, Technical Digest Series, (Optica Publishing Group), paper CTuP8A_03.(2022).

木星の氷衛星であるエウロパは内部海を持ち、生命の存在可能性が期待されている。その内部海と表層の間では物質の輸送が示唆されているため、表層組成の理解は内部海組成の理解につながる。しかし、表層物質は、木星磁気圏プラズマ等が照射され変性するため、内部海から輸送された直後の表層物質の組成は未解明である。内部海物質の噴出が活発であると推定されるカオス地形は斑点模様の地形が多く存在する。その地形の一部であるタラ地域では、450 nm と 230 nm に太陽光反射スペクトルの吸収構造が観測されている [Trumbo et al.,2022]。これらは、室内実験における NaCl への電子照射によって発生する反射率スペクトルの吸収構造と一致しており、NaCl 結晶中の格子欠陥に対応する色中心である可能性がある [Trumbo et al.,2022]。しかし、色中心による吸収の深さと照射条件の関連性は未解明な点が多く、色中心の観測から NaCl 中の格子欠陥等の結晶構造を推定することは困難であり、エウロパ表層の NaCl の変性の状態は推定できていない。

そこで本研究では、エウロパ表層を再現した環境下で、木星磁気圏を模した電子やイオンを、NaCl 試料に照射し、複数の光学的な物質分析を適用することで、色中心の吸収構造、照射条件、結晶構造を初めて関連付けることを試みた。粉体の NaCl に対し、室温 (300 K) でエネルギー 10 keV の電子を、総照射量 (2.3×10^{14}—3.2×10^{18}/cm^2) やフラックス (1.9×10^{12}—1.5×10^{15}/s/cm^2) のいずれかを一定に保ちつつ、他方を変化させて照射した。その結果、総照射量が大きいほど 460nm 付近の F 中心が減少し、720 nm 付近の M 中心は増加した。これは、Denman et al. [2022] の電子照射実験の結果と同様に、照射による変成によって F 中心が飽和した後、M 中心に変化した可能性を示す。また、総照射量が一定値のもとでは、フラックスが大きいほど F 中心、M 中心ともに増加したが、M 中心の方がより多く生成された。電子と水素分子イオンの両方を NaCl に照射した結果、水素分子イオン照射によって電子照射による F 中心や M 中心が減退した。これは、試料表面のイオンスパッタリングによる色中心生成の抑制を示唆している。Denman et al. [2022] のハッブル宇宙望遠鏡によって観測されたエウロパ昼夜の F 中心の分布と、電子照射実験との比較によると、フォトブリーチングによっても F 中心が崩壊し、M 中心生成には達しない可能性もある。これらの結果を総合すると、エウロパ表層では電子照射で生成された F 中心や M 中心が、スパッタリングとフォトブリーチングによって減退している可能性がある。

今後は、Sadgrove et al. [2022] で開発された、試料が変性しにくい結晶構造分析であるカソードルミネッセンス法を用いて、照射後の NaCl 試料の結晶構造を直接評価し、格子欠損と色中心の関連付けを行い、より厳密に表層状態を分析して表層年代の推定に紐づけていく。

3 次元磁気流体力学シミュレーションを用いた土星風及び太陽風によるタイタン大気散逸過程の比較

#高田 亮馬 [1)], 木村 智樹 [1)], 堺 正太朗 [2)], 前田 優樹 [3)], 中田 英太朗 [4)], 草野 百合 [1)], 寺田 直樹 [5)]
([1] 東京理科大学, [2] 東北大・理・地球物理, [3] 東京大学, [4] 北海道大学, [5] 東北大・理

Comparison of Titan's atmospheric escape processes by Saturn and Solar winds using 3D magnetohydrodynamic simulations

#Ryoma Takada[1)], Tomoki Kimura[1)], Shotaro Sakai[2)], Yuki Maeda[3)], Eitaro Nakada[4)], Yuri Kusano[1)], Naoki Terada[5)]
([1]Tokyo University of Science, [2]Department of Geophysics, Graduate School of Science, Tohoku University, [3]The University of Tokyo, [4]Hokkaido University, [5]Graduate School of Science, Tohoku University

Titan is the only body in our solar system with an abundant atmosphere of 1 atm pressure on the surface. Titan's atmosphere is nitrogen-dominated (nitrogen: 94%, methane: 5%, hydrogen: 1% Magee et al., 2009), like the atmospheric composition of past Earth just before biotic oxygen began to increase. Therefore, the evolutionary process of Titan's atmosphere is essential for elucidating the atmospheric evolution of the past Earth. The energy deposition to the atmosphere by Saturn's magnetospheric plasma precipitation responsible for the non-thermal atmospheric ion pickup and sputtering is likely more dominant than EUV in the upper atmosphere (Micheal et al., 2005), which is important for elucidating atmospheric evolution. Titan is located in Saturn's magnetosphere in almost all orbital phases and is blown by mainly the O^+ and H^+ in the magnetospheric plasma (Saturn wind). However, solar wind protons H^+ should significantly affect the atmosphere when the magnetosphere shrinks as the solar wind dynamic pressure increases, and Titan moves out of Saturn's magnetosphere (Bertucci et al., 2008). Since the global extent of non-thermal escape by the external plasma flows, the Saturn and solar winds are difficult to study only with spacecraft observations, numerical simulations have been used in comparison with observations (Modolo et al., 2008; Strobel, 2009; Gu et al., 2019). However, the previous studies did not treat the non-thermal escape for hydrogen and also not the Saturn and solar winds by the same method, thus the differences in the escape rates for the two external plasma flows were not fully discussed.

In this study, we simulated the global non-thermal escape of nitrogen and hydrogen, which are the main components of the atmosphere, using a 3D multi-component ion magnetohydrodynamic simulation developed by Terada et al. (2009), and evaluated the escape rate by the Saturn wind in comparison with that by the solar wind for the first time.

The non-thermal atmospheric escape was simulated under the Saturn wind conditions of O^+:0.2[/cm^3] density, 120 [km/s] velocity, H^+:0.1[/cm^3] density, 120 [km/s] velocity and 7.0 [nT] magnetic flux density (Sittler et al., 2009), resulting in an escape rate of 3.6×10^{23} [/s] for nitrogen-associated ions and 9.9×10^{23} [/s] for hydrogen-associated ions. On the other hand, under solar wind conditions with a density of 0.35 [/cm^3], a velocity of 360[km/s], and 0.5[nT] magnetic flux density (Bertucci et al., 2015), it resulted in 1.4×10^{23} [/s] for the nitrogen-associated ions and are 9.1×10^{24} [/s] for the hydrogen-associated ions. These results indicate that the Saturn wind suppresses the escape of the hydrogen-associated ions and enhances that of nitrogen-associated ions compared to the solar wind. This suggests that Saturn and solar winds control the abundance of hydrogen in Titan's atmosphere. The Saturn wind promotes a more hydrogen-rich reduced atmospheric composition, and the solar wind promotes oxidation. The quantitative evaluation of the escape rates for each ion species and the escape mechanisms still need to be evaluated, which we investigate in detail in the future. In this presentation, we report the current status of the above.

土星の衛星タイタンは、太陽系惑星の衛星の中で唯一豊富な表面で 1 気圧の大気を持つ。タイタン大気の組成は、酸素が増え始める直前の初期地球の窒素大気のそれと類似している (窒素:94%、メタン:5%、水素:1% Magee et al.,2009)。タイタン大気の進化過程を明らかにできれば、初期地球の大気進化の解明に寄与すると考えられる。特にイオンピックアップやスパッタリング等によって駆動される非熱的散逸過程は、大気粒子へのエネルギー付与率が EUV によるものよりも上層大気で優位であることが示唆されている (Micheal et al.,2005) ため、大気進化解明の上で重要である。タイタンは通常、土星磁気圏内に位置し磁気圏プラズマ中の主に O^+ や H^+(以下、土星風) に吹き付けられている。しかし太陽風動圧が強くなると磁気圏が縮小し、タイタンが土星磁気圏界面の外に出て (Bertucci et al.,2008)、大気は太陽風 H^+ の影響を大きく受けるはずである。土星風や太陽風といった外部プラズマ流による非熱的散逸の全容を解明するには、断片的な探査機観測では困難であるため、数値シミュレーションによる再現が観測と併用されてきた (Modolo et al., 2008; Strobel, 2009; Gu et al., 2019)。しかし先行研究では、水素について非熱的散逸の取り扱いがなく、また土星風と太陽風を同じ手法で扱っていないため、2 つの外部プラズマ流に対する散逸率の相違点等は議論はなされていない。

そこで本研究は、3 次元多成分イオン MHD シミュレーション (Terada et al.,2009) を用いて、大気の主成分である窒素と水素について非熱的散逸を全球的に模擬し、太陽風と土星風による散逸率の評価を初めて行った。カッシーニのその場観測データをもとに、土星風条件を O^+：密度 0.2[/cm^3]、速度 120[km/s]、H^+：密度 0.1[/cm^3]、速度 120[km/s]、磁場強度 7.0[nT] (Sittler et al., 2010) として散逸率を見積もった結果、散逸率が、窒素系イオン:3.6×10^{23}[/s]、水素系イオン:9.9×10^{23}[/s] であった。一方、太陽風条件を密度 0.35[/cm^3]、速度 360[km/s]、磁場強度 0.5[nT] (Bertucci et al.,2015)

として、散逸率を見積もった結果、窒素系イオン:1.4×10^{23}[/s]、水素系イオン:9.1×10^{24}[/s] となった。これらの結果から、土星風は太陽風に比べて水素系イオンの散逸を抑制し、窒素系イオンの散逸を促進させることがわかった。これは土星風と太陽風がタイタン大気の水素の存在率を制御することを示唆しており、土星風はより水素が豊富な還元型の大気組成を促進し、太陽風は酸化を促進する働きがあると考えられる。本研究ではタイタン大気の主要成分である窒素、水素について非熱的散逸の合計散逸率を推定したが、今後は、各イオン種の散逸率の定量評価や散逸のメカニズムについて精査していく予定である。本発表では、上記の現状を報告する。

R009-P14
ポスター 4 ：11/26　AM1/AM2 （9:00-12:00）

公転運動に起因するタイタン大気の時間変動

#中嶋 瑞穂 [1)], 高木 聖子 [1)], 有馬 銀河 [1)], 佐藤 光輝 [1)], 高橋 幸弘 [1)]
([1] 北海道大学

Time variations in the atmosphere of Titan caused by its orbital motion

#Mizuho NAKAJIMA[1)], Seiko Takagi[1)], Kirara Arima[1)], Mitsuteru SATO[1)], Yukihiro Takahashi[1)]
([1]Hokkaido University

The atmosphere of Saturn's moon Titan has a layered structure (troposphere, stratosphere, mesosphere, and thermosphere) similar to that of the Earth's atmosphere, and is composed mainly of nitrogen and methane. The methane concentration is 5% in the troposphere and about 1% in the upper atmosphere, and the other components are mostly nitrogen. Titan orbits Saturn with a period of about 16 days and passes through the plasma sheet in Saturn's magnetosphere. The Cassini spacecraft observed the heating of the thermosphere by energetic particles in the plasma sheet (e.g., Westlake et al., 2011). High-energy particles in Saturn's magnetosphere ionize nitrogen and methane, producing tholins that form the haze layer of the upper atmosphere (Sagan et al., 1984). Therefore, as Titan passes through the plasma sheet, variations in methane concentration and the optical thickness of the haze layer can be expected. Conventional observations avoid the methane absorption wavelengths, and the variation of methane concentration due to orbital motion remains unresolved. Observations of the haze layer by ground-based telescopes (Nichols-Fleming et al., 2021) report that the opacity of the haze layer fluctuates by 5 - 10% in a few weeks. However, no analysis of temporal variation in the haze layer has focused on orbital motion, and it is unclear whether there is any variation caused by orbital motion.

In this study, we conducted multi-wavelength imaging observations including methane absorption wavelengths (727 and 889 nm) from 2021 to 2024 using the Multispectral Imager (MSI) on the Pilika Telescope owned by Hokkaido University. Spectral analysis was performed based on aperture photometry to determine the reflectance of the methane absorption lines. The relationship between the reflectance and Titan's orbital motion was investigated. The reflectance was compared with an atmospheric radiative transfer model to quantify the methane concentration and the optical thickness of the haze layer. Data from the Huygens probe (Niemann et al., 2010; Tomasko et al., 2007) and HITRAN (Kochanov et al., 2016) were used as input to the atmospheric radiative transfer model and the optical properties of the tholins. The analysis suggests that reflectance at methane absorption wavelengths is related to orbital motion and tends to be smaller at the perihelion and larger at the aphelion. Three hypotheses were considered as possible reasons for this: energetic particle flux from Saturn's magnetosphere, solar flux, and variations in the height of the Haze layer. In this presentation, we discuss the validity of the hypotheses based on the quantitative evaluation of temporal variations in methane absorption and the optical thickness of the haze layer.

土星衛星タイタンの大気圏は地球大気圏と同様に層構造 (対流圏，成層圏，中間圏，熱圏) を持ち，主に窒素とメタンで構成されている．対流圏の上には光学的に厚いヘイズ層が存在する．タイタンは約 16 日周期で土星を公転し，土星磁気圏のプラズマシートを通過する．カッシーニ探査機はプラズマシート内の高エネルギー粒子が熱圏加熱を観測した (e.g., Westlake et al., 2011)．高エネルギー粒子は窒素とメタンを電離させ，ヘイズ層を形成する (Sagan et al., 1984)．したがって，タイタンのプラズマシート通過に伴う，メタン濃度及びヘイズ層の光学的厚さの変動が予想できる．しかし，従来の観測はメタン吸収波長を避けており，公転運動によるメタン濃度の変動は未解明である．また，地上望遠鏡によるヘイズ層の観測では，ヘイズ層の不透明度が数週間で 5 - 10% 変動すると報告している (Nichols-Fleming et al., 2021) が，ヘイズ層の時間変動について公転運動に注目して解析した例はなく，公転運動に起因する変動は不明である．

本研究は北海道大学が所有するピリカ望遠鏡のマルチスペクトル撮像装置 (MSI) を用いて，2021 年から 2024 年にわたりメタン吸収波長 (727, 889 nm) を含む多波長撮像観測を行った．得られた観測データからメタン吸収波長付近の反射率を導出し，さらに反射率とタイタン公転運動との関連性を調査した．得られた反射率を，大気放射伝達モデルと比較し，メタン濃度とヘイズ層の光学的厚さを定量した．大気放射伝達モデルに入力する大気モデルとヘイズ粒子の光学特性は，ホイヘンス探査機 (Niemann et al., 2010; Tomasko et al., 2007) 及び HITRAN(Kochanov et al., 2016) のデータを用いた．解析の結果，メタン吸収波長の反射率は公転運動に関係し，近土点で小さく，遠土点で大きい傾向が示唆された．この要因として，高エネルギー粒子フラックス，太陽光フラックス，ヘイズ層高度の変動の 3 つの仮説を検討した．本発表ではメタン吸収量及びヘイズ層の光学的厚さの時間変動の定量的評価に基づき，仮説の妥当性について議論する．

R009-P15
ポスター 4 ：11/26　AM1/AM2 （9:00-12:00）

#田所 裕康 [1)], 加藤 雄人 [2)]
([1] 東北学院大学, [2] 東北大・理・地球物理

Elastic scattering of keV electrons by water molecules around Enceladus: A test particle simulation

#Hiroyasu Tadokoro[1)], Yuto Katoh[2)]
([1]Tohoku Gakuin University, [2]Department of Geophysics, Graduate School of Science, Tohoku University

Saturn's inner magnetosphere is primarily composed of water group neutrals originated from Enceladus, which play a crucial role in plasma loss. Previous our studies have focused on electron loss due to elastic collisions with water molecules. We have previously estimated the electron loss rate and energy input into the atmosphere due to the elastic collisions between 500 eV to 50 keV electrons and water molecules. However, the peak energy of electron energy input has remained unidentified. We show this peak energy and re-evaluate the energy input into the atmosphere.

R009-P16
ポスター 4 ：11/26　AM1/AM2 （9:00-12:00）

系外惑星のオーロラ検出に向けた磁気圏-電離圏結合過程の汎用モデル開発

#アサ サティアグラハ [1)], 木村 智樹 [1)], 藤井 友香 [2)], 森野 隆盛 [1)]
([1] 東京理科大学, [2] 国立天文台

Development of Analytical Model Generalized for Exoplanetary Auroral Radio Emission

#Satyagraha Asa[1)], Tomoki Kimura[1)], Yuka Fujii[2)], Ryusei Morino[1)]
([1]Tokyo University of Science, [2]National Astronomical Observatory of Japan

Planetary aurora is believed to be a key for the direct detection of planetary magnetic fields and atmosphere. The circular polarization of the auroral radio emissions (Wu & Lee, 1979) enables them to be easily differentiated from other radio sources, and their emission frequency is theoretically proportional to the magnetic flux density in the radio source region. Therefore, auroral radio observations can directly constrain the magnetic field without relying on complex model assumptions. The auroral radio emission, however, has not been observationally detected from any exoplanet yet. Modeling of auroral radio emission is needed to predict which exoplanets are appropriate for auroral detection. Past modeling of exoplanetary aurora has been conducted, focusing on the Magnetosphere-Ionosphere coupling (Nichols, 2011, 2012) and Star-Planet Interaction mechanism (Saur et al., 2013), but have not been able to generally explain emissions from a variety of exoplanets. Here, we developed a new generalized analytical model of the Magnetosphere-Ionosphere(M-I) coupling that predicts the exoplanetary auroral radio power, based on the pioneering exoplanetary M-I coupling model by Nichols (2011, 2012). Our model assumes the flow speed distribution of the magnetosphere to estimate the auroral current density. This model is applicable to both Earth-like and Jupiter-like planets which have been addresed independently in previous models (Jupiter-like: Nichols et al., 2011, 2012; Earth-like: Nichols & Milan, 2016). Validation of our model with Jupiter and Saturn suggests that our model successfully describes the total auroral energy dissipated as Joule heating in the planet's magnetosphere (Jupiter: ˜450 TW; Saturn: ˜5 TW) within one order of magnitude of observations, and consistent with past modeling. We believe that our results on the total power dissipated as Joule heating will allow us to understand the polar atmospheric escape associated with the aurora of exoplanets when we apply our model to exoplanets in the future (Cowley et al., 2004; Gronoff et al., 2020). Furthermore, analysis of past models shows a 0.1% conversion efficiency of energy dissipated as Joule heating to radio emission (Cowley et al., 2002, 2004). Application of the convertion efficiency to our results suggests that the predicted radio emission power from Jupiter and Saturn agrees with obsrvational results within one order of magnitude (Jupiter: ˜450 GW; Saturn: ˜5 GW). We are currently validating and modifying our model based on comparative study with the auroral radio emission observations for other solar system bodies, ultracool (e.g., Kao et al., 2023) and brown dwarfs (e.g., Berger et al., 2001; Kao et al., 2016, 2018) before application to exoplanets. Here, we present the current status of our modeling and validation.

木星オーロラ電波の長期変動特性-II

#三澤 浩昭 [1)], 土屋 史紀 [1)]
[(1] 東北大・理・惑星プラズマ大気研究センター

Long-term variable nature of Jupiter's auroral radio emissions - II

#Hiroaki Misawa[1)], Fuminori Tsuchiya[1)]
[(1]Planetary Plasma and Atmospheric Research Center, Graduate School of Science, Tohoku Univeristy

It is known that Jupiter's auroral radio emission (hereafter "JAR") shows long term occurrence variations with the time scale of about a decade. The variations were first considered to be initiated by the solar and/or solar wind activities since the variations seemed to inversely correlate with the solar activity in 1960's. A longer term analysis were made in 1970's and showed that the variations relate with the Jovicentric declination of the earth (De) rather than the solar and/or solar wind activities. So far, their plausible causalities are considered to be mainly brought by the two geometrical effects; i.e., De relates to amount of reachable rays to the earth from the source regions, and the geocentric declination of Jupiter relates to incidence angle of the radio wave to the terrestrial ionosphere and varies the ionospheric shielding level (e.g. Oya+, 1984). However, when we think the solar cycle dependence on the terrestrial auroral radio activity (e.g. Kumamoto+, 2003), the solar and/or solar wind control directly affecting JAR may not be negligible for the long term variations.

In order to assess such the proposed causalities and the other effects, we have investigated occurrence features of Jupiter's radio emissions using the radio wave data observed by the WIND satellite with equal-quality for almost 30 years. We have derived occurrence probabilities from the data observed in the frequency range of about 0.7 to 14MHz ("HOM" to "DAM" radio wave ranges) for each timing around Jupiter's opposition. In the presentation, we will show the long time variable nature of JAR particularly for its CML (Central Meridian Longitude) occurrence dependence and evaluate possible causalities.

R009-P18
ポスター 4 ：11/26　AM1/AM2 （9:00-12:00）

#松岡 彩子 [1)], Dougherty Michele[2)], Brown Patrick[2)], Auster Hans-Ulrich[3)]
([1 京都大学, ([2Imperial College London, ([3Institut fur Geophysik und extraterrestrische Physik, Technische Universitat Braunschweig

Magnetic field experiment by Jupiter Icy Moons Explorer (JUICE) J-MAG and sensor alignment evaluation at the lunar-Earth flyby

#Ayako Matsuoka[1)], Michele Dougherty[2)], Patrick Brown[2)], Hans-Ulrich Auster[3)]
([1Graduate School of Science, Kyoto University, ([2Imperial College London, ([3Institut fur Geophysik und extraterrestrische Physik, Technische Universitat Braunschweig

The magnetometer (J-MAG) is one of the core instruments on the JUICE spacecraft and is critical for examining prime scientific objectives of the mission. Firstly, we are expecting to gain an understanding of the interior structure of the icy moons of Jupiter, specifically those of Ganymede, Callisto and Europa. We will be able to obtain the knowledge of the depth at which the liquid oceans reside beneath their icy surfaces. We are also interested in the configuration of internal magnetic fields and the induced magnetic fields arising within these oceans. Secondary, the magnetic field drives the plasma processes within the Jupiter system. Magnetic field observations allow for a better interpretation of dynamical plasma processes, auroral phenomena and various current systems within the Jovian magnetosphere.

Defined J-MAG science targets result in a requirement to determine accurate knowledge of the sensing orientation by two fluxgate sensors, MAGIBS and MAGOB, on the spacecraft. Due to the long MAG boom it is not possible to meet J-MAG's alignment requirement by mechanical stability alone. To evaluate the alignment error of the sensing direction, the spacecraft includes two orthogonal coils mounted around its body. The coils, JACS, can be driven with a current which produces a measurable magnetic field vector at the fluxgate sensors. This signal can then be used by the fluxgates to track the variation in the sensor alignment by the method that was developed for the Kaguya mission,

After the launch of JUICE we have operated JACS several times and made preliminary analysis of the fluxgate sensor alignment. And we operated JACS before and after the lunar-Earth flyby in August 2024. It is very valuable opportunity to examine the variation of the alignment, because the alignment could be determined also by the fitting the magnetometer data to the geomagnetic model. In the presentation we show the tentative results of the alignment calibration at the lunar-Earth flyby, and discuss the perspective of the feasibility of the alignment calibration at the Jovian orbit.

R009-P19
ポスター 4 ：11/26　AM1/AM2 （9:00-12:00）

#大畑 元 [1)], 中川 広務 [2)], 笠羽 康正 [1)], 村田 功 [3)], 片桐 崇史 [4)], 松浦 祐司 [5)], 平原 靖大 [6)], 山崎 敦 [7)]
([1] 東北大・理, [2] 東北大・理・地球物理, [3] 東北大院・環境, [4] 富山大・工, [5] 東北大院・医工, [6] 名古屋大院・環境学研究科, [7]JAXA/宇宙研

Test observations of natural lights by the mid-infrared laser heterodyne spectrometer with the hollow optical fiber coupler

#Hajime Ohata[1)], Hiromu Nakagawa[2)], Yasumasa Kasaba[1)], Isao Murata[3)], Takashi Katagiri[4)], Yuji Matsuura[5)], Yasuhiro Hirahara[6)], Atsushi Yamazaki[7)]
([1]Planetary Plasma and Atmospheric Research Center, Graduate School of Science, Tohoku University, [2]Department of Geophysics, Graduate School of Science, Tohoku University, [3]Department of Environmental Studies, Graduate School of Environmental Studies, Tohoku University, [4]Faculty of Engineering, University of Toyama, [5]Graduate School of Biomedical Engineering, Tohoku University, [6]Graduate School of Environmental Studies, Nagoya University, [7]The Institute of Space and Astronautical Science, Japan Aerospace Exploration Agency

Mid-infrared (IR) laser heterodyne spectroscopy can achieve an ultra-high wavelength resolution of λ/d λ >1,000,000 (frequency resolution: <30 MHz) at ˜10 μ m in wavelength (˜30 THz in frequency). The high dispersion observations for planetary atmosphere enables to measure wind velocities with a resolution of several 10 m/s and to detect trace gases including isotopomers. Notable successes for those targets have been accomplished on Venus, Mars, Jupiter, and Titan, by ground-based telescopes with heterodyne spectrometers. The spectrometers used in those observations consist of many optical elements to combine observed and laser lights. The size and weight become large, and their optical geometry requires high stability.

Fiber optics can simplify, downsize, and reduce the weight for those instruments. With this benefit, a near-IR heterodyne system with fiber couplers has been proposed as a space-borne instrument (Rodin et al., 2015). On the other hand, in mid-IR, there has been no fiber coupler with high transmission yet. In this study, we applied a new hollow optical fiber coupler to mid-IR laser heterodyne spectrometer. The coupler developed by Toyama University has high transmittance (˜61%) for CO2 laser light. The next step is to utilize them in the application for natural light measurements.

We evaluated the capability of the mid-IR laser heterodyne spectrometer with fibers and a fiber coupler for natural lights from the Sun and black body source. The results are as follows: (1) For the hollow fiber, the transmission efficiency of 89.6 %/m was achieved for incoherent natural light from the Sun. (2) Incoherent light from a black body source and coherent light from CO2 gas laser through fibers are mixed by a beam splitter. This heterodyne spectroscopy could achieve a similar sensitivity as the heterodyne instrument without fibers. (3) Two kinds of incoherent lights and a coherent light from CO2 gas laser through fibers are mixed by a hollow fiber coupler. The two lights are from a black body absorbed by a C2H4 gas cell and from the Sun absorbed by the Earth's atmosphere. Obtained spectra are similar to spectra generated by numerical calculation.

Our current heterodyne test system with the fibers and the fiber coupler showed 10,000K of system noise temperature. It is about 3 times worse than our system without the fiber coupler, indicating that the test system with the fiber coupler needs an integration time of 9 times longer to achieve the same noise intensity. We are now justifying the coupling of natural light source to the fiber input, because the incident angle of observed light from the expected telescope is larger than the ideal angle for the input of the fiber. We will also report the results of this evaluation and improvement.

R009-P20
ポスター４：11/26　AM1/AM2（9:00-12:00）

金属合金を用いた多層膜反射鏡の開発

#吉川 一朗[1)], 桑原 正輝[2)], 吉岡 和夫[3,4)], 村上 豪[5)], 鈴木 雄大[6)]
([1)] 東大, ([2)]Rikkyo Univ., ([3)] 東大・新領域, ([4)] 東大・新領域, ([5)]ISAS/JAXA, ([6)]JAXA/ISAS

Development of Multilayer Mirrors Using Metak Alloys

#Yoshikawa Ichiro[1)], Masaki Kuwabara[2)], Kazuo Yoshioka[3,4)], Go Murakami[5)], Yudai Suzuki[6)]
([1)]University of Tokyo, ([2)]Rikkyo University, ([3)]Department of Complexity Science and Engineering, The University of Tokyo,, ([4)]Department of Complexity Science and Engineering, The University of Tokyo,, ([5)]Institute of Space and Astronautical Science, Japan Aerospace Exploration Agency, ([6)]Institute of Space and Astronautical Science, Japan Aerospace Exploration Agency

At the beginning of the 21st century, imaging of the Earth's inner magnetosphere using extreme ultraviolet light (EUV) became possible, bringing significant achievements to the field of geophysics. A multilayer mirror that efficiently collects the resonance scattering line of singly ionized helium (wavelength 30.4 nm) played a key role in this success. By stacking 20 layers of molybdenum (Mo) and silicon (Si) on the mirror surface, the reflection rate, which would normally be less than a few percent, was increased to 20%, leading to the success of the "Nozomi" satellite's inner magnetosphere imaging. The "Kaguya" satellite carried out an ambitious attempt to provide a comprehensive view of the Earth's magnetosphere from lunar orbit, where Mo/Si multilayer mirrors also contributed to new achievements.

The Mo/Si multilayer mirrors possess numerous advantages, such as high resistance to environmental changes like temperature, humidity, and pressure, and can sometimes be cleaned if contaminated. For this reason, they are also utilized in the field of extreme ultraviolet lithography (EUVL), which uses a 13.5 nm wavelength as a light source.

As EUV imaging became recognized as one of the observational methods in the field of earth and planetary sciences, a team combining science and engineering was recently formed at the University of Tokyo, which developed the ultra-small (6U) satellite "EQUULEUS." To mount an EUV imager on a 6U-sized satellite, it was necessary to reduce the mirror surface area to about half of the conventional size, which required improving the multilayer reflectivity by at least twofold. At that time, the project leader focused on the fact that multilayer mirrors composed of magnesium (Mg) and silicon carbide (SiC) (and also B4C and Mg) exhibited high reflectivity, aiming to miniaturize the imager.

The reflectivity of the Mg/SiC multilayer mirror that was manufactured reached over twice that of the Mo/Si multilayer mirror (about 50%) in laboratory calibration experiments, but it was discovered that exposing the mirror to slightly high humidity (˜65%) or high temperature (˜55° C) for a short period led to the formation of spots, as shown in Figure 2, resulting in a decline in reflectivity. It was identified that these spots did not occur on the surface of the multilayer mirror, but rather at the interfaces between the layers, where Mg was found to diffuse into the SiC layer, causing interfacial degradation. However, no decisive solution to this problem has been found.

Because Mg and Al have low absorption (k) and high refractive index in the EUV wavelength region (making them optimal as one part of a multilayer pair), researchers in space science worldwide, as well as in the EUV lithography field (EUVL), have attempted to use them in multilayer mirrors. However, through joint research with industrial researchers in the EUVL field, it was found that Mg and Al exhibit significant diffusion at the interfaces, making it difficult to create stable interfaces. It seems that researchers around the world share this understanding.

In this study, we present experimental results on the use of Mg and Al alloys, which cannot form stable interfaces as single elements, as materials for multilayer mirrors.

２１世紀の初頭、極端紫外光（ＥＵＶ）を用いた地球内部磁気圏の撮像が可能となり、ヘリウム一価イオンの共鳴散乱線（波長 30.4nm）を効率よく集光する多層膜反射鏡が、地球物理学の分野に大きな成果をもたらした。Ｍｏ（モリブデン）とＳｉ（シリコン）を２０層、鏡の表面に積層することにより通常では数%にも満たない鏡の反射率が２０%にまで向上し、「のぞみ」衛星の内部磁気圏撮像を成功に導いた。「かぐや」衛星では月の周回から地球磁気圏を一望するという野心的な試みを遂行し、ここでもＭｏ/Ｓｉの多層膜反射鏡が新しい成果の創出に貢献した。Ｍｏ/Ｓｉ多層膜は、温度、湿度や圧力などの環境変化に対する耐力が高く、汚染しても洗浄できる場合がある等の利点が多い。そのため、１３．５ nm を光源とする極端紫外光リソグラフィ（ＥＵＶＬ）分野でも利用されている。
地球惑星科学分野における観測手段の一つとしてＥＵＶによる撮像が認知されるに至り、最近、東京大学内で理工一体チームを編成し、超小型（６Ｕ）衛星エクレウスを開発した。６Ｕサイズの衛星にＥＵＶ撮像機を搭載するには従来の反射鏡面積を約半分に縮小する必要があり、それを補うために多層膜の反射率を最低でも２倍程度にまで向上させる必要が

ある。当時、研究代表者は、Mg と SiC（並びに B4C と Mg）からなる多層膜が高い反射率を持つ事に注目し、撮像機の小型化を図った。

製造した Mg/SiC 多層膜鏡の反射率は、室内校正実験ではＭｏ／Ｓｉ多層膜の２倍以上の反射率（５０％程度）を製造直後には達成していたが、やや高い湿度（～６５％）や高温（～５５℃）に短時間曝すだけで、図２に示す斑点が多層膜反射鏡に発生し、反射率が低下することが解ってきた。これらの斑点は多層膜の表面に発生したのではなく、多層膜の層の界面においてＭｇがＳｉＣ層に拡散し、界面を犯していることが原因であるところまでは突き止めたが、決定的な改善策は見つかっていない。

ＭｇとＡｌはＥＵＶ波長領域においてｋが小さく（吸収が小さい)、屈折率が大きい（多層膜のペアの一方としては最適である）事から、これまでにも世界各国の宇宙科学研究者のみならず、極端紫外光露光リソグラフィ分野（ＥＵＶＬ）が、多層膜反射鏡への利用を試みてきた。様々な材料の組み合わせを極端紫外光露光リソグラフィ分野（ＥＵＶＬ）の民間企業の研究者と検討したが、Ｍｇ、Ａｌは界面での拡散が大きく、安定した界面ができないことが分かってきた。世界の研究者もそのように理解しているようである。

本研究では、単体では安定な界面を生成できない Mg や Al を合金として用いた場合の実験結果について紹介する。

R009-P21
ポスター 4 ：11/26　AM1/AM2 （9:00-12:00）

#村上 豪 [1)], 土屋 史紀 [2)], 鍵谷 将人 [3)], 山崎 敦 [4)], 吉岡 和夫 [5)], 木村 智樹 [6)], 桑原 正輝 [7)], 亀田 真吾 [8)]
([1]ISAS/JAXA, [2 東北大・理・惑星プラズマ大気, [3 東北大・理・惑星プラズマ大気研究センター, [4]JAXA/宇宙研, [5 東大・新領域, [6]Tokyo University of Science, [7]Rikkyo Univ., [8 立教大

LAPYUTA mission: instrument overview and technical developments

#Go Murakami[1)], Fuminori Tsuchiya[2)], Masato Kagitani[3)], Atsushi Yamazaki[4)], Kazuo Yoshioka[5)], Tomoki Kimura[6)], Masaki Kuwabara[7)], Shingo Kameda[8)]
([1]Institute of Space and Astronautical Science, Japan Aerospace Exploration Agency, [2]Planetary Plasma and Atmospheric Research Center, Graduate School of Science, Tohoku University, [3]Planetary Plasma and Atmospheric Research Center, Graduate School of Science, Tohoku University, [4]The Institute of Space and Astronautical Science, Japan Aerospace Exploration Agency, [5]Graduate School of Frontier Sciences, The University of Tokyo,, [6]Tokyo University of Science, [7]Rikkyo University, [8]Rikkyo University

The Life-environmentology, Astronomy, and PlanetarY Ultraviolet Telescope Assembly (LAPYUTA) mission aims to carry out spectroscopy with a large effective area (>300 cm2) and a high spatial resolution (0.1 arc-sec) and imaging in far ultraviolet spectral range (110-190 nm) from a space telescope. The main part of the science payload is a Cassegrain-type telescope with a 60 cm-diameter primary mirror. As a current design, three main UV instruments are installed on the focal plane of the telescope: a mid-dispersion spectrograph, a high-dispersion spectrograph, and a slit imager. The mid-dispersion spectrograph contains a movable slit with different slit width, a holographic toroidal grating with 2110 lines/mm, and an MCP detector coupled with CMOS imaging sensors. Spectral resolution of 0.02 nm and field-of-view of 100 arc-sec will be achieved. The high-dispersion spectrograph consists of a slit, a toroidal mirror, an echelle gating, a cross disperser, and a detector. Highest spectral resolution of 3 pm will be achieved at the target wavelength (130.5 nm). The UV slit imager consists of imaging optics, several bandpass filters with a rotation wheel, and a same type of UV detector as the one installed in the spectrometer. In order to achieve a high spatial resolution of 0.1 arc-sec, we will install a target monitoring camera at 0th order position inside the spectrometer and slit imager for both attitude control and image accumulation process. We also plan to install a fine guidance sensor to monitor guidance stars. In addition, new technologies such as funnel-type MCPs and CMOS-coupled readout system and highly reflective UV coating will be applied to satisfy requirements of LAPYUTA. Here we present the LAPYUTA concept design, the overview of the spacecraft and instruments, and the status of technical developments.

R009-P22
ポスター 4 ：11/26　AM1/AM2 （9:00-12:00）

#横田 勝一郎 [1)], 北村 悠稀 [1)], 齋藤 義文 [2)], 浅村 和史 [3)], 笠原 慧 [4)]
([1] 大阪大, [2] 宇宙研, [3] 宇宙研, [4] 東京大学

Calibration test of an ion energy mass spectrum analyzer onboard the Martian Moons eXploration (MMX) spacecraft

#Shoichiro Yokota[1)], Yuki Kitamura[1)], Yoshifumi Saito[2)], Kazushi Asamura[3)], Satoshi Kasahara[4)]
([1]Osaka University, [2]Institute of Space and Astronautical Science, Japan Aerospace Exploration Agency, [3]Institute of Space and Astronautical Science, Japan Aerospace Exploration Agency, [4]The University of Tokyo

We will report the results of the calibration test of the ion energy mass spectrum analyzer for the Martian Moons eXploration (MMX) mission. The MMX mission is a sample return project planned by the Japan Aerospace Exploration Agency (JAXA) to investigate the origin of the Martian moons and physical processes in the Martian environment. The ion analyzer is a component of the mass spectrum analyzer (MSA), along with the two magnetometers, which measures distribution functions and mass distributions of low-energy (<~10s keV) ions. The MSA will measure ions emitted from Phobos and its torus as well as escaping ions from the Martian atmosphere with monitoring the solar wind to address the MMX science goals.

The ion analyzer employs nearly the same measurement techniques as that of Ion energy Mass Analyzer (IMA) for the Kaguya mission and mass spectrum analyzer (MSA) for BepiColombo/MIO. The ion analyzer is cylindrically symmetric in shape and consists of an energy analyzer and a mass analyzer (see the figure). The aperture of 360 degrees near the sensor top and neighboring angular scanning deflectors provide a 2-pi steradian field-of-view (FOV). The energy analyzer measures energy/charge using a top-hat electrostatic method in which the inner spherical electrode is applied with a sweeping negative high voltage. In the mass analyzer, mass/charge is measured by a time-of-flight (TOF) method that uses a linear-electric field (LEF) for the higher mass resolution. At the entrance of the mass analyzer, ultra-thin carbon foil is mounted on a metal grid to emit secondary electrons for start signals. The TOF chamber is longer than that of the previous analyzers and is optimized to achieve a high mass resolution (m/dm~100).

Calibration tests of the ion analyzer were conducted at JAXA's Sagamihara Campus from Fall 2022 to Winter 2024. When acquiring detailed calibration data, the tests were separated into the energy analysis section and the mass spectrometry section, and each performance test was conducted. Through a series of tests, it was confirmed that all performance requirements were met.

R009-P23
ポスター 4 ：11/26　AM1/AM2 （9:00-12:00）

#原田 裕己 [1)], Cravens Thomas E.[2)], Brain David A.[3)], Halekas Jasper S.[4)]
([1 京大・理, ([2 カンザス大学, ([3LASP, ([4 アイオワ大学

Exploring Magnetic Reconnection at Mars With MAVEN: A Unique Natural Laboratory of Multi-Ion and Collisional Plasmas

#Yuki Harada[1)], Thomas E. Cravens[2)], David A. Brain[3)], Jasper S. Halekas[4)]
([1Graduate School of Science, Kyoto University, ([2Department of Physics and Astronomy, University of Kansas, ([3Laboratory for Atmospheric and Space Physics, University of Colorado, Boulder, ([4Department of Physics and Astronomy, University of Iowa

Thanks to accumulated data of comprehensive plasma and field measurements at Mars by MAVEN, a growing number of papers have reported observational signatures associated with magnetic reconnection in the Martian plasma environment. The recent results collectively indicate that magnetic reconnection occurs in a wide variety of plasma regions around Mars: in the magnetotail, above strong crustal magnetic fields, at magnetospheric boundaries, and in the ionosphere. Here we explore two frontiers of Martian reconnection research: (i) reconnection and aurora and (ii) collisional reconnection.

(i) Based on recent auroral observations, it is proposed that the discrete aurora at Mars is driven by reconnection between the draped IMF and crustal fields. This hypothesis provides a testable prediction of the location and condition of reconnection occurrence. We investigate ion flow patterns above strong crustal fields in comparison to the predicted location of X-lines. We analyze velocity distribution functions of multiple ion species in detail.

(ii) MAVEN's orbit is designed to explore the collisional ionosphere of Mars below the exobase around the periapsis. We upgrade Harada et al. (2020)'s algorithm to identify low-altitude current sheets and reconnection jets within them. From the identified current sheets and ion jet events, we investigate ion-neutral friction effects on reconnection outflows as proposed by Cravens et al. (2020).

R009-P24
ポスター 4 ：11/26　AM1/AM2 （9:00-12:00）

#中村 勇貴 [1)], 関 華奈子 [2)], 吉田 辰哉 [3)], 寺田 直樹 [3)], 小山 俊吾 [4)], 堺 正太朗 [5)]
([1] 東大, [2] 東大理・地球惑星科学専攻, [3] 東北大・理, [4] 東北大, [5] 東北大・理・地球物理

Enhancement of hydrogen escape from the early Martian atmosphere induced by the precipitation of solar energetic particles

#Yuki Nakamura[1)], Kanako Seki[2)], Tatsuya Yoshida[3)], Naoki Terada[3)], Shungo Koyama[4)], Shotaro Sakai[5)]
([1]Graduate School of Science, The University of Tokyo, [2]Department of Earth and Planetary Science, Graduate School of Science, University of Tokyo, [3]Graduate School of Science, Tohoku University, [4]Tohoku University, [5]Graduate School of Science, Tohoku University

Hydrogen escape from the Martian atmosphere is crucial for understanding its redox state and water loss. The Jeans escape flux of hydrogen on Mars is regulated to be twice the nonthermal escape flux of oxygen, called self-regulation (e.g., McElroy and Donadue, 1972; Koyama et al., 2021).

Nakamura et al. (2023) suggested that the precipitation of solar energetic particles into the present-day Martian atmosphere enhances the production of H and OH pair due to cluster ion chemistry driven by SEP-induced atmospheric ionization. The flare observations of solar-type G stars by the Kepler mission suggested that our Sun should have been much more active, and intense SEP events could have hit the planetary atmospheres repeatedly 4 billion years ago (e.g., Shibayama et al. 2013; Lingam et al., 2018). Such a continuous precipitation of SEPs into the early Martian atmosphere could have enhanced the dissociation of water vapor and increased hydrogen escape.

In this study, we explored the impacts of SEPs on the escape rate of hydrogen from the early Martian atmosphere using an atmospheric ionization model based on continuous slowing down approximation and a one-dimensional photochemical model (Nakamura et al., 2023a, 2023b). We found that the dissociation of water vapor by SEP-induced ion chemistry is more than an order of magnitudes higher than the photolysis rate. In an atmosphere without H2 degassing, the precipitation of SEPs establishes a new steady state solution of atmospheric composition, and the hydrogen escape rate is no longer self-regulated. The escape rate of hydrogen increases proportionally to the energy flux of SEPs if the continuous SEP energy flux is more than ˜1 erg cmˆ-2 sˆ-1. Such an effect of SEPs on hydrogen escape suppresses as the H2 degassing rate increases.

References:

McElroy, M. B., and Donahue, T. M. (1972) Science, 177, 986-988.
Koyama, S., et al. (2021). The Astrophysical Journal, 912(2), 135.
Lingam, M., et al. (2018). The Astrophysical Journal, 853(1), 10.
Shibayama, T., et al. (2013). The Astrophysical Journal, 209:5.
Nakamura, Y., et al. (2023). Earth Planets and Space, 75(1), 140.
Nakamura, Y., et al. (2023). Journal of Geophysical Research: Space Physics, 128, e2022JA031250.

R009-P25
ポスター 4 ：11/26　AM1/AM2 （9:00-12:00）

初期の火星・地球大気における太陽高エネルギー荷電粒子照射によるペプチドの非生物合成

#櫻井 悠貴 [1)], 木村 智樹 [1)], 鳥越 秀峰 [1)], 小林 憲正 [2)], 奥村 宣明 [3)], 福井 康祐 [1)], 小木 菜々夏 [1)], 吉村 弥生 [1)], 寺田 直樹 [4)]
([1] 東京理科大学, [2] 横浜国立大学大学院工学研究院, 東京工業大学理学院, [3] 大阪大学蛋白質研究所, [4] 東北大学大学院理学研究科地球物理学専攻

Abiotic synthesis of peptides driven by the solar energetic particles in early Martian and terrestrial atmospheres

#Yuki Sakurai[1)], Tomoki Kimura[1)], Hidetaka Torigoe[1)], Kensei Kobayashi[2)], Nobuaki Okumura[3)], Kosuke Fukui[1)], Nanaka Kogi[1)], Yayoi Yoshimura[1)], Naoki Terada[4)]
([1]Tokyo University of Science, [2]Faculty of Engineering, Yokohama National Univ., Tokyo Institute of Technology, School of Science, [3]Institute for Protein Research, Osaka University, [4]Department of Geophysics, Graduate School of Science, Tohoku University

The origin of amino acids, peptides, proteins, and their precursors is the most important issue for elucidating the origin and evolution of life on planets with the atmosphere and ocean. It has been theoretically predicted that these prebiotic substances were synthesized abiotically from atmospheric molecules by any energy injections: e.g., lightning discharge, solar ultraviolet photon, and Solar Energetic Particles (SEP). Many laboratory experiments have been conducted for the abiotic synthesis of prebiotic substances from the atmosphere by various energy injections [e.g., Miller, 1953]. Most of these laboratory experiments modeled the early Martian and terrestrial environments with mildly reduced (CO or CO_2, H_2O, N_2) and strongly reduced (CH_4, H_2O, NH_3) atmospheres. Proton irradiation experiment for modeling the solar energetic particle (SEP) injections most effectively produced amino acids and their bound macromolecules called tholins [Sagan and Khare, 1979] from both the mildly and strongly reduced atmospheric molecules [Kobayashi et al., 1990, 2023]. However, because only the amino acids and tholins were found in the previous studies, the formation of peptides from amino acids bounding and abiotic evolution to the protein have been not evaluated yet.

Here we focused on the sulfur dioxide, which is abundant around the volcanoes on early Mars and Earth and highly reactive for the chemical process in the atmosphere. With the assumption that the sulfur-containing amino acid was abiotically synthesized from the volcanic atmosphere as well as the non-sulfuric amino acids, we evaluated the abiotic synthesis of peptides from these starting substances based on the laboratory plasma irradiation experiment. We irradiated a powder sample of non-sulfuric amino acids composed of 74.6% glycine, 19.9% alanine, and 5.49% serine, and a sample with sulfur-containing amino acid (cysteine) composed of 73.3% glycine, 19.6% alanine, 5.39% serine, and 1.77% cysteine with hydrogen ions at 10 keV with a beam current of 7 μ A for an hour. Based on the high-performance liquid chromatographic analysis, we detected peaks only in irradiated samples containing sulfur-containing amino acids. The N-terminal amino acid sequence analysis of the detected peaks showed that the product substance have multiple peptide bonds, suggesting that it may contain alanine as one of the constituents. The mass spectrometry analysis of peptide constituents other than alanine showed no values consistent with proteinogenic amino acids. The peptides formed are considered to consist of alanine and non-proteinogenic amino acids. This demonstrated that sulfur-containing amino acids promote the bonding of amino acids to form peptides under hydrogen irradiation.

These results suggested that the peptides were abiotically synthesized in the atmosphere around the volcanoes on early Mars and Earth. We are going to address the structural analysis of the peptide, and abiotic synthesis of peptide and protein from gases based on energetic proton irradiation of atmospheric molecules containing sulfur.

Kobayashi, K., Tsuchiya, M., Oshima, T. and Yanagawa, H.: 1990, Origins of Life and Evolution of the Biosphere 20, 99-109.

Kobayashi, K., Ise, J., Aoki, R., Kinoshita, M., Naito, K., Udo, T., Kunwar, B., Takahashi, J., Shibata, H., Mita, H., Fukuda, H., Oguri, Y., Kawamura, K., Kebukawa, Y. and Vladimir, S. A.: 2023, Life 2023, 13, 1103. Miller, S. L.: 1953, Science 117, 528.

Sagan, C. and Khare, B. N.: 1979, Nature 277, 102-107.

大気や海洋を有する惑星において、生命の発生に必要なアミノ酸やタンパク質の起源は未解明である。タンパク質の基礎となるペプチド、アミノ酸や、その前駆体の起源を解明することは、生命の起源や発生条件の理解をする上で最重要の課題である。これらの生命前駆物質が、大気へのエネルギー入射により大気分子から非生物的に合成されたとする説があり、様々な初期惑星大気とエネルギーの組み合わせで非生物的合成実験が行われてきた [e.g. Miller, 1953]。初期の火星や地球の大気は主に弱還元型（CO または CO_2, H_2O, N_2）と強還元型（CH_4, H_2O, NH_3）の 2 種類が提案されているが、いずれの場合も太陽高エネルギー粒子 (Solar Energetic Particles, SEP) を模した陽子照射室内実験により大気分子からアミノ酸や、構造が一定でないソリンと呼ばれる高分子の物質 [Sagan and Khare, 1979] が生成されることが分かっている

[Kobayashi et al., 1990, 2023]。しかし、先行研究はアミノ酸とソリンの合成までにとどまっており、アミノ酸の重合によるペプチド形成や、タンパク質への非生物的進化は未検証である。

そこで本研究は、初期の火星・地球の火山周辺に豊富に存在し、反応性の高い硫黄ガスに注目した。硫黄を含むアミノ酸が、他のアミノ酸と同様に SEP により大気中で非生物的に合成されたと仮定し、それらを母物質としたペプチドの非生物的合成をプラズマ照射実験で検証した。実験室において初期の火星・地球大気から生成されるアミノ酸組成（グリシン 74.6%、アラニン 19.9%、セリン 5.49%, Kobayashi et al., 1989）を模した粉体サンプルと、含硫アミノ酸（システイン）を含む粉体サンプル（グリシン 73.3%、アラニン 19.6%、セリン 5.39%、システイン 1.77%）へ、水素分子イオン（10keV, 7 μ A）を 1 時間照射した。高速液体クロマトグラフィー分析の結果から、含硫アミノ酸を含む照射サンプルのみから検出されるピークが確認された。検出されたピークを分取し、N 末端シーケンス解析をした結果、生成物質はペプチド結合を複数持ち、構成物質としてアラニンが含まれている可能性が示唆された。アラニン以外のペプチドの構成物質について精密質量分析した結果、タンパク質合成アミノ酸に合致する値は観測されなかった。このことから、含硫アミノ酸はアミノ酸同士からのペプチド形成を促進することが明らかになった。また、生成したペプチドは、アラニンと非タンパク質構成アミノ酸から成ると考えられる。これらは、初期火星・地球の火山付近の大気中において、ペプチドが SEP により非生物合成されていることを示唆する。今後は、ペプチドのさらなる構造分析や、硫黄を含む大気分子への高エネルギープロトン照射実験により、気体からペプチドやタンパク質の非生物合成に取り組む予定である。

R009-P26
ポスター 4 ：11/26　AM1/AM2 （9:00-12:00）

火星全球気候モデル（MGCM）を用いたグローバルダストストーム中における下層・中層大気の非移動熱潮汐の解析

#長田 章嗣 [1)], Liu Huixin[1)], Rafkin Scot[2)], Hartwick Victoria[2)], 中川 広務 [3)]
([1] 九大・理・地惑, [2]Southwest Research Institute, Boulder Office, [3] 東北大・理・地球物理

Analysis of Mars Non-Migrating Tides in Lower-Middle Atmosphere during Global Dust Storms using Mars Global Climate Model (MGCM)

#Noritsugu Nagata[1)], Huixin Liu[1)], Scot Rafkin[2)], Victoria Hartwick[2)], Hiromu Nakagawa[3)]
([1]Department of Earth and Planetary Sciences, Graduate School of Science, Kyushu University, [2]Southwest Research Institute, Boulder Office, [3]Department of Geophysics, Graduate School of Science, Tohoku University

To understand the Martian atmosphere, the study of dust storms, which play a critical role in its dynamics, is crucial. In particular, the atmosphere is greatly impacted by Global Dust Storms (GDS), which cover the entire planet and occur roughly once every decade. Spacecraft observations, such as MAVEN, have provided important insights regarding the effects of GDS on the upper atmosphere of Mars. Due to the difficulties in detecting the lower and middle atmospheres during dust storms, little is known about the process of its vertical propagation from the lower atmosphere (~50 km), where dust storms happen, to the upper atmosphere.

In this study, we aim to investigate how non-migrating thermal tides are influenced by GDS, using the Mars Global Climate Model (GCM). Non-migrating tides are a specific type of thermal tide, that is primarily driven by solar radiation. While thermal tides typically propagate westward in the opposite direction with Mars's rotation, non-migrating tides look fixed in relation to the planet's surface.

The production of non-migrating tides is mostly dependent on heating in the dust layer, which is significantly altered during dust storms, particularly GDS. Dust can modify the formation and vertical propagation of non-migrating tides, with effects potentially extending to the upper atmosphere.

Using the NASA Ames Global Climate Model (GCM), this study analyzes the formation and propagation of non-migrating tides and changes in atmospheric circulation during GDS. By comparing these findings to normal Martian Years, we aim to further unravel the influence that GDS has on the atmosphere of Mars.

火星大気を理解する上で、ダストストームはとても重要な現象である。特に、約 10 年に一度発生する惑星全体を覆う全球ダストストーム（Global Dust Strom: GDS）は、大気に多大な影響を及ぼす。MAVEN 探査機などの観測により、GDS が火星の超高層大気に与える影響については広く研究が進められている。しかし、下層・中層大気の観測の難しさなどから、GDS 発生が発生する下層大気（～高度 50 km）から超高層大気に至る伝播過程については、未だ十分に解明されていない。

そこで本研究では、火星全球気候モデル（GCM）を用いて、GDS が火星大気の非移動熱潮汐（non-migrating tide）に与える影響の解明を目指す。非移動熱潮汐は、主に太陽放射により形成される熱潮汐の一種である。熱潮汐は太陽の動きに伴って火星の自転と反対方向、すなわち西向きに移動するが、非移動熱潮汐は太陽放射に加えて、大気中の熱放射や地形などの影響を受けるため、自転に対して静止しているように見える。

非移動熱潮汐の形成に関与する大気中の熱放射は、ダストストーム（特に GDS）によって大きく変化する。大気中に巻き上げられたダストが層を形成し、その上下で異なる熱放射が生じる。これにより、非移動熱潮汐の形成や鉛直伝播過程も変化し、その影響は超高層大気にまで及ぶと考えられている。

本研究では、NASA Ames Global Climate Model (GCM) を用いて、GDS 中における非移動熱潮汐の形成・伝播過程及び大気循環の変化を解析し、通常時との違いを考察することで、GDS が火星大気に与える影響の解明に繋げる。

火星全球気候モデル DRAMATIC MGCM の現状：マルチスケールモデリングとデータ同化に向けて

#黒田 剛史 [1)], 鎌田 有紘 [1)], 古林 未来 [1)], 杉本 憲彦 [2)]
([1] 東北大・理, [2] 慶應大

The current state of DRAMATIC MGCM: Towards the multi-scale modeling and data assimilation

#Takeshi Kuroda[1)], Arihiro Kamada[1)], Mirai Kobayashi[1)], Norihiko Sugimoto[2)]
([1]Department of Geophysics, Tohoku University, [2]Keio University

The DRAMATIC (Dynamics, RAdiation, MAterial Transport and their mutual InteraCtions) MGCM (Mars Global Climate Model) has been developed on the dynamical core of MIROC (Model for Interdisciplinary Research On Climate) spectral solver for the terrestrial climate modeling, and used for the investigations of atmospheric dynamics (baroclinic waves, semi-annual oscillation, winter polar warming induced by a global dust storm, etc.) and material transport (CO_2, water, and dust cycles) on Mars, as well as the collaborations with observations.

Now we have updated the dynamical and physical schemes of the MGCM. Now the MGCM is based on MIROC6 [Tatebe et al., 2019] and the definition of vertical layers has been updated to the hybrid sigma-pressure coordinate. Also, we have implemented the dust cycle with 6 particle mode radii (0.0625, 0.125, 0.25, 0.5, 1, and 2 μ m), in whch dust is injected from surface along with 3-dimensional (latitude, longitude, and time) dust scenarios for past observations [Montabone et al., 2015, 2020] and part of the dust particles works as nuclei of water ice clouds. The formation of water ice clouds is based on Montmessin et al. [2004], and the radiative effects of water ice clouds, CO_2 ice clouds, and water vapor have been newly implemented.

In the current simulations with horizontal resolution of T21 (~5.6 degrees or ~333km), we have reproduced the zonal-mean temperature fields and water ice distributions consistently with MRO-MCS observations [McCleese et al., 2010] as well as their diurnal changes (note that MRO-MCS has observed them for local times of 3PM and 3AM). Now we are starting the simulation with higher horizontal resolution of T106 (~1.1 degrees or ~333km) for the reproduction of the generation and propagation of gravity waves as our simulations with the previous version of MGCM [Kuroda et al., 2015, 2015, 2019, 2020].

In addition, we are developing a regional mesoscale model using the SCALE (Scalable Computing for Advanced Library and Environment) 3-dimensional fully compressible non-hydrostatic dynamical core [Nishizawa et al., 2015] and common physical schemes with DRAMATIC MGCM. We have made test simulations with the horizontal resolution of down to 1 km in Acidalia Planitia. Moreover, we are planning the data assimilation using available observational datasets, such as MRO-MCS, using the LETKF (Local Ensemble Transform Kalman Filter) method based on our experiences for Venus atmosphere [Sugimoto et al., 2017; Fujisawa et al., 2022]. The reanalysis data being produced will be used as boundary conditions of the regional mesoscale model for the reproductions of past multi-scale meteorology on Mars to investigate the mechanisms of the occurrences and expansions of dust storms which have been observed.

Our multi-scale simulation and data assimilation aim to collaborate with the future Mars missions, such as MMX (Martian Moons eXploration) [Kuramoto et al., 2022; Ogohara et al., 2022] which is launching in 2026, towards the realization of weather forecasting on Mars for the era of human activities on Mars.

R009-P28
ポスター 4 ：11/26　AM1/AM2 （9:00-12:00）

#侯 成澤 [1)], 今村 剛 [2)], 杉山 耕一朗 [3)], ラフキン スコット [4)]
([1] 東京大学, [2] 東京大学, [3] 松江高専, [4] サウスウエスト・リサーチ・インスティテュート

Numerical Simulation of Arsia Mons Cloud on Mars

#Chengze Hou[1)], Takeshi Imamura[2)], Koichiro Sugiyama[3)], Scot Rafkin[4)]
([1]The University of Tokyo, [2]Graduate School of Frontier Sciences, The University of Tokyo, [3]National Institute of Technology, Matsue College, [4]Southwest Research Institute

Arsia Mons is located on the Tharsis Plateau near Mars' equator and is the southernmost of the three major shield volcanoes. It features a large caldera at its summit and a gentle slope. Recent studies by Hernandez et al. (2021, 2022) have investigated the elongated clouds over Arsia Mons through long-term observations and mesoscale modeling. Their research supports the mechanisms described by Michaels et al. (2006), demonstrating how the mountain disturbs the atmosphere.

The formation of water-ice over Arsia Mons is a natural laboratory for understanding the distribution of water vapor and the lifecycle of water-ice clouds on Mars. Our study focuses on the Arsia Mons Elongated Cloud, beginning with the use of NASA's Global Climate Model (GCM) to understand the cloud's seasonal dynamics. Subsequent numerical simulations suggest that while the GCM may not fully represent Martian conditions, the clouds over Arsia Mons are the result of multiple factors interacting at different scales.

R009-P29
ポスター 4 ：11/26　AM1/AM2 （9:00-12:00）

#今井 正尭 [1)], 高木 征弘 [2)], 安藤 紘基 [2)]
[(1] 東大 天文センター, [(2] 京産大

Synoptic-scale vortices in the lower cloud layer reproduced by AFES-Venus GCM

#Masataka Imai[1)], Masahiro Takagi[2)], Hiroki Ando[2)]
[(1]Institute of Astronomy, The University of Tokyo, [(2]Kyoto Sangyo University

The Japanese Venus Climate Orbiter Akatsuki captures Venus images of lower latitudes. The onboard 2-μ m camera (IR2) detected a synoptic-scale vortex between 20^o and 30^o latitude, exclusively in the northern hemisphere, appearing as spiral-shaped clouds on the planet's nightside. Similar large-scale vortices were simulated using a general circulation model (GCM) named AFES-Venus.

In these simulations, the vortex forms around 60 km high within the lower cloud layer, featuring poleward and upward winds on the east (leading) side and equatorward and downward winds on the west (trailing) side. By comparing this structure with the observed spiral-shaped cloud distribution around the vortex, the upward (downward) winds correspond to the dark (bright) region, implying that the cloud could be formed by the upward winds. The AFES-Venus model also suggests the existence of a mid-latitudinal jet with an asymmetry between the northern and southern hemispheres, potentially triggering shear (barotropic) instability with an e-folding period of around 5 days, which could impact vortex development. When a vortex becomes more prominent in one hemisphere, the jet's peak shifts to the opposite hemisphere, enhancing meridional shear and leading to the creation of a new vortex. This interaction between the mature and newly formed vortices in both hemispheres creates winds that cross the equator, reversing the direction of momentum transport and causing the strength of the vortex and jet to alternate between hemispheres over time. While the exact process behind the periodic alternation of these asymmetric vortices between the hemispheres is not yet understood, the formation of mid-latitudinal jets with north-south asymmetry and barotropic instability within the cloud layer may help explain the complex cloud patterns seen on Venus' nightside.

R009-P30
ポスター 4 ：11/26　AM1/AM2 （9:00-12:00）

金星電波掩蔽観測による気温と硫酸蒸気混合比の長期変動に関する研究

#安藤 紘基 [1)], 野口 克行 [2)], 今村 剛 [3)], 佐川 英夫 [1)], Oschlisniok Janusz[4)], Tellmann Silvia[4)], Pätzold Martin[4)]
([1 京都産業大学, ([2 奈良女子大学, ([3 東京大学, ([4 ケルン大学

Long-term variations of temperature and H2SO4 gas mixing ratio in the Venusian atmosphere

#Hiroki Ando[1)], Katsuyuki Noguchi[2)], Takeshi Imamura[3)], Hideo Sagawa[1)], Janusz Oschlisniok[4)], Silvia Tellmann[4)], Martin Pätzold[4)]
([1]Kyoto Sangyo University, ([2]Nara Women's University, ([3]The University of Tokyo, ([4]Universität zu Köln

It is well known that planetary atmospheres have a wide range of time-scale variations that have a significant impact on the surface environment of the planet. Taking the Earth as an example, long-term scale atmospheric variations such as ENSO and QBO are affecting the Earth's weather and climate. On the other hand, whether such long-term scale atmospheric variations exist in planetary atmospheres other than Earth has not been much studied in the past. A change in this situation has been brought by the recent realization of long-term observations of the Venusian atmosphere by Venus Express and Akatsuki: the presence of significance long-term variations in UV albedo and the zonal mean wind speed at cloud levels have been reported. In addition, the measurements using ground-based telescopes also have indicated the long-term variations in the mixing ratios of H2O and SO2 gases at the cloud top level. In this study, we used the vertical profiles of temperature and H2SO4 gas mixing ratio obtained by the Venus Express and Akatsuki radio occultation measurements and investigated their long-term variations in the low latitude region. As a preliminary result, we found that both temperature and H2SO4 gas mixing ratio around the cloud bottom level (46-50 km altitudes) in 2006-2014 obtained from the radio occultation measurements by Venus Express are generally higher than those in 2016-2022 from the Akatsuki data. In addition, the trend of the annual variation of H2SO4 gas mixing ratio almost follows that of its saturated mixing ratio which is mainly determined by the temperature. In the presentation, we will also discuss the long-term variations of temperature in a wider vertical range from the mesosphere down to the sub-cloud region (~40-85 km altitudes).

惑星の大気中には様々な時間・空間規模の現象が存在しており、惑星の表層環境に大きな影響を与える。地球の場合、ENSO や QBO といった長期変動が地球気象に影響する。一方、地球以外の惑星におけるそのような長期変動の有無については、あまり研究が為されていない。近年、Venus Express やあかつきによって、金星でも有意な長期変動があることが示唆されている。また、地上観測によって、雲頂高度における水蒸気や SO2 の混合比が長期的に変動している可能性が指摘されている。本研究では、Venus Express とあかつきの電波掩蔽観測によって得られた気温と硫酸蒸気混合比の高度分布データを用いて、金星低緯度におけるそれらの長期変動を調べた。初期的な結果として、雲底付近（高度 46-50km）における気温と硫酸蒸気混合比は、Venus Express の観測時期の方があかつきより大きいことがわかった。また、硫酸蒸気混合比の年変化は、気温によって決まる飽和混合比におおよそ従っていることもわかった。本発表では、より広い高度範囲での温度の長期変動についても議論する。

R009-P31
ポスター 4 ：11/26　AM1/AM2 （9:00-12:00）

#郭 祝安 [1)], 今村 剛 [1)]
[(1] 東京大学

Image restoration experiment for infrared images of Venus

#Zhuan Guo[1)], Takeshi Imamura[1)]
[(1]the University of Tokyo

Thermal infrared images captured by Longwave Infrared Camera (LIR) onboard Akatsuki provide valuable information about the dynamics of the Venusian atmosphere. LIR successfully detects thermal emission in a waveband 8-12 μ m from the cloud deck of Venus on dayside and nightside with equal quality[1]. However, the noise in the infrared images prevents from further investigation of the Venusian atmosphere. Enhancement of the image quality is thereby needed to reveal more detailed morphology and structures of clouds.

Image restoration has been a popular topic and extensively studied for decades. It is the task of recovering a true unknown image from a degraded observed one. Numerous traditional and deep learning methods have been developed and proven to be powerful in image restoration for fields like remote sensing[2], medical imaging[3], etc. Regarding the LIR images, the previous study reduced random noise by taking a moving average of successive images with an interval of a few hours[4,5]. Stable structures are thereby highlighted, while transient ones are suppressed simultaneously.

Therefore, this study seeks new approaches to enhance the remote sensing images while refraining the transient structures from reduction. We selected a traditional algorithm, BM3D, and a learning-based algorithm, KBNet, to restore the infrared images of Venus. Both methods provided distinguishable major cloud structures. Enhanced images were compared with the original infrared image and the moving averaged images. The noise power spectrum (NPS) of the results obtained by BM3D, KBNet, and moving average was produced to investigate the characteristics of the noise and demonstrate the reliability and effectiveness of the two methods in the restoration of LIR images. The comparative analysis provides insights into the performance and efficacy of the traditional and learning-based algorithms on the LIR images, which contribute to the image process routine and analysis of remote sensing of Venus in the future.

[1] Taguchi, M., Fukuhara, T., Imamura, T., Nakamura, M., Iwagami, N., Ueno, M., Suzuki, M., Hashimoto, G. L., and Mitsuyama, K. (2007). Longwave Infrared Camera onboard the Venus Climate Orbiter. Advances in Space Research, 40(6), 861-868.
[2] B. Rasti, Y. Chang, E. Dalsasso, L. Denis, and P. Ghamisi. Image restoration for remote sensing: Overview and toolbox. IEEE Geoscience and Remote Sensing Magazine, 10(2):201 – 230, 2022.
[3] Jiri Jan. Medical image processing, reconstruction and restoration. Boca Raton, Fl: Taylor Francis, 2006.
[4] Fukuya, K., Imamura, T., Taguchi, M., Fukuhara, T., Kouyama, T., Horinouchi, T., Peralta, J., Futaguchi, M., Yamada, T., Sato, T. M., Yamazaki, A., Murakami, S.-Y., Satoh, T., Takagi, M., and Nakamura, M. (2021). The nightside cloud-top circulation of the atmosphere of Venus. Nature, 595(7868), 511-515.
[5] Fukuya, K., Imamura, T., Taguchi, M., and Kouyama, T. (2022). Horizontal structures of bow-shaped mountain wave trains seen in thermal infrared images of Venusian clouds taken by Akatsuki LIR. Icarus, 378, 114936.